Spring 2015

Biochemical investigation of the ubiquitin carboxyl-terminal hydrolase family

Joseph Rashon Chaney
Purdue University

Graduate School Form 30
(Updated 11/20/2014)

PURDUE UNIVERSITY
GRADUATE SCHOOL
Thesis/Dissertation Acceptance

This is to certify that the thesis/dissertation prepared

By Joseph Rashon Chaney

Entitled BIOCHEMICAL INVESTIGATION OF THE UBIQUITIN CARBOXYL-TERMINAL HYDROLASE FAMILY

For the degree of Doctor of Philosophy

Is approved by the final examining committee:

Chittaranjan Das

Angeline Lyon

Christine A. Hrycyna

George M. Bodner

To the best of my knowledge and as understood by the student in the Thesis/Dissertation Agreement, Publication Delay, and Certification/Disclaimer (Graduate School Form 32), this thesis/dissertation adheres to the provisions of Purdue University's "Policy on Integrity in Research" and the use of copyrighted material.

Approved by Major Professor(s): Chittaranjan Das

Approved by: R. E. Wild 04/24/2015

Head of the Department Graduate Program Date

BIOCHEMICAL INVESTIGATION OF THE UBIQUITIN CARBOXYL-TERMINAL HYDROLASE FAMILY

Dissertation

Submitted to the Faculty

of

Purdue University

by

Joseph Rashon Chaney

In Partial Fulfillment of the

Requirements for the Degree

of

Doctor of Philosophy

May 2015

Purdue University

West Lafayette, Indiana

All of this I dedicate wife, Millicent, to my faithful and beautiful children, Josh and Caleb. To my supportive father, Joseph Sr., mother, Janetta, sister, Jessica and my blessed in-laws Edmore, Alice and Marcia. I love you all!!!

ACKNOWLEDGMENTS

John 1: 2-5

Consider it pure joy, my brothers and sisters,[a] whenever you face trials of many kinds,3because you know that the testing of your faith produces perseverance. 4Let perseverance finish its work so that you may be mature and complete, not lacking anything.5If any of you lacks wisdom, you should ask God, who gives generously to all without finding fault, and it will be given to you.

I want to acknowledge my wife for her unwavering support. My children, Joshua and Caleb, follow after the things that God put in your heart to do and you will never be led astray. My family for all their support and prayers.

Thank you Chitta for all your wisdom, support and encouragement and mentorship. Thank my committee for good direction. I want to acknowledge my lab members, Chris (my brother), David, Tushar, Judy, Mike, and Marie. You all supported me and provided hope for me. God bless you all.

I especially want to acknowledge Kathy Dixon and the AGEP program for all their support and opportunities provided me. I wouldn't have made it without you.

TABLE OF CONTENTS

Page

LIST OF TABLES

LIST OF FIGURES

Figure Page

Figure Page

LIST OF SCHEMES

ABSTRACT

Chaney, Joseph Rashon. Ph.D., Purdue University, May 2015. Biochemical Investigation of the Ubiquitin Carboxyl-Terminal Hydrolase Family Major Professor: Chittaranjan Das.

The proteasome is the machinery in eukaryotic cells that degrades protein and recycles the amino acids. Protein degradation is a highly regulated process which starts by the attachment of chains of ubiquitin, which serves as a tag that marks a protein for degradation. This function involves the work of several proteins at the proteasome that work either as ubiquitin chaperones, ubiquitin binders or cleave ubiquitin from the protein that is to be degraded. As this is a highly regulated process, various irregularities can have deleterious effects including the onset of disease, including cardiovascular, cancer, and neurological.

The focus of this dissertation is to study how residues located within and outside the active site of Ubiquitin Carboxyl Terminal Hydrolase (UCH) deubiquinating enzymes (DUBS) help regulate these enzymes interaction with the ubiquitin. I will provide evidence that the putative oxyanion glutamine does function contribute to stabilization of the oxyanion intermediate. Secondly, I will show that evidence that glutamine may also serve another function within the active site by providing a CHO hydrogen bond that was previously thought not to exist within the active sites of cysteine proteases. Lastly, I will show that a conserved tryptophan in UCH37 has an effect on its catalytic viability.

CHAPTER 1: INTRODUCTION

1.1 Ubiquitin-Proteasome System

The proteasome is the machinery in eukaryotic cells that degrades protein and recycles the amino acids. Protein degradation is a highly regulated process. Ubiquitin is attached to proteins marked for degradation. Ubiquitin however is not degraded by the proteasome. Instead, the ubiquitin chain is cleaved by an enzyme at the proteasome cap called deubiquitinating enzymes or DUBS. Proteins are tightly regulated in the cell by the ubiquitin proteasome system. Ubiquitination is the covalent attachment of the 76 amino acid containing eukaryotic polypeptide ubiquitin and is an important reversible post-translational modification of proteins in the cell. It helps regulates a wide variety of biological process, such as cell cycle control, transcription, and protein quality control [3-5]. Ubiquitin is attached through an isopeptide bond between the C-terminal carboxy-terminal group of ubiquitin and the Ɛ-amino group of a lysine side chain[1]. This reaction is catalyzed by the sequential action of three enzymatic systems termed E1, E2, and E3 [4]. Ubiquitin is first activated by E1 in an ATP-dependent reaction that results in its installation on the E1 enzyme through a thioester bond between the c-terminal carboxylic acid of ubiquitin and the catalytic cysteine of E1. The activated ubiquitin is then transferred to the E2 enzymes catalytic cysteine residue. The E3 enzyme serves the function of a protein ligase. E3 links ubiquitin to the acceptor protein's lysine residue.

Once this isopeptide bond is formed, more ubiquitins are linked to form a polyubiquitin chain. There are estimated to be more than 600 E3 proteins found in the human genome [5]. E3 are responsible for the type of polyubiquitin chain tagged to the proteins. The type polyubiquitin linkages are identified by the lysine on ubiquitin and the carboxy terminus of the next ubiquitin where the bond is formed. The linkages that have been identified are K6, K11, K27, K29, K33, K48, and K63. Of these only the roles of K11, K48, and K63 have been determined[6-10]. K11 and K48 both have been found to be the primary linkage to confer proteasome degradation. While K63 linked substrates are responsible for non-degradative functions such as cellular signaling, intracellular trafficking, and ribosomal biogenesis [8-12]. The process is ultimately regulated by deubiquinating enzymes (DUBs), which catalytic activities oppose that of the E3 enzymes by editing the polyubiquitin chain or cleaving the ubiquitin directly from the substrate, creating more fee ubiquitin [12]. There are five classes of over 90 DUBs in the human genome: the cysteine protease comprising the ubiquitin c-terminal hydrolases (UCHs) family, the ubiquitin specific proteases (USPs) family, the ovarian tumor proteases (OTU) family, the Machado-Josephin Domain protease (MJDs) family and the last family, the JAB1/MPN/MOV34 (JAMM) protease family, are metalloproteases [13-15].

1.2 Ubiquitin C-Terminal Hydrolases

Of the five DUB families, the ubiquitin c-terminal hydrolase family is unique because there active sites contain a cross-over loop that restricts the substrate access . There are four members of the UCH family; UCHL1, UCHL3, UCHL5 (UCH37), and

BAP1 . It is the first DUB family to be identified however the substrate preference for each enzyme has not yet been determined [18]. Each family member is composed of a UCH domain with UCH37 and BAP1 having extensions at their c-terminus [1-3]. Ubiquitination is the covalent attachment of the 76 amino acid containing eukaryotic polypeptide ubiquitin and is an important reversible post-translational modification of proteins in the cell. It helps regulates a wide variety of biological process, such as cell cycle control, transcription, and protein quality control [3-5]. Ubiquitin is attached through an isopeptide bond between the C-terminal carboxy-terminal group of ubiquitin and the Ɛ-amino group of a lysine side chain[1]. This reaction is catalyzed by the sequential action of three enzymatic systems termed E1, E2, and E3 [13, 19]. Ubiquitin is first activated by E1 in an ATP-dependent reaction that results in its installation on the E1 enzyme through a thioester bond between the c-terminal carboxylic acid of ubiquitin and the catalytic cysteine of E1. The activated ubiquitin is then transferred to the E2 enzymes catalytic cysteine residue. The E3 enzyme serves the function of a protein ligase. E3 links ubiquitin to the acceptor protein's lysine residue. Once this isopeptide bond is formed, more ubiquitins are linked to form a polyubiquitin chain. The process is ultimately regulated by deubiquinating enzymes, which catalytic activities oppose that of E3 enzymes.

1.2.1 UCHL3

UCHL3 was one of the first structurally characterized in the UCH family and also the smallest at just 8.6 kDa [15, 21]. The primary responsibility of UCHL3 has yet to be determined. It is understood from structure that it has a crossover loop presumably for

conferring substrate specificity [13, 20]. The loop is found to be disordered in the human enzyme but takes an ordered conformation when bound to ubiquitin [15, 22]. UCHL3 shows hydrolase activity to linearly fused ubiquitin to small peptides [22]. It has been found to be upregulated in uterine cervical neoplasms and to be a novel regulator in prostate cancer cell lines [22, 23].

1.2.2 UCHL1

UCHL1 is a (223 amino acid), 24 kDa protein that belongs the UCH family of DUBs. It is selectively expressed in the brain comprising 1-2% of all brain protein. Mutations in UCHL1 have been linked to neurodegenerative diseases. UCHL1 has been identified in lewy bodies in Parkinson's disease [25]. UCHL1 is not expressed in normal lung tissue. This gives UCHL1 implications in lung cancer tumor regulation and metastasis[10]. UCHL1 monomer is composed of two lobes, a right and left. The right lobe of L1 consisting of five αα helixes [10]. The left lobe of L1 consists of two αα helices and six β strands. Between the lobes is a cleft that contains the catalytic residues. The active site is composed of three secondary structural elements; αa helix, a ββ sheet, and a loop. The helix contains the catalytic cysteine (Cys90). The β sheet contains the catalytic histidine (His 161). The loop contains the catalytic aspartic acid (Asp 176) [26]. These three residues make up UCHL1 catalytic triad and are responsible for UCHL1's ability to cleave the isopeptide bond linked substrates from ubiquitin.

1.2.3 UCHL5

UCHL5 (UCH37) is a 329 amino acid DUB of the UCH family. Its specific function is for ubiquitin chain editing, presumably at the distal end, at the 19S proteasome [27]. It has been found to dock to the 19S regulatory particle through the interactions with the subunit Rpn13. UCHL5 and RPN13 share a similar construct in their c-terminal region called a KEKE motif. The KEKE motif is a series of repetitive lysine and glutamate residues. This motif is believed to be responsible for this interaction. UCHL5's activity toward poly-ubiquitin chains is mediated by its association with RPN13, which provides an additional ubiquitin binding site for the poly-ubiquitin chain. RPN13 is linked to the proteasome through an association with RPN2[28].

1.2.4 BAP1

BRCA1 associated protein 1 (BAP1) is the largest member of the UCH family. In addition to the N-terminal UCH domain, it contains several interacting domains along with a nuclear localization site (NLS) [28]. BAP1 interactes with the RING finger domain of BRCA1 [29]. Sequence analysis identified the amino-terminal segment of BAP1 as a ubiquitin hydrolase, which was confirmed through activity measurements against a Ub-OEt substrate mimic[30]. BAP1 is the last member of the UCH family that has not had its structure determined. Further characterization of the enzyme revealed that BAP1 contained two nuclear localization sites and that BAP1 co-immunprecipitated with a splicing variant of BRCA1. This led to the understanding that the ubiquitin degradation pathway could play a role in the regulation of BRCA1. Because the sequence of BAP1 that interacts with BARD1 overlaps with the UCH domain (residues 182-365),

it is still unclear if the deubiquitinating activity of BAP1 has any link to its role is breast cancer[31].

1.3 References

1. Glickman MH, Ciechanover A. The ubiquitin-proteasome proteolytic pathway: destruction for the sake of construction. Physiol Rev. 2002;82(2):373-428. PubMed PMID: 11917093.

2. Ciechanover A, Heller H, Elias S, Haas AL, Hershko A. ATP-dependent conjugation of reticulocyte proteins with the polypeptide required for protein degradation. Proc Natl Acad Sci U S A. 1980;77(3):1365-8. Epub 1980/03/01. PubMed PMID: 6769112; PubMed Central PMCID: PMC348495.

3. Wilkinson KD, Urban MK, Haas AL. Ubiquitin is the ATP-dependent proteolysis factor I of rabbit reticulocytes. J Biol Chem. 1980;255(16):7529-32. Epub 1980/08/25. PubMed PMID: 6249803.

4. Li W, Bengtson MH, Ulbrich A, Matsuda A, Reddy VA, Orth A, et al. Genome-wide and functional annotation of human E3 ubiquitin ligases identifies MULAN, a mitochondrial E3 that regulates the organelle's dynamics and signaling. PLoS One. 2008;3(1):e1487. doi: 10.1371/journal.pone.0001487. PubMed PMID: 18213395; PubMed Central PMCID: PMC2198940.

5. Komander D, Rape M. The ubiquitin code. Annu Rev Biochem. 2012;81:203-29. doi: 10.1146/annurev-biochem-060310-170328. PubMed PMID: 22524316.

6. Pickart CM. Ubiquitin in chains. Trends Biochem Sci. 2000;25(11):544-8. PubMed PMID: 11084366.

7. Pickart CM, Eddins MJ. Ubiquitin: structures, functions, mechanisms. Biochim Biophys Acta. 2004;1695(1-3):55-72. doi: 10.1016/j.bbamcr.2004.09.019. PubMed PMID: 15571809.

8. Spence J, Sadis S, Haas AL, Finley D. A ubiquitin mutant with specific defects in DNA repair and multiubiquitination. Mol Cell Biol. 1995;15(3):1265-73. PubMed PMID: 7862120; PubMed Central PMCID: PMC230349.

9. Arnason T, Ellison MJ. Stress resistance in Saccharomyces cerevisiae is strongly correlated with assembly of a novel type of multiubiquitin chain. Mol Cell Biol. 1994;14(12):7876-83. PubMed PMID: 7969127; PubMed Central PMCID: PMC359326.

10. Das C, Hoang QQ, Kreinbring CA, Luchansky SJ, Meray RK, Ray SS, et al. Structural basis for conformational plasticity of the Parkinson's disease-associated ubiquitin hydrolase UCH-L1. Proc Natl Acad Sci U S A. 2006;103(12):4675-80. PubMed PMID: 16537382.

11. Clague MJ, Barsukov I, Coulson JM, Liu H, Rigden DJ, Urbe S. Deubiquitylases from genes to organism. Physiol Rev. 2013;93(3):1289-315. doi: 10.1152/physrev.00002.2013. PubMed PMID: 23899565.

12. Reyes-Turcu FE, Ventii KH, Wilkinson KD. Regulation and cellular roles of ubiquitin-specific deubiquitinating enzymes. Annu Rev Biochem. 2009;78:363-97. doi: 10.1146/annurev.biochem.78.082307.091526. PubMed PMID: 19489724; PubMed Central PMCID: PMC2734102.

13. Johnston SC, Larsen CN, Cook WJ, Wilkinson KD, Hill CP. Crystal structure of a deubiquitinating enzyme (human UCH-L3) at 1.8 A resolution. Embo J. 1997;16(13):3787-96. PubMed PMID: 9233788.

14. Johnston SC, Riddle SM, Cohen RE, Hill CP. Structural basis for the specificity of ubiquitin C-terminal hydrolases. Embo J. 1999;18(14):3877-87. PubMed PMID: 10406793.

15. Maiti TK, Permaul M, Boudreaux DA, Mahanic C, Mauney S, Das C. Crystal structure of the catalytic domain of UCHL5, a proteasome-associated human deubiquitinating enzyme, reveals an unproductive form of the enzyme. FEBS J. 2011;278(24):4917-26. doi: 10.1111/j.1742-4658.2011.08393.x. PubMed PMID: 21995438; PubMed Central PMCID: PMC3336103.

16. Nishio K, Kim SW, Kawai K, Mizushima T, Yamane T, Hamazaki J, et al. Crystal structure of the de-ubiquitinating enzyme UCH37 (human UCH-L5) catalytic domain. Biochem Biophys Res Commun. 2009;390(3):855-60. doi: 10.1016/j.bbrc.2009.10.062. PubMed PMID: 19836345.

17. Rose IA, Warms JV. An enzyme with ubiquitin carboxy-terminal esterase activity from reticulocytes. Biochemistry. 1983;22(18):4234-7. PubMed PMID: 6313036.

18. Wilkinson KD, Deshpande S, Larsen CN. Comparisons of neuronal (PGP 9.5) and non-neuronal ubiquitin C-terminal hydrolases. Biochem Soc Trans. 1992;20(3):631-7. Epub 1992/08/01. PubMed PMID: 1426603.

19. Artavanis-Tsakonas K, Weihofen WA, Antos JM, Coleman BI, Comeaux CA, Duraisingh MT, et al. Characterization and structural studies of the Plasmodium falciparum ubiquitin and Nedd8 hydrolase UCHL3. J Biol Chem. 2010;285(9):6857-66. Epub 2010/01/01. doi: M109.072405 [pii]

10.1074/jbc.M109.072405 [doi]. PubMed PMID: 20042598; PubMed Central PMCID: PMC2825479.

20. Misaghi S, Galardy PJ, Meester WJ, Ovaa H, Ploegh HL, Gaudet R. Structure of the ubiquitin hydrolase UCH-L3 complexed with a suicide substrate. J Biol Chem. 2005;280(2):1512-20. PubMed PMID: 15531586.

21. Larsen CN, Krantz BA, Wilkinson KD. Substrate specificity of deubiquitinating enzymes: ubiquitin C-terminal hydrolases. Biochemistry. 1998;37(10):3358-68. Epub 1998/04/02. doi: 10.1021/bi972274d [doi]bi972274d [pii]. PubMed PMID: 9521656.

22. Song HM, Lee JE, Kim JH. Ubiquitin C-terminal hydrolase-L3 regulates EMT process and cancer metastasis in prostate cell lines. Biochem Biophys Res Commun. 2014;452(3):722-7. doi: 10.1016/j.bbrc.2014.08.144. PubMed PMID: 25194810.

23. Rolen U, Kobzeva V, Gasparjan N, Ovaa H, Winberg G, Kisseljov F, et al. Activity profiling of deubiquitinating enzymes in cervical carcinoma biopsies and cell lines. Mol Carcinog. 2006;45(4):260-9. doi: 10.1002/mc.20177. PubMed PMID: 16402389.

24. Maraganore DM, Lesnick TG, Elbaz A, Chartier-Harlin MC, Gasser T, Kruger R, et al. UCHL1 is a Parkinson's disease susceptibility gene. Ann Neurol. 2004;55(4):512-21. PubMed PMID: 15048890.

25. Kim HJ, Kim YM, Lim S, Nam YK, Jeong J, Kim HJ, et al. Ubiquitin C-terminal hydrolase-L1 is a key regulator of tumor cell invasion and metastasis. Oncogene. 2009;28(1):117-27. doi: 10.1038/onc.2008.364. PubMed PMID: 18820707.

26. Yao T, Song L, Jin J, Cai Y, Takahashi H, Swanson SK, et al. Distinct modes of regulation of the Uch37 deubiquitinating enzyme in the proteasome and in the Ino80 chromatin-remodeling complex. Mol Cell. 2008;31(6):909-17. doi: 10.1016/j.molcel.2008.08.027. PubMed PMID: 18922472; PubMed Central PMCID: PMC2577292.

27. He J, Kulkarni K, da Fonseca PC, Krutauz D, Glickman MH, Barford D, et al. The structure of the 26S proteasome subunit Rpn2 reveals its PC repeat domain as a closed toroid of two concentric alpha-helical rings. Structure. 2012;20(3):513-21. doi: 10.1016/j.str.2011.12.015. PubMed PMID: 22405010.

28. Jensen DE, Proctor M, Marquis ST, Gardner HP, Ha SI, Chodosh LA, et al. BAP1: a novel ubiquitin hydrolase which binds to the BRCA1 RING finger and enhances BRCA1-mediated cell growth suppression. Oncogene. 1998;16(9):1097-112. Epub 1998/04/07. PubMed PMID: 9528852.

29. Jensen DE, Rauscher FJ, 3rd. Defining biochemical functions for the BRCA1 tumor suppressor protein: analysis of the BRCA1 binding protein BAP1. Cancer Lett. 1999;143 Suppl 1:S13-7. Epub 1999/11/05. PubMed PMID: 10546591.

30. Mallery DL, Vandenberg CJ, Hiom K. Activation of the E3 ligase function of the BRCA1/BARD1 complex by polyubiquitin chains. EMBO J. 2002;21(24):6755-62. PubMed PMID: 12485996; PubMed Central PMCID: PMC139111.

31. Lill JR, Wertz IE. Toward understanding ubiquitin-modifying enzymes: from pharmacological targeting to proteomics. Trends Pharmacol Sci. 2014;35(4):187-207. doi: 10.1016/j.tips.2014.01.005. PubMed PMID: 24717260.

32. Morrow ME, Kim MI, Ronau JA, Sheedlo MJ, White RR, Chaney J, et al. Stabilization of an unusual salt bridge in ubiquitin by the extra C-terminal domain of the proteasome-associated deubiquitinase UCH37 as a mechanism of its exo specificity. Biochemistry. 2013;52(20):3564-78. Epub 2013/04/27. doi: 10.1021/bi4003106. PubMed PMID: 23617878; PubMed Central PMCID: PMC3898853.

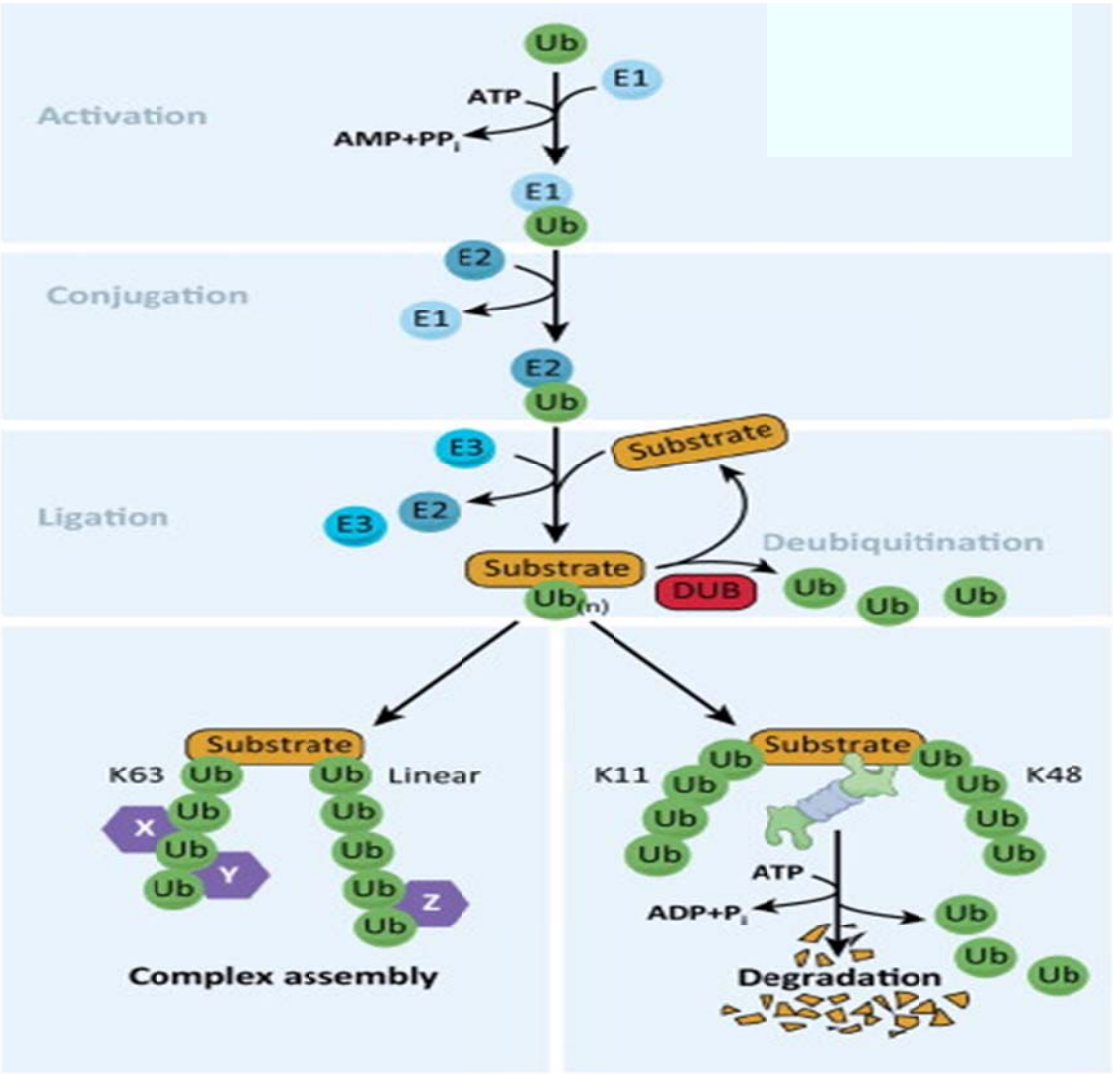

Figure 1.1: Ubiquitin (Ub) is covalently attached to substrates via an isopeptide bond by sequential action of E1, E2, and E3 enzymes. Deubiquitinases (DUBs) hydrolyze isopeptide linkages, thus reversing the action of ubiquitin machinery [32].

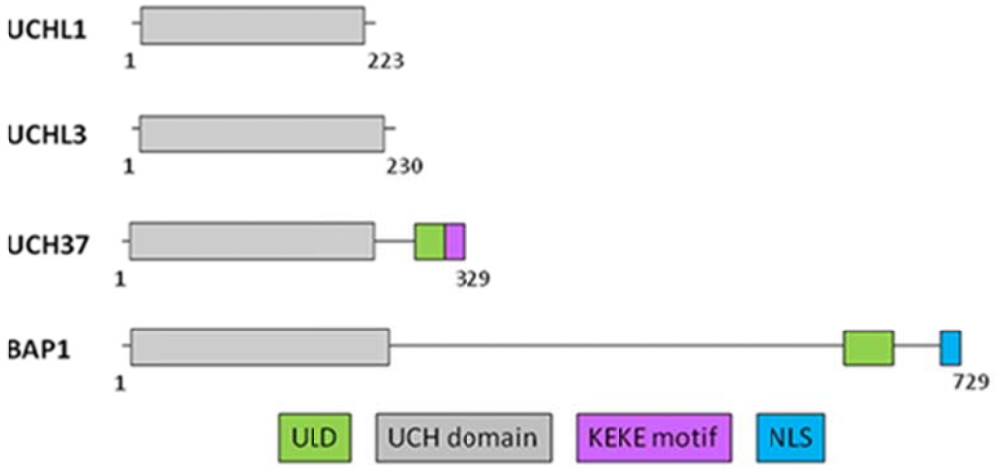

Figure 1.2: Domain maps of proteins that make up the UCH family of DUBs [1-3]

CHAPTER 2: CONTRIBUTION OF PUTATIVE OXYANION HOLE RESIDUE TO CATALYSIS IN UCHL1, UCHL3 AND UCHL5

(Previously published as Boudreaux D, Chaney J, Maiti TK, Das C. Contribution of active site glutamine to rate enhancement in ubiquitin C-terminal hydrolases. FEBS J. 2012.)

2.1 Abstract

Ubiquitin carboxy terminal hydrolases (UCHs) catalyze the hydrolytic removal of ubiquitin from ubiquitinated proteins. These deubiquinating enzymes are cysteine proteases featuring a classical cysteine-histidine-aspartate catalytic triad, also a highly conserved glutamine thought to be a part of the oxyanion hole. However, the contribution of this side chain to the catalysis by UCH enzymes is not known.

In this study, we demonstrate through mutational analysis that the putative oxyanion-stabilizing side chain contributes to rate enhancement in UCHL1, UCHL3 and UCHL5. Mutation of the glutamine to alanine in these enzymes reduces the catalytic efficiency, mainly due to a 16 to 30-fold reduction in k_{cat} (2 kcal/mol).

2.2 Introduction

Ubiquitin carboxy-terminal hydrolases (UCHs) belong to a larger group of enzymes collectively called deubiquitinases (DUBs), which catalyze the hydrolysis of the peptide or isopeptide bond through which ubiquitin is attached to other proteins or other

ubiquitin moieties in polyubiquitin chains [12, 35, 36]. The UCH family members are cysteine proteases featuring a classical cysteine-histidine-aspartate catalytic triad [12, 15, 16, 22]. The active site of these enzymes also features a highly conserved glutamine residue (Fig. 2.1) believed to be a part of the so-called oxyanion hole, an arrangement of spatially proximal peptide dipoles aligned in a way that creates a positively charged pocket facing the thiol group of the catalytic cysteine. It is also possible that, by virtue of being located at the N-terminus of a helix, the electropositive character of this pocket is enhanced by the helix macro dipole effect [6]. In cysteine proteases, nucleophilic attack of the carbonyl group on the scissile peptide bond proceeds through a tetrahedral transition state bearing a negative charge on the oxygen atom of the carbonyl group. This negative charge is stabilized by electrostatic and hydrogen-bonding interactions with the oxyanion hole, which is proposed to be one of the factors leading to the lowering of activation energy for the hydrolysis reaction [6].

The relative orientation of the carbonyl oxygen of the scissile peptide group with respect to the oxyanion-stabilizing groups, as in the tetrahedral transition state, may be approximately visualized in the crystal structure of the yeast ubiquitin hydrolase Yuh1 bound covalently to the suicide substrate ubiquitin aldehyde (Ubal) (Fig. 2) [6]. Attack of the catalytic thiol on Ubal results in the formation of the thiohemiacteal product, which mimics the oxyanion-bearing tetrahedral transition state (Fig. 2). As seen in Figure 2, the hydroxyl oxygen of the thiohemiacetal moiety is within a relatively short distance from the backbone NH groups of the catalytic Cys90, Ala89, Asn88 and the side chain NH_2 group of Gln84, the putative oxyanion-stabilizing side chain. It has been proposed that in a general cysteine protease, the negatively charged oxygen in the tetrahedral transition

state would occupy nearly the same position as the thiohemiacteal hydroxyl oxygen seen in the Yuh1-Ubal structure and would be coordinated through electrostatic and hydrogen-bonding interactions by the groups lining the oxyanion hole [7].

Papain, an extensively studied cysteine protease, revealed that Gln19, the oxyanion side chain in the protein, plays a role in the catalytic mechanism of the enzyme contributing to rate enhancement [7]. Mutation of this side chain to alanine reduces the catalytic efficiency approximately 60-fold, mostly affecting k_{cat} (20-fold lower) with a relatively smaller change in K_M (3-fold higher) [8]. Ignoring the relatively small change in K_M, the 20-fold change in k_{cat} was attributed to a loss of the contribution of the glutamine side chain to oxyanion stabilization. The catalytic Cys-His-Asp triad of structurally characterized UCH enzymes, such as UCHL1, UCHL3 and UCHL5, adopts a similar geometric relationship as found in the Cys-His-Asn triad of papain and the triads of other papain-like cysteine proteases. Additionally, the active-site glutamine in UCH enzymes is located in an identical location as the as Gln19 in papain. However, the role played by this side chain in the catalysis by UCH enzymes has not been studied thus far. Considering the importance of the UCH group of proteases in diseases such as Parkinson's disease and cancer, understanding the role of active site residues in catalysis is important for our overall understanding of the mechanism of these enzymes[9]. We sought to determine the contribution to rate enhancement by the putative oxyanion glutamine.

2.3 Materials and Methods

Ubiquitin 7-amido-4-methylcoumarin (Ub-AMC) used for hydrolysis assays was acquired from Boston Biochem (Boston, MA). The glutathione affinity column (GSTPrep FF 16/10), gel filtration column (HiLoad 16/60 Superdex 75) and PreScission protease were purchased from GE Biosciences (USA). All fluorescence assays were performed on a TECAN Genios microplate spectrofluorometer. Buffer and salt components were purchased from either Sigma-Aldrich (St. Louis, MO) or RPI Corp (Mount Prospect, IL).

2.3.1 Mutagenesis, Protein Expression and Purification

UCHL1, UHCL3, UCHL5N240 were cloned into the pGEX-6P-1 vector using standard protocols and subsequently used to mutate the active-site glutamine to alanine through PCR reactions using the Quickchange II (Agilent; Santa Clara, CA) site-directed mutagenesis kit. All plasmids were transformed into Rosetta2 *E. coli* cells and grown to an $OD_{\lambda 600nm}$= 0.6 in LB media supplemented with 100 μg/mL ampicillin then induced with 0.5 mM isopropyl β-thiogalactoside and grown overnight at 18°C. Cells were harvested at 6,000 × *g* and resuspended in 1X PBS + 400 mM KCl (buffer A). Cells were passed through a French press twice at 1,200 psi and the lysate cleared by centrifugation at 30,000 × *g* for 1 hour. The supernatant was loaded onto a glutathione affinity column, washed with 3 column volumes of buffer A and eluted with 250 mM Tris, 500 mM KCl, 10 mM reduced L-glutathione, pH 8.0. The eluted sample was dialyzed against 1X PBS, 400 mM KCl, 1 mM DTT to which PrecissionProtease was added to remove the glutathione S-transferase (GST) tag, which was captured onto a glutathione-agarose affinity column. The resulting GST-cleaved protein solution was passed through a

Superdex S75 gel filtration column with 50 mM TRIS-HCl (pH 7.6), 150 mM NaCl and 1mM DTT. Fractions containing purified protein were pooled, concentrated then flash frozen in liquid nitrogen and stored at -80 °C until use.

2.3.2 Analysis of Oxyanion Mutants

Each of the UCH enzymes was diluted in assay reaction buffer (50 mM Tris pH 7.6, 0.5 mM EDTA, 0.1% BSA, 5 mM DTT) so the final concentration in the reaction is the following: UCHL1 (2 nM), UCHL1 Q84A (8 nM), UCHL3 (5 pM), UCHL3 Q89A (175 pM), UCHL5N240 (500 pM), UCHL5N240 Q82A (3 nM), UCHL3 Q89E (12 pM), UCHL3 Q89K (50 pM). Enzyme was added to a 96-well plate and incubated at 30°C for 5 min prior to addition of Ub-AMC diluted in assay reaction buffer to initiate the reaction. Rates of Ub-AMC cleavage was monitored with an excitation λ = 380 nm and an emission λ = 465 nm at 30°C. Initial reaction rates were calculated and plotted versus Ub-AMC concentration in SigmaPlot and fitted to the Michaelis-Menten equation to determine K_M and k_{cat} values.

2.4 Results

2.4.1 Alanine Mutants Show Modest Loss of Activity

In order to determine if the conserved glutamine residue found in the active site of UCH enzymes (fig. 2.3) contributes to rate enhancement, hydrolysis assays using the fluorogenic substrate Ub-AMC were conducted using identical conditions for each set of enzyme and its glutamine to alanine mutant. These results show that the rate of

hydrolysis leading to AMC release is significantly reduced in the mutants compared to their wild-type enzymes seen in figure 2.3, suggest that this side chain plays some role in the catalytic mechanism of the enzymes. Since glutamine is located in the solvent-accessible active site of the enzymes, the mutation of this residue to alanine is not expected to cause any significant perturbation in the active-site structure or gross changes in the three-dimensional fold of the protein. In fact, the circular dichroism spectra of the mutants produce a pattern that is nearly identical in shape and intensities to their corresponding wild-type proteins confirming that the mutation has no observable structural effect in these proteins [10-12].

The loss in catalytic activity observed upon mutation could be attributed to two possible factors: an increase in the Michaelis constant K_M, or a reduction in k_{cat}, the rate constant of the rate determining step in the hydrolysis reaction. In order to know which parameters are affected by the mutation, we set out to analyze the Michaelis-Menten kinetics of the mutants and the wild-type enzymes. Additional activity assays were conducted with varying substrate concentration and plots of the initial velocities versus substrate concentration are shown in figure 2.4 All enzymes with the exception of UCHL5N240 Q82A were fit to the Michaelis-Menten equation (figure 2.4). Non-linear regression analysis of the plots yielded the kinetic parameters k_{cat} and K_M for each UCH variant and their values are provided in Table 2.1. The values of the kinetic parameters obtained with wild-type enzymes are consistent with previously reported values . The glutamine to alanine mutants showed a 30 and 18-fold decrease in k_{cat}, for UCHL1 and UCHL3, respectively, compared to their corresponding wild-type enzymes. However, K_M values were relatively unchanged due to the mutation, which is consistent with the

hypothesis that the glutamine residue is involved in the catalytic mechanism of the enzyme.

In the case of UCHL5N240 Q82A, k_{cat} and K_M could not be determined individually because, even at concentrations of Ub-AMC as high as 12 μM, the Michaelis-Menten plot was still rising linearly with substrate concentration, not reaching the plateau that is diagnostic of saturation. Substrate concentrations greater than 12 μM result in DMSO concentrations higher than 5%, which can diminish the enzyme's activity. Instead, the ratio k_{cat}/K_M was determined by dividing the slope of this linear plot by the total enzyme concentration since it can be assumed that in this region of the Michaelis-Menten plot, [Ub-AMC] << K_M. Comparison of this value for the wild-type and Q82A variant of UCHL5N240 shows a 16-fold reduction in catalytic efficiency, which is comparable to the reductions seen with UCHL1 and UCHL3 suggesting that the Gln82 residue is likely performing the same function as in the other UCH enzymes.

In order to determine the effect of these mutations on the stabilization of the transition state, we sought to estimate the change in free energy of activation associated with the mutation. The calculation was carried out using equation 2.1 and the k_{cat}/K_M values mentioned above and reported in Table 2.1 [11]. The free energy change for the three enzymes is approximately 2 kcal/mol, which is consistent with the value reported for the same mutation in papain [11].

$$\Delta\Delta G^{\neq} = -RT \ \ln\left[\frac{(k_{cat}/K_M)_{mutant}}{(k_{cat}/K_M)_{wild\text{-}type}}\right] \qquad \text{Equation 2.1}$$

The active-site glutamine in UCH enzymes is involved in a C—H•••O hydrogen bond with CεH of the catalytic histidine

2.5 Discussion

The UCH subfamily of dubiquitinases are cysteine proteases with a catalytic triad similar to that seen in the papain family. In each member of this family, like papain, there is a conserved glutamine residue located in the active site of the enzymes believed to stabilize the incipient negative charge on the carbonyl of the scissile bond during the transition state of the hydrolysis reaction (Scheme 2.1). Indeed, mutation of the Gln19 in papain to alanine resulted in a 60-fold decrease in catalytic efficiency due mainly to a diminished catalytic rate (20-fold) and a small loss in substrate binding (3-fold). These results support the claim that the conserved glutamine side chain contributes to the stabilization of the oxyanion transition state. Given the similarity in certain active-site residues between papain and members of the UCH family, we wondered if the glutamine would perform a similar role in the UCH family. Our study sought to address the role of the conserved glutamine in rate enhancement in three UCH enzymes.

Through site-directed mutagenesis, the active-site glutamine in three structurally characterized members of the UCH family was replaced with alanine in order to assess the contribution of this side chain to rate enhancement. Deubiquitination assays show there is a significant loss of activity in mutant enzymes compared to their wild-type counterparts. Comparison of the kinetic parameters shows a 16 to 30-fold loss (~2 kcal/mol) in the catalytic efficiency for the glutamine mutants, which is due mainly to a decrease in the k_{cat} parameter, as seen in UCHL1 and UCHL3 (for the mutant UCHL5,

k_{cat} and K_M could not be separately determined). These results are in agreement with the aforementioned results from papain, although the UCH enzymes did not exhibit the same change in the K_M value. The kinetic scheme for UCHL1 has been worked out by Case and Stein using the same Ub-AMC substrate [10]. Their study shows that the rate of acylation is rate-limiting for k_{cat}, which means K_M reduces to the dissociation constant (K_d) of the Michaelis complex. The fact that we are not seeing any significant change in K_M suggests that Gln84 in UCHL1 does not contribute to the enzyme-ground state-substrate complex. Therefore, in UCHL1, according to our studies, the active site glutamine does not make any appreciable contact with the substrate in the Michaelis complex; rather it helps to stabilize the transition state.

The kinetic scheme for UCHL3 remains to be worked out. However, k_{cat} values of UCHL3 catalyzed hydrolysis of ubiquitin ethylester and Ub-lysine are very similar to that obtained with Ub-AMC as the substrate, suggesting that deacylation might be the rate-limiting step [13]. In such a case, K_M is not the simple dissociation constant of the Michaelis complex. Nevertheless, the fact that K_M changes only slightly upon glutamine to alanine mutation in UCHL3 is consistent with the inference that the glutamine does not appreciably contribute to Michaelis complex.

As discussed before, we could not separately measure k_{cat} and K_M for UCHL5N240 Q82A; rather, the ratio was measured, which is about 16-fold less than the wild-type protein. It is possible that the ratio reflects a change mostly in k_{cat}, like UCHL1 and UCHL3, due to the structural similarity between the proteins. However, it cannot be ruled out that UCHL5N240 employs a different mechanism than UCHL1 and UCHL3. It is possible that there was a much larger change in k_{cat} that was compensated by an

opposite change in K_M. Alternatively, there was little or no change in k_{cat} and the observed effect was due mostly to a change in K_M. The latter possibility seems rather unreasonable since the glutamine is located in an almost identical position as in the other enzymes and therefore its effect on stabilizing the Michaelis-Menten complex is expected to be the same.

Our results indicate the mutation of glutamine to alanine results in a significant decline in the catalytic rate, which supports the hypothesis that glutamine is functioning to stabilize the transition state intermediate(s). However, one expects that the change would be much greater than 30-fold as seen in our system if the mechanism were through the stabilization of the oxyanion, which has been proposed to involve hydrogen bonding between the NH_2 group of the side chain of glutamine and the negatively charged oxygen ion, given that such hydrogen bonds are particularly strong. For example, mutation of the oxyanion-stabilizing residue Tyr16 to phenylalanine in ketosteroid isomerase results in a 20,000-fold (6.3 kcal/mol) reduction in k_{cat} [9]. One explanation for the discrepancy between the result of the mutation of the oxyanion-stabilizing side chain in ketosteroid isomerase compared to our system is that, in the latter, the side chain of glutamine is not solely responsible for stabilizing the oxyanion through hydrogen bonding; rather, it is playing a role in contributing to the overall electropositive character of the oxyanion hole. As shown in Figure 2.2, a number of αNH dipoles from surrounding backbone residues can still support a significant degree of oxyanion stabilization even in the absence of the glutamine side chain. Since main-chain atoms cannot be removed by traditional mutagenesis methods, the individual contribution of each atom cannot be determined, nor can we determine if the glutamine plays a more significant role than the individual

backbone atoms. The alternative possibility that the transition-state stabilization by the glutamine side chain is reflecting a somewhat weaker hydrogen bond owing to a longer distance between the donor and the acceptor (discussed further in Chapter 4) cannot be ruled out.

2.6 References

1. Komander D, Clague MJ, Urbe S. Breaking the chains: structure and function of the deubiquitinases. Nat Rev Mol Cell Biol. 2009;10(8):550-63. doi: 10.1038/nrm2731. PubMed PMID: 19626045.

2. Nijman SM, Luna-Vargas MP, Velds A, Brummelkamp TR, Dirac AM, Sixma TK, et al. A genomic and functional inventory of deubiquitinating enzymes. Cell. 2005;123(5):773-86. Epub 2005/12/06. doi: S0092-8674(05)01169-4 [pii]

10.1016/j.cell.2005.11.007 [doi]. PubMed PMID: 16325574.

3. Das C, Hoang QQ, Kreinbring CA, Luchansky SJ, Meray RK, Ray SS, et al. Structural basis for conformational plasticity of the Parkinson's disease-associated ubiquitin hydrolase UCH-L1. Proc Natl Acad Sci U S A. 2006;103(12):4675-80. PubMed PMID: 16537382.

4. Johnston SC, Larsen CN, Cook WJ, Wilkinson KD, Hill CP. Crystal structure of a deubiquitinating enzyme (human UCH-L3) at 1.8 A resolution. Embo J. 1997;16(13):3787-96. PubMed PMID: 9233788.

5. Misaghi S, Galardy PJ, Meester WJ, Ovaa H, Ploegh HL, Gaudet R. Structure of the ubiquitin hydrolase UCH-L3 complexed with a suicide substrate. J Biol Chem. 2005;280(2):1512-20. PubMed PMID: 15531586.

6. Johnston SC, Riddle SM, Cohen RE, Hill CP. Structural basis for the specificity of ubiquitin C-terminal hydrolases. Embo J. 1999;18(14):3877-87. PubMed PMID: 10406793.

7. Leroy E, Boyer R, Auburger G, Leube B, Ulm G, Mezey E, et al. The ubiquitin pathway in Parkinson's disease. Nature. 1998;395(6701):451-2. PubMed PMID: 9774100.

8. Fang Y, Fu D, Shen XZ. The potential role of ubiquitin c-terminal hydrolases in oncogenesis. Biochim Biophys Acta. 1806(1):1-6. Epub 2010/03/23. doi: S0304-419X(10)00026-0 [pii]

10.1016/j.bbcan.2010.03.001 [doi]. PubMed PMID: 20302916.

9. Boudreaux D, Chaney J, Maiti TK, Das C. Contribution of active site glutamine to rate enhancement in ubiquitin C-terminal hydrolases. FEBS J. 2012. Epub 2012/01/31. doi: 10.1111/j.1742-4658.2012.08507.x. PubMed PMID: 22284438.

10. Luchansky SJ, Lansbury PT, Jr., Stein RL. Substrate recognition and catalysis by UCH-L1. Biochemistry. 2006;45(49):14717-25. PubMed PMID: 17144664.

11. Case A, Stein RL. Mechanistic studies of ubiquitin C-terminal hydrolase L1. Biochemistry. 2006;45(7):2443-52. PubMed PMID: 16475834.

12. Dang LC, Melandri FD, Stein RL. Kinetic and mechanistic studies on the hydrolysis of ubiquitin C-terminal 7-amido-4-methylcoumarin by deubiquitinating enzymes. Biochemistry. 1998;37(7):1868-79. Epub 1998/03/04. doi: 10.1021/bi9723360

bi9723360 [pii]. PubMed PMID: 9485312.

13. Kraut DA, Sigala PA, Fenn TD, Herschlag D. Dissecting the paradoxical effects of hydrogen bond mutations in the ketosteroid isomerase oxyanion hole. Proc Natl Acad Sci U S A. 107(5):1960-5. Epub 2010/01/19. doi: 0911168107 [pii]

10.1073/pnas.0911168107 [doi]. PubMed PMID: 20080683.

```
UCH-L1     80 YFMKQTIGNSCGTIGLIHAVANN 102
UCH-L3     85 YFMKQTISNACGTIGLIHAIANN 107
UCH-L5     78 FFAKQVINNACATQAIVSVLLNC 100
BAP1       81 FFAHQLIPNSCATHALLSVLLNC 103
Yuh1       80 IWFKQSVKNACGLYAILHSLSNN 102

UCH-L1    159 NFHFILFNNVDGHLYELDGRMPF 181
UCH-L3    167 DLHFIALVHVDGHLYELDGRKPF 189
UCH-L5    162 AFHFVSYVPVNGRLYELDGLREG 184
BAP1      167 AFHFVSYVPITGRLFELDGLKVY 189
Yuh1      164 NLHYITYVEENGGIFELDGRNLS 186
```

Figure 2.1: Sequence alignment for the five human Ubiquitin Carboxyl Terminal Hydrolase enzymes and the yeast homolog YUH1. Active site catalytic residues are featured in red while the putative oxyanion residue is featured in blue [9]

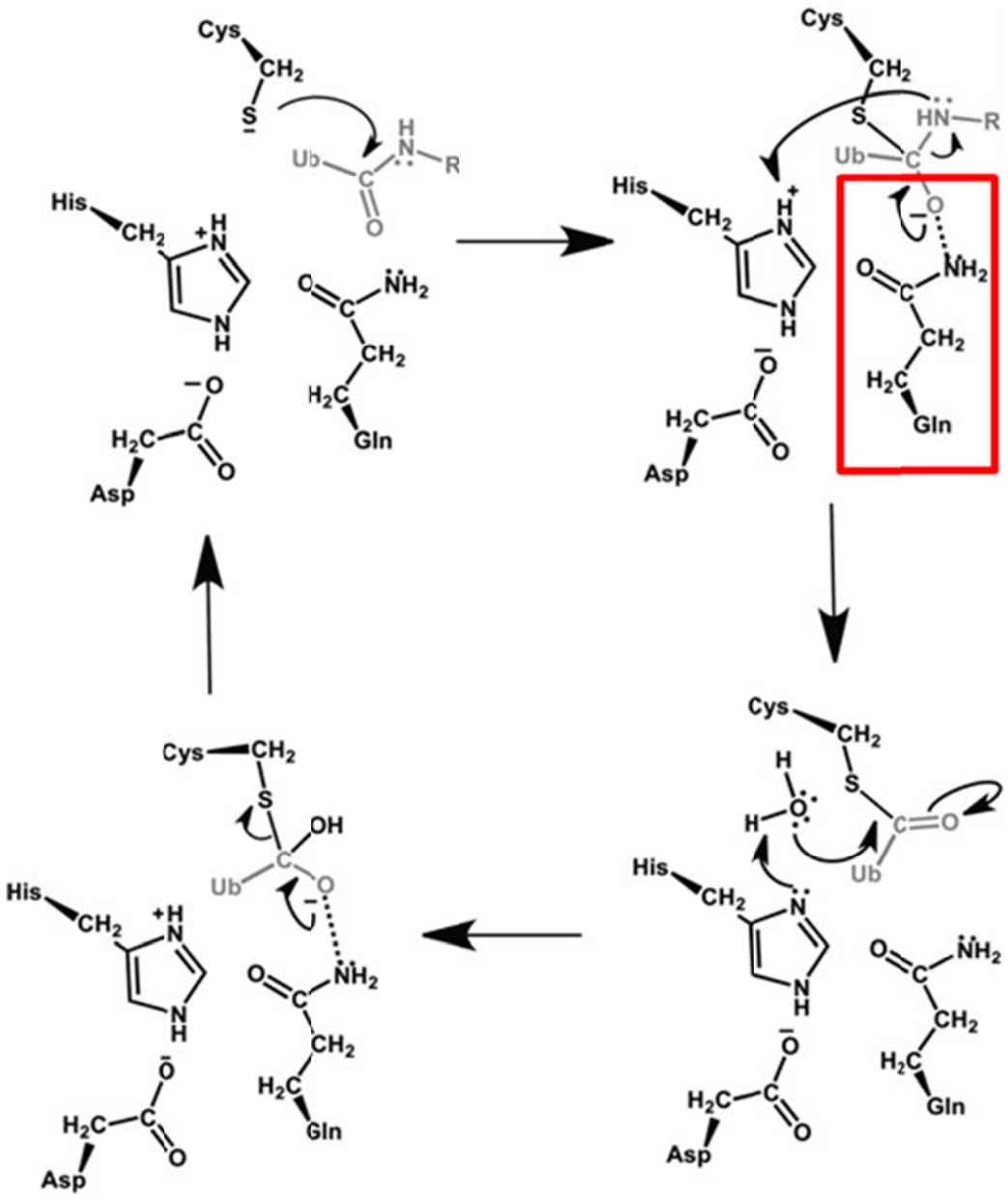

Scheme 2.1: Proposed mechanism for deubiquination by UCH enzymes. Putative oxyanion residue glutamine is boxed in red [5].

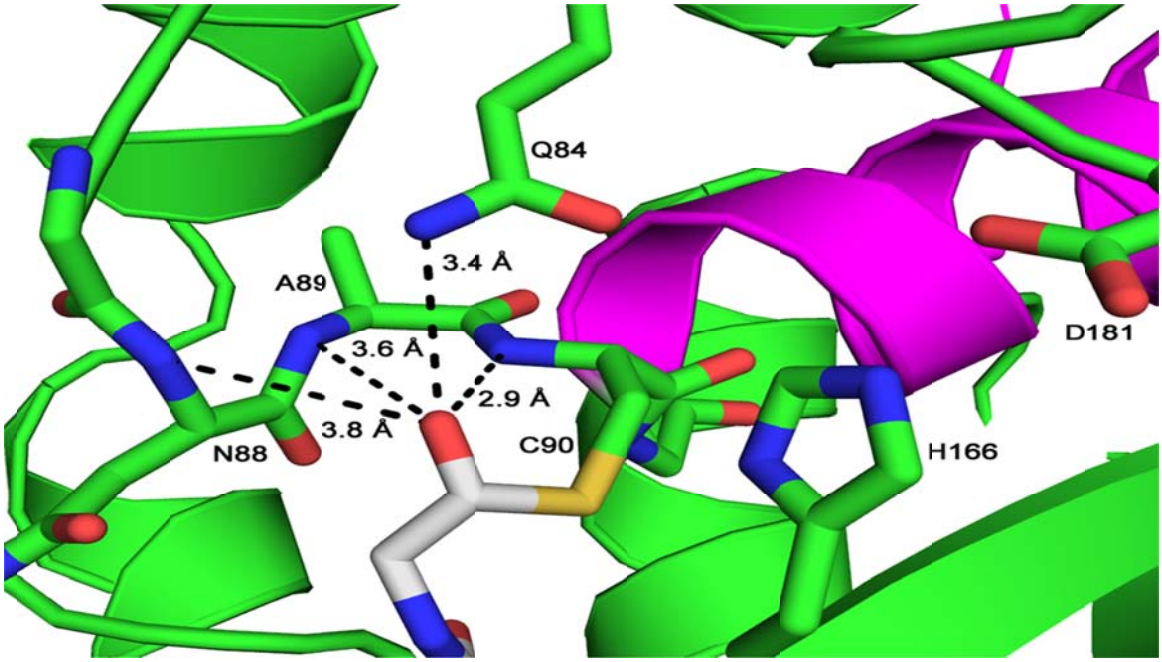

Figure 2.2: An illustration of oxyanion hole in a UCH enzyme. The structure of yeast UCHL3 homologue, Yuh1 (PDB entry **1CMX**) (green), covalently bound to Ubiquitin aldehyde (gray). Hydrogen bonding distances are shown for Yuh1 residues stabilizing the thiohemiacetal hydroxyl oxygen on the aldehyde moiety [9]

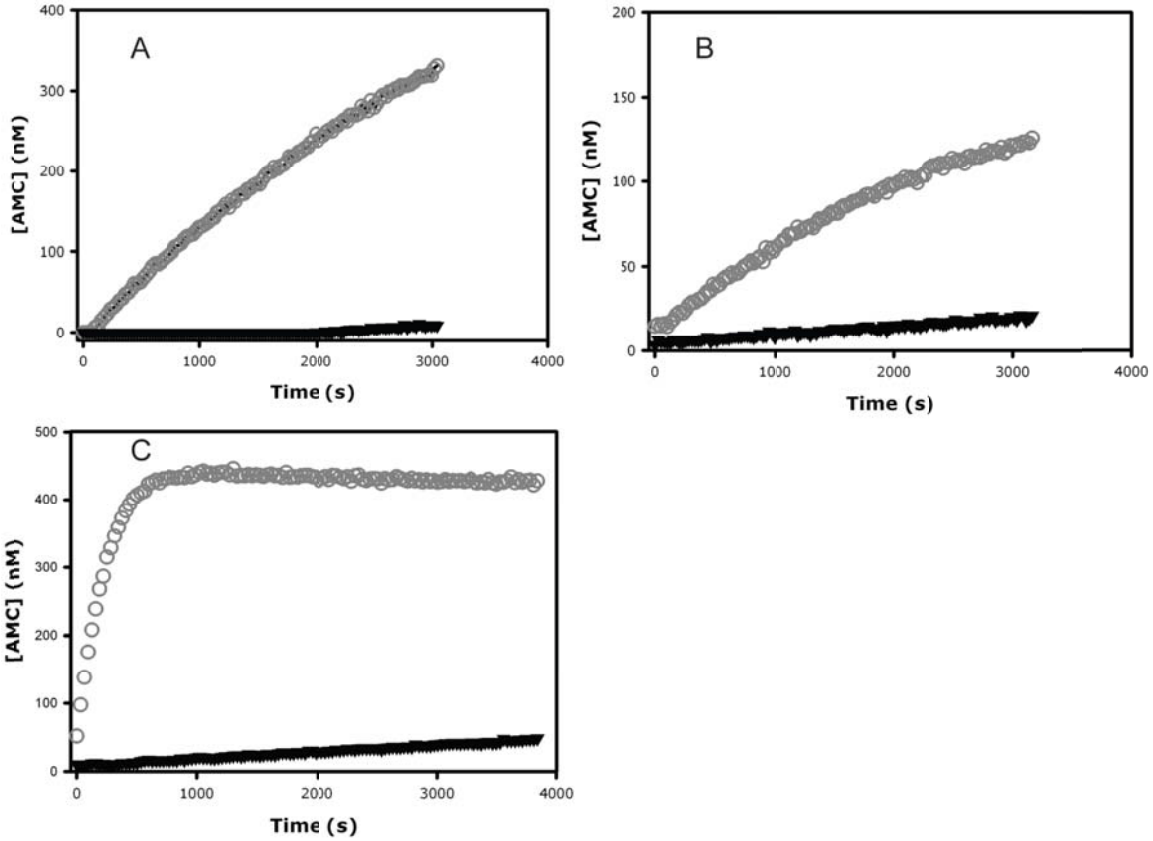

Figure 2.3: Comparative activity assay of wild-type and mutant UCH enzymes. A, UCHL1 (5 nM) and UCHL1(Q89A) (5 nM) with 600 nM Ub-AMC. B, UCHL3 (5 pM) and UCHL3(Q89A) (5 pM) with 300 nM Ub-AMC. C, UCHL5N240 (1 nM) and UCHL5N240(Q82A) (1 nM) with 480 nM Ub-AMC. Wild-type UCH's are shown in open gray and glutamine mutants are shown in solid black [9].

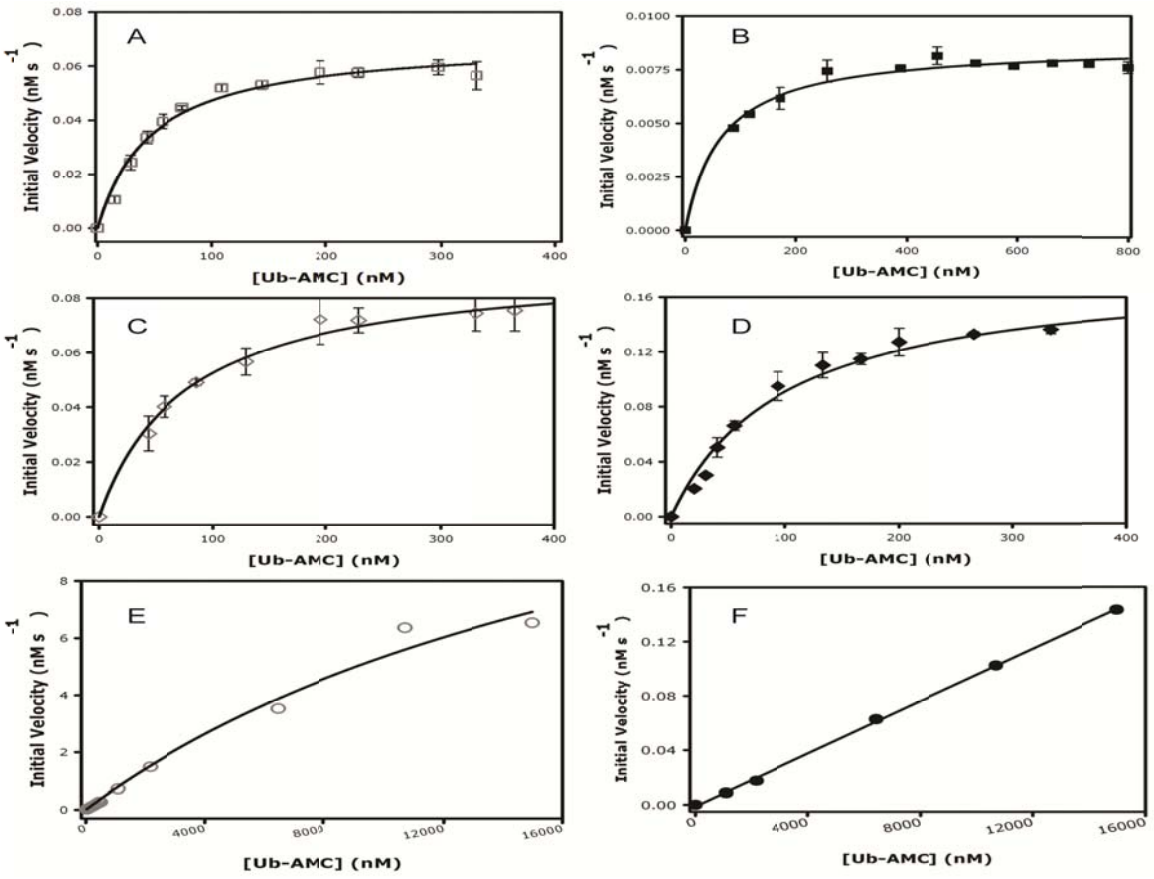

Figure 2.4: Glutamine to alanine mutants in UCH enzymes show impaired catalysis suggesting that the active site glutamine plays a role in rate enhancement. A. UCHL1 WT B. UCHL1 Q84A C. UCHL3 WT D. UCHL3 Q89A E. UCHL5N240 F. UCHL5N240 Q82A[9]

Table 2.1: Kinetic Parameters for UCH Enzymes showing decrease in k_{cat}/K_M from wild type to Ala mutants [1]

Enzyme	K_M (nM)	k_{cat} (s^{-1})	$k_{cat}/K_M \times 10^4$ (M^{-1} s^{-1})	$\Delta\Delta G^{\ddagger}$ (kcal/mol)
UCHL3	77.1 ± 8.2	18.60 ± 0.60	24140	1.89
UCHL3 Q89A	99.1 ± 13.5	1.03 ± 0.05	1040	
UCHL1	47.0 ± 6.0	0.0348 ± 1.25×10^{-3}	74.1	2.19
UCHL1 Q84A	56.1 ± 2.3	0.0011 ± 1.50×10^{-4}	1.96	
UCHL5N240	21493.2	33.67	15.7	1.68
UCHL5N240 Q82A	—	—	0.966	

CHAPTER 3: CONSERVED HYDROPHOBIC MUTATION IN UCH ENZYMES HAS VARIED ROLE AS IT RELATES TO UBIQUITIN

3.1 Abstract

Ubiquitin carboxyl terminal hydrolase (UCH) enzymes release small peptide and protein leaving groups from the C-terminus of ubiquitin. Although the interaction with ubiquitin is fairly well understood in these enzymes, recognition of the isopeptide moiety of the substrate at the active site has not been well characterized. The crystal structure of TsUCH37 (*T.* spiralis) bound to the suicide substrate, UbVMe, reveals a conserved tryptophan residue that may play a role in stabilizing the isopeptide linkage in the active site. To study the contribution of this tryptophan residue, the equivalent residue in human UCH37, W58, was mutated to alanine and phenylalanine. The phenylalanine mutant retained most of its ubiquitin-AMC (Ub-AMC) hydrolysis activity as compared to the wild type enzyme, but the alanine mutant was substantially impaired. The loss of activity with the alanine mutant is not due to any alteration in the three-dimensional fold of the enzyme. Considering the distance of this tryptophan residue from G76 of ubiquitin (>5 Å), this observation suggests that W55 may be involved in binding to the AMC portion of the Ub-AMC substrate, which may indicate that it makes contact with the isopeptide moiety in ubiquitin-linked substrates. This has been further investigated using UCHL3 as a model.

3.2 Introduction

Uch37 is a member of the ubiquitin carboxyl terminal hydrolase family. It is the only member of the family that has been found to be a resident of the proteasome. Uch37 binds to the 19s cap through an interaction at its C-terminus with the C-terminus of Rpn13 [2]. It is believed that this interaction activates Uch37 for cleavage of polyubiquitin chains by relieving the auto inhibition of the active site by helix 9, though this has yet to be experimentally proven [3, 4]. However this interaction provides additional ubiquitin binding sites that may contribute to the effectiveness of Uch37 cleaving polyubiquitin chains. Uch37 has not shown to be activated unless it is bound to the 19S proteasome cap. At the proteasome Uch37 takes the role of chain as it process polyubiquitin chains at the distal end. Ubiquitin carboxyl terminal hydrolase (UCH) enzymes release small peptide and protein leaving groups from the C-terminus of ubiquitin . Although the interaction with ubiquitin is fairly well understood in these enzymes, recognition of the isopeptide moiety of the substrate at the active site has not been well characterized. It was recently found that the tryptophan residue (Trp55) of TsUCH37 which is near the active site was in a particular confirmation that suggested it may interact with the isopeptide bond between ubiquitin and its linked substrates [5].

The crystal structure of TsUCH37 (*T.* spiralis) bound to the suicide substrate, UbVMe, reveals a conserved tryptophan residue that may play a role in stabilizing the isopeptide linkage in the active site [5]. Considering the distance of this tryptophan residue from G76 of ubiquitin (>5 Å), this observation suggests that W55 may make contact with the isopeptide moiety in ubiquitin-linked substrates and have a role in ubiquitin binding or substrate release. We found this interaction to be very intriguing, as

it made us wonder the significance of this individual residue. We hoped to identify if this tryptophan assists with monoubiquitin binding or does it have an effect on the ability of Uch37 to cleave ubiquitin bound substrates. It has been further suggested that the Trp55 residue may provide important contacts with the isopeptide link, properly positioning for cleavage at the active site [5].

3.3 Materials and Methods

Mutagenesis primers were ordered from Sigma Aldrich for Uch37(1-240) W58A and W58F. Using a Bioneer mutagenesis kit the mutagenesis was performed using standard parameters on the PCR thermocycler. After PCR thermocylcling was compete the resulting mixtures were treated with the DPN1 enzyme to remove methylated parental DNA. The resulting mutagenesis reaction was transformed using Rosetta cells and plated overnight in a 37˚C incubator. The resulting plate produced a number of colonies. The mutant DNA was extracted using a mini-prep purification kit. The mutant DNA was submitted for sequencing to the Purdue Genomics Facility. The sequence results confirmed each mutation was successful (figure 3.2, 3.3, 3.4). The resulting DNA was transformed into Rosetta Component Cells.

3.3.1 Mutagenesis, Protein Expression and Purification

A 75 mL starter culture of Lennox broth (LB) inoculated with 100 $\mu g/mL$ Ampicillin and Escherichia coli cells containing the desired protein construct. This culture was incubated at 37℃ with vigorus shaking overnight. The next day 6 x 1L of LB media was

inoculated with 100 $\mu g/mL$ Ampicilin and 8 mls of the starter culture. The 6L cultures were grown to an optical density ($O.D._{\lambda=600nm}$) = 0.400 and then induced with 1.0 mM isopropyl B-D-1-thiogalactopyranoside (IPTG). The cultures were then allowed to grow overnight at 18°C.

Cells were harvested by centrifugation at 7000 x g for 10 minutes and resuspended in 60 mL of 1 X PBS buffer (phosphate-buffered saline plus 400 mM KCl). The cells were then lysed by French press at 1,000 psi after incubating for 30 minutes with approximately 600 mg of Lysozyme. The pressed cells were then centrifuged at 1200 rpm (30,000 x g) to pellet the cell debris. The supernatant collected was then loaded on to a GSTPrep FF 16/10 glutathione sepharose affinity column, equilibrated with the 1 X PBS solution, at a flow rate of 1ml/min. The column was then washed with the 60 ml of 1 X PBS buffer plus 400 mM KCl to remove non-specific binding elements. The desired protein was eluted with approximately 30 ml of elution buffer (250 mM Tris•HCL, 500 mM KCl, 10 mM reduced glutathione, pH 8.0). About 500 units of PreScission Protease, a 47 kDa protein that recognizes and cleaves GST region of the protein between a Gln and Gly residues, was added to the eluted solution (citation needed GE website). This results in free GST (26 kDa) and free protein containing plus GPLGS peptide on the N-terminal. The solution was dialyzed overnight at 4°C in a 1 X PBS buffer plus 400 mM KCl, to allow for sufficient cleavage of the GST tag. The solution was then loaded on to the GSTPrep FF 16/10 glutathione sepharose affinity column allowing the GST free protein to pass through the column while the cleaved GST stays bound in a process called GST subtraction. Fractions were taken from each step of the purification process and run on an SDS PAGE Gel for successful verification of the

isolated protein of interest. The protein was then concentrated by centrifugation to 4 ml, filtered through a .25 micron syringe filter and loaded onto an S75 gel filtration column on an Akta protein purification system (GE Healthcare Life) with a running buffer of 50 mM Tris-HCL 50 mM NaCl and 1 mM DTT (pH 7.4). The protein was collected in 2 ml fractions. An SDS PAGE Gel was run on the collected fractions to quantify were the protein eluted. The fractions containing the most concentrated eluted protein was then pooled and concentrated to around 2 ml. A small sample of protein taken for concentration measurement and the rest was aliquoted into 100 ml epindorf tubes, flash frozen in liquid nitrogen, and stored in -80˚C Ultra Freezer.

3.3.2 Kinetic Analysis of Oxyanion Mutants

Each of the hUCH37 (hUch37N240 WT, hUch37N240 W58A and hUch37N240 W58F) and UCHL3 (UCHL3 and UCHL3 I58A) enzymes were diluted in assay reaction buffer (50 mM Tris pH 7.6, 0.5 mM EDTA, 0.1% BSA, 5 mM DTT) so the final concentration in the reaction is the following: Uch37N240 WT (1 nM), Uch37N240 W58A (1 nM), Uch37(N240)W58F (1 Nm), UCHL3 (50 pM), UCHL3 I58A (50 pM). Enzymes were added to a 96-well plate and incubated at 30°C for 5 min prior to addition of Ub-AMC diluted in assay reaction buffer to initiate the reaction. Rates of Ub-AMC cleavage were monitored with an excitation λ = 380 nm and an emission λ = 465 nm at 30°C.

3.3.3 Circular Dichroism

Each of the hUCH37 (hUch37N240 WT, hUch37N240 W58A and hUch37N240 W58F) were buffer exchanged into 1 X PBS buffer pH 7.4, to remove all traces of Tris HCL which absorbs strongly at 210 nm. Each protein was diluted to the final following concentrations: Uch37N240 WT (5 nM), Uch37N240 W58A (5 nM), Uch37N240 W58F (5 nM). CD spectra were obtained using a wavelength scan on a JASCO J-810 spectrophotometer. Scans were conducted in the region of 260 to 190 nm. Scans were corrected for blank and raw data converted to molar ellipticity.

3.3.4 Isothermal Titration Calorimetry

All solutions were dialyzed against 50 mM Tris-HCl 1mM TCEP. In the titration of hUCH37N240 (WT) and ubiquitin, ubiquitin was diluted in buffer to 10 mM in syringe. hUCH37N240 (WT) was at a diluted to a concentration of 200 uM in cell. In the titration of UCH37-RPN13N268 complex and Ubiquitin, the complex was diluted to a concentration of 100 uM in cell. Ubiquitin was diluted in buffer to 2 mM in syringe. In the titration of hUCHL3 (WT) and ubiquitin and hUCHL3 I58A, ubiquitin was diluted in buffer to 500 μM in syringe. Both hUCHL3 (WT) and hUCHL3 I58A were diluted to a concentration of 59 μM for each titration. All ITC experiments were carried out by titrating free ubiquitin in syringe into the cell containing the respective UCH enzyme. Data was analyzed and fitted to a one-site binding model corresponding to a single site binding free ubiquitin to the perspective UCH enzyme being tested. Binding isotherm plots were produce from the integration of the heat of release vs. time for each ubiquitin-enzyme pair.

3.4 Results

3.4.1 hUCH37N240 W58A and hUCH37N240 W58F

The tryptophan (55) residue of TsUCH37 was observed to make contact with the OMe group, in the structurally characterized, TsUCH37^{cat}-UBVME which suggest an important contact with the hydrocarbon area of the isopeptide bond of an actual ubiquitin attached substrate [1]. We mutated this tryptophan (58) residue, conserved in all UCH37 homologs, in hUCH37 to alanine and phenylalanine to test whether this contact is important for substrate binding or ubiquitin interaction with UCH37. The result was that the UCH37 enzyme showed no difference in Ub-AMC release between the hUCH37(1-240) (wild-type) and the W58F mutant. This comes as no surprise because the phenylalanine (F) mutation was a hydrophobic and structurally conservative mutation from the tryptophan (W) of that position and no change was expected. However, the non-conservative mutation of W58A, gave a significant decrease in UCH37 ability to hydrolyze the Ub-AMC in comparison to the truncated wild-type and W58F mutation as revealed in figure 3.5. We attempted to quantify this change using Isothermal Calorimetry measurements of the hUCH37N240 (WT) and hUCH37N240 W58A. ITC of the hUCH37N240 showed a very weak interaction with ubiquitin because it was outside of the K_D of the ITC ($K_D \leq 1$ mM) and is estimated to be near 10.5 mM. ITC of the mutant hUCH37N240 W58A was not performed because the due to the WT protein not showing measurable binding to ubiquitin. We decided instead to measure the K_D of UCH37-RPN13N268 complex. This is because previous literature indicates that UCH37 has an increased affinity to ubiquitin when in complex with Rpn13, a resident of the

proteasome [5]. The ITC measurement of the complex also proved to be just outside of the range of the instrument and is estimated to be a K_D: 1.6 ± 0.7 mM. So ITC proved to be not a conclusive way to determine whether the tryptophan mutation affects ubiquitin binding to hUCH37.

3.4.2 UCHL3I28A

The tryptophan of the hUCH37 is conserved in and other homologs [5]. However sequence alignment of the UCH family as seen in figure 3.1 shows an isoleucine present in a similar position in UCHL3. We decided to test whether mutation to alanine would have the same effect as witnessed in hUCH37. Also UCHL3 provides an excellent model substrate because of its high affinity to ubiquitin. However, we observed that this mutation had almost no effect on UCHL3 ability to catalyze Ub-AMC as seen in figure 3.11. Similarly, analysis of the ITC data (figure 3.12) indicates that UCHL3 wild type protein and UCHL3I28A bind ubiquitin with dissociation constants (K_D) of 669 ± 60 nM and 456 ± 62 nM, respectively. We interpret from this that this isoleucine has no significant impact in ubiquitin binding or AMC release.

3.5 Discussion

We sought to determine the contribution the role of the conserved tryptophan found near the active site of hUCH37N240. Through site-directed mutagenesis, the tryptophan residue, the equivalent residue in human UCH37, W58, was mutated to alanine and phenylalanine. The phenylalanine mutant retained most of its ubiquitin-AMC (Ub-AMC) hydrolysis activity as compared to the wild type enzyme, but the alanine mutant was

substantially impaired. The loss of activity with the alanine mutant is not due to any alteration in the three-dimensional fold of the enzyme. Considering the distance of this tryptophan residue from G76 of ubiquitin (>5 Å), this observation suggests that W55 may be involved in binding to the AMC portion of the Ub-AMC substrate, which may indicate that it makes contact with the isopeptide moiety in ubiquitin-linked substrates. UCHL3, another structurally characterized member of the UCH family and excellent model DUB, was also studied by mutating the isoleucine, analogous to hUCH37 tryptophan, in order to assess the contribution to the isopeptide link near the active site. UB-AMC deubiquination assays show there is a significant loss of activity in the UCH37 W58A mutant enzymes compared to its wild-type counterparts. However, no effect was observed in the same assay with UCHL3 I58A and UCHL3 wild-type. ITC analysis indicates that UCH37 does not tightly bind ubiquitin. We tested UCH37, UCH37 W58A, and UCH37-RPN13N268 complex but not able to observe appreciable binding to mono-ubiquitin. We can reasonably determine that the tryptophan does have an appreciable impact on hUCH37 ability to cleave ubiquitnated substrates based on the Ub-AMC experimental results. It would be reasonable to assume that this interaction is with the isopeptide bond and substrate and not with ubiquitin binding just based on distance (> 5 Å). What we also can determine is that this interaction is not seen in UCHL3 and based on structural similarity we can also rule out this effect in UCHL1. However, at this time we are not able to experimentally rule out its effect on ubiquitin binding.

3.6 References

1. Yao T, Song L, Xu W, DeMartino GN, Florens L, Swanson SK, et al. Proteasome recruitment and activation of the Uch37 deubiquitinating enzyme by Adrm1. Nat Cell Biol. 2006;8(9):994-1002. doi: 10.1038/ncb1460. PubMed PMID: 16906146.

2. Burgie SE, Bingman CA, Soni AB, Phillips GN, Jr. Structural characterization of human Uch37. Proteins. 2012;80(2):649-54. doi: 10.1002/prot.23147. PubMed PMID: 21953935; PubMed Central PMCID: PMC3251636.

3. Amerik AY, Hochstrasser M. Mechanism and function of deubiquitinating enzymes. Biochim Biophys Acta. 2004;1695(1-3):189-207. Epub 2004/12/02. doi: S0167-4889(04)00253-8 [pii]

10.1016/j.bbamcr.2004.10.003 [doi]. PubMed PMID: 15571815.

4. Dang LC, Melandri FD, Stein RL. Kinetic and mechanistic studies on the hydrolysis of ubiquitin C-terminal 7-amido-4-methylcoumarin by deubiquitinating enzymes. Biochemistry. 1998;37(7):1868-79. Epub 1998/03/04. doi: 10.1021/bi9723360

bi9723360 [pii]. PubMed PMID: 9485312.

5. Morrow ME, Kim MI, Ronau JA, Sheedlo MJ, White RR, Chaney J, et al. Stabilization of an unusual salt bridge in ubiquitin by the extra C-terminal domain of the proteasome-associated deubiquitinase UCH37 as a mechanism of its exo specificity. Biochemistry. 2013;52(20):3564-78. Epub 2013/04/27. doi: 10.1021/bi4003106. PubMed PMID: 23617878; PubMed Central PMCID: PMC3898853.

6. Lander GC, Estrin E, Matyskiela ME, Bashore C, Nogales E, Martin A. Complete subunit architecture of the proteasome regulatory particle. Nature. 2012;482(7384):186-91. doi: 10.1038/nature10774. PubMed PMID: 22237024; PubMed Central PMCID: PMC3285539.

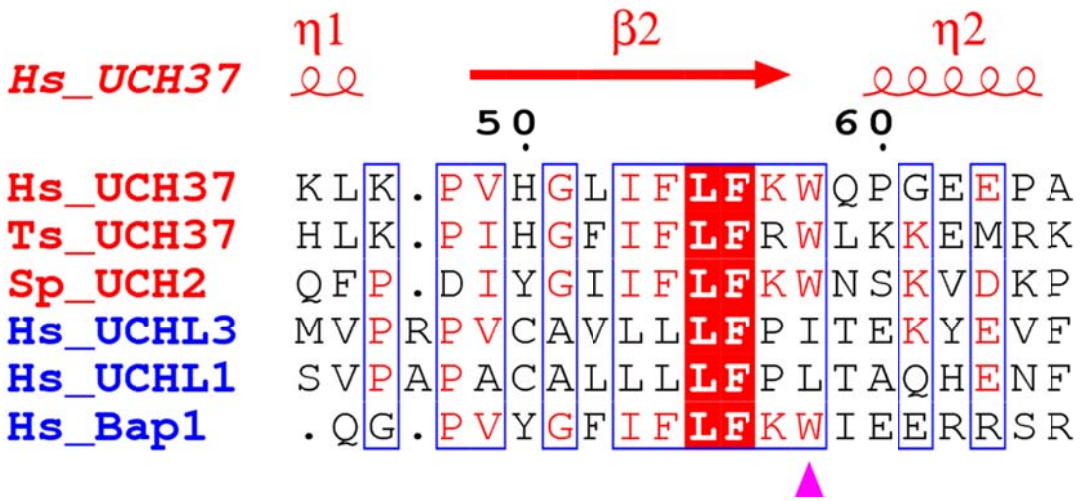

Figure 3.1: Sequence comparison of UCH37 enzymes (red) and other UCH members (blue) from residues 45-65 (human UCH37 numbering). Trptophan is conserved UCH37 and Hs_Bap1

```
                                  10         20         30
                          ....|....| ....|....| ....|....| ....
L5cat W58A        1       MXGMXGDWCI LAREXGVLTE LIKGFGCRGA QVEE
L5cat (1-240)     1       MTGNAGEWCL MESDPGVFTE LIKGFGCRGA QVEE

                                  60         70         80
                          ....|....| ....|....| ....|....| ....
L5cat W58A        51      GLIFLFKAQP GEEPAGSVVQ DSRLDTIFFA KQVI
L5cat (1-240)     51      GLIFLFKWQP GEEPAGSVVQ DSRLDTIFFA KQVI

                                 110        120        130
                          ....|....| ....|....| ....|....| ....
L5cat W58A        101     THQDVHLGET LSEFKEFSQS FDAAMKGLAL SNSD
L5cat (1-240)     101     THQDVHLGET LSEFKEFSQS FDAAMKGLAL SNSD

                                 160        170        180
                          ....|....| ....|....| ....|....| ....
L5cat W58A        151     FDTKTSAKEE DAFHFVSYVP VNGRLYELDG LREG
L5cat (1-240)     151     FDTKTSAKEE DAFHFVSYVP VNGRLYELDG LREG

                                 210        220        230
                          ....|....| ....|....| ....|....| ....
L5cat W58A        201     RPVIEKRIQK YSEGEIRFNL MAIVSDRKMI YEQK
L5cat (1-240)     201     RPVIEKRIQK YSEGEIRFNL MAIVSDRKMI YEQK
```

Figure 3.2 Sequencing results verifying the mutation of L5cat W58A (UCH37N240 W58A)

```
                                10         20         30
                        ....|....| ....|....| ....|....| ....
L5cat (1-240)     1     MTGNAGEWCL MESDPGVFTE LIKGFGCRGA QVEE
L5catW58F         1     MTGNAGEWCL MESDPGVFTE LIKGFGCRGA QVEE

                                60         70         80
                        ....|....| ....|....| ....|....| ....
L5cat (1-240)    51     GLIFLFKWQP GEEPAGSVVQ DSRLDTIFFA KQVI
L5catW58F        51     GLIFLFKFQP GEEPAGSVVQ DSRLDTIFFA KQVI

                               110        120        130
                        ....|....| ....|....| ....|....| ....
L5cat (1-240)   101     THQDVHLGET LSEFKEFSQS FDAAMKGLAL SNSD
L5catW58F       101     THQDVHLGET LSEFKEFSQS FDAAMKGLAL SNSD
```

Figure 3.3 Sequencing results verifying the mutation of L5cat W58F (UCH37N240 W58F)

```
                    10         20         30         40         50         60
            ....|....| ....|....| ....|....| ....|....| ....|....| ....|....|
UCHL3    1  MEGQRWLPLE ANPEVTNQFL KQLGLHPNWQ FVDVYGMDPE LLSMVPRPVC AVLLLFPITE  60
L3I58A   1  MEGQRWLPLE ANPEVTNQFL KQLGLHPNWQ FVDVYGMDPE LLSMVPRPVC AVLLLFPATE  60

                    70         80         90        100        110        120
            ....|....| ....|....| ....|....| ....|....| ....|....| ....|....|
UCHL3   61  KYEVFRTEEE EKIKSQGQDV TSSVYFMKQT ISNACGTIGL IHAIANNKDK MHFESGSTLK  120
L3I58A  61  KYEVFRTEEE EKIKSQGQDV TSSVYFMKQT ISNACGTIGL IHAIANNKDK MHFESGSTLK  120

                   130        140        150        160        170        180
            ....|....| ....|....| ....|....| ....|....| ....|....| ....|....|
UCHL3  121  KFLEESVSMS PEERARYLEN YDAIRVTHET SAHEGQTEAP SIDEKVDLHF IALVHVDGHL  180
L3I58A 121  KFLEESVSMS PEERARYLEN YDAIRATHET SAHEGQTEAP SIDEKVDLHF IALVHVDGHL  180

                   190        200        210        220        230        240
            ....|....| ....|....| ....|....| ....|....| ....|....| ....|....|
UCHL3  181  YELDGRKPFP INHGETSDET LLEDAIEVCK KFMERDPDEL RFNAIALSAA *           231
L3I58A 181  YELDGRKPFP INHGETSDET LLEDAIEVCK KFMERDPDEL RFNAIALSAA *LERPHRD*L  240
```

Figure 3.4 Sequencing results verifying the mutation of L3 I58A (hUCHL3 I58A)

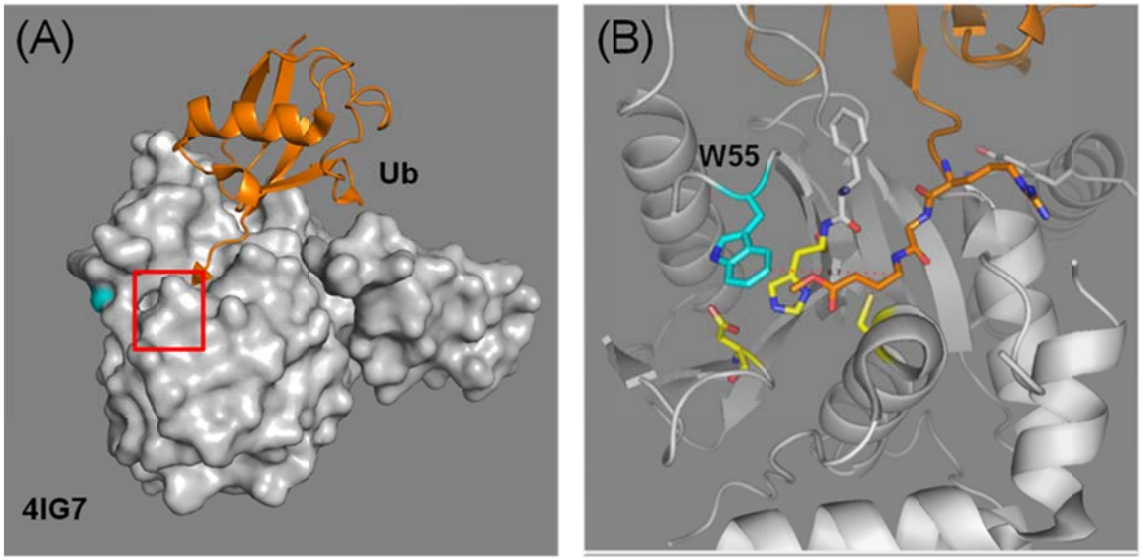

Figure 3.5: (A) The crystal structure of *Trichinella spiralis* UCH37 (gray) bound to the suicide substrate, UbVMe (orange), revealed insights into how the isopeptide bond of a ubiquitinated substrate may be stabilized at the active site (red box). (B) A conserved tryptophan (W55) may play a significant role in stabilizing the isopeptide bond in the active site. The distance (8.7 Å) between W55 (cyan) and ubiquitin G76 (orange) is too great for an interaction with the bound distal Ub, however the lysine side chain of a substrate or proximal Ub could be stabilized by W55 [6].

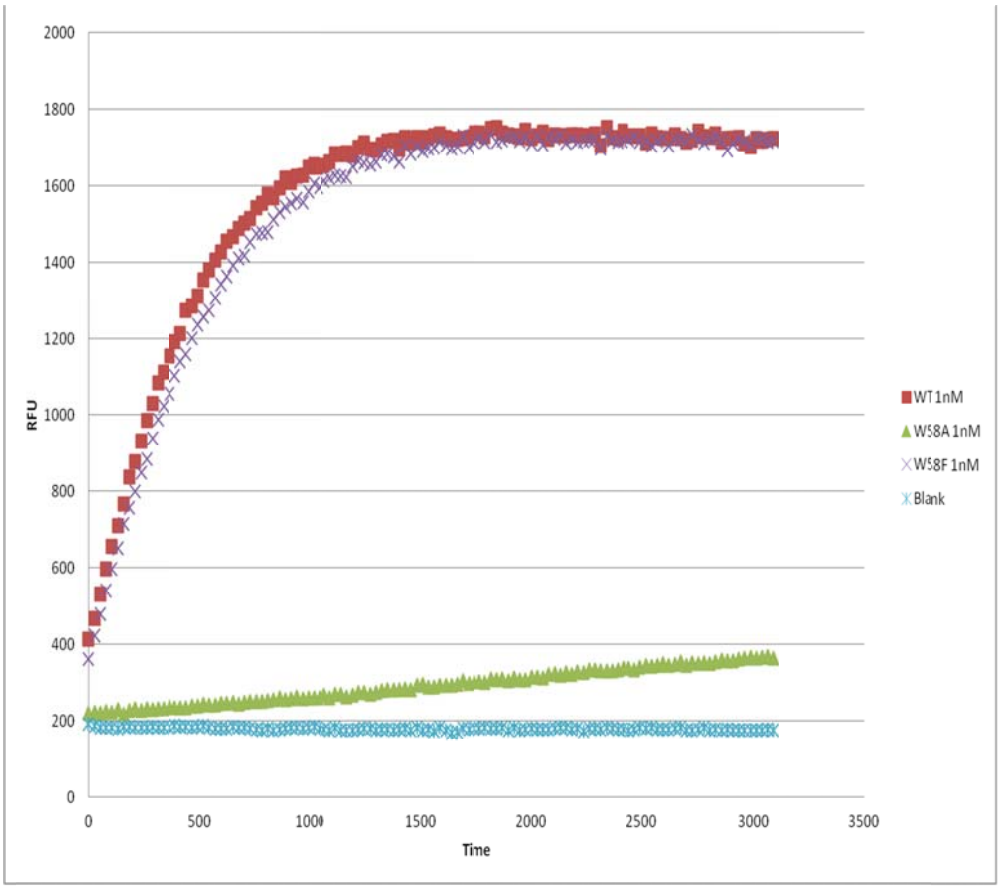

Figure 3.6: Tryptophan to alanine mutant (W58A) in hUCH37N240 shows impaired catalysis suggesting that the active site tryptophan plays a role in Ub-AMC hydrolysis, while the phenylalanine mutant (W58F) confers the same Ub-AMC activity as wild type (WT).

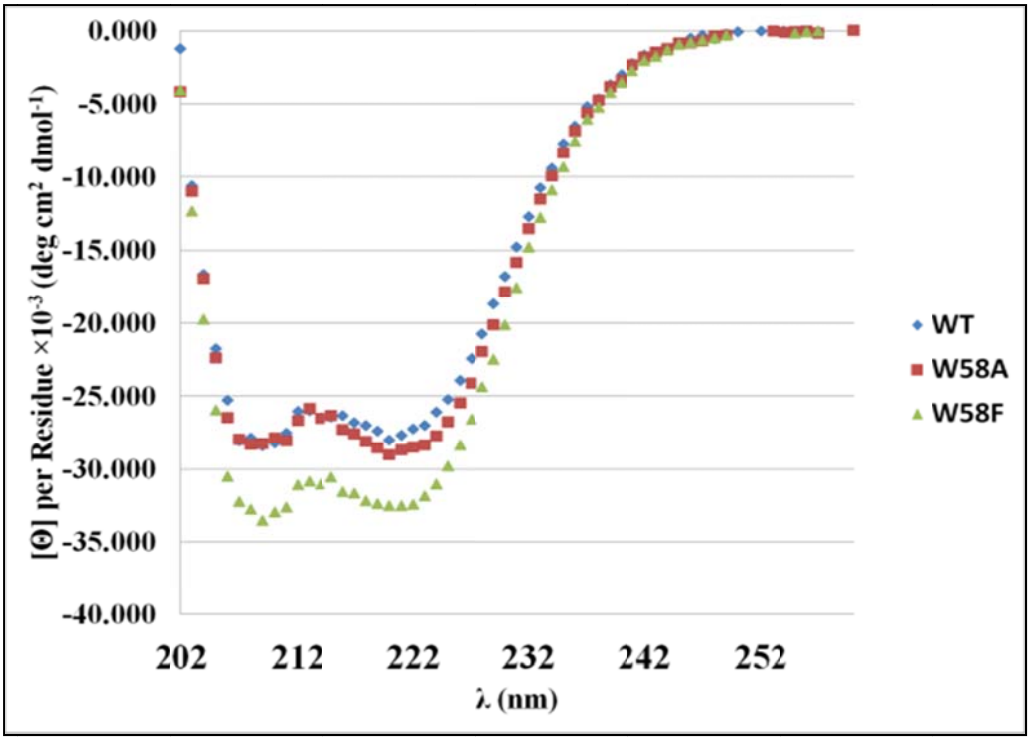

Figure 3.7: Far UV C.D. spectrum for hUCH37 WT, hUCH37 W58A, and hUCH37 W58F reveals the mutations cause no structural perturbations.

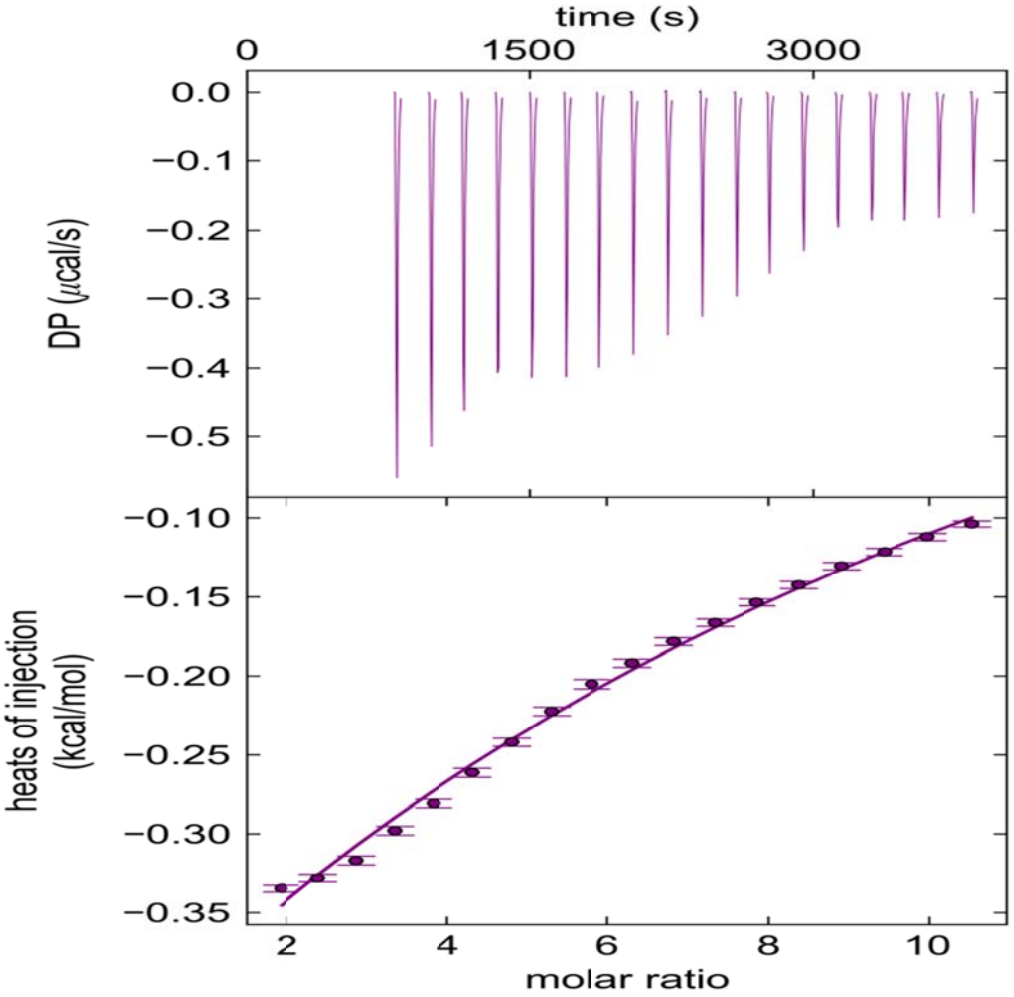

Figure 3.8: ITC analysis of hUCH37N240 (WT) showed very weak interaction with ubiquitin K_D: 10.5 ± 5.1 mM.

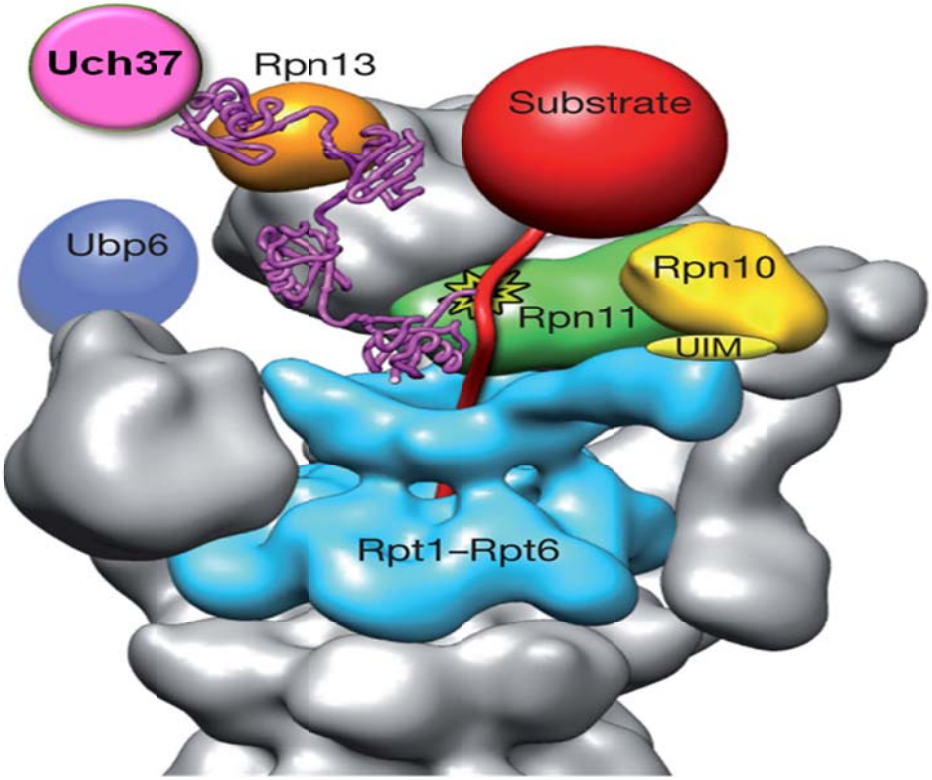

Figure 3.9: UCH37 resides in the 19S cap of the proteasome and its DUB activity is known to be activated by association with Rpn13[1]

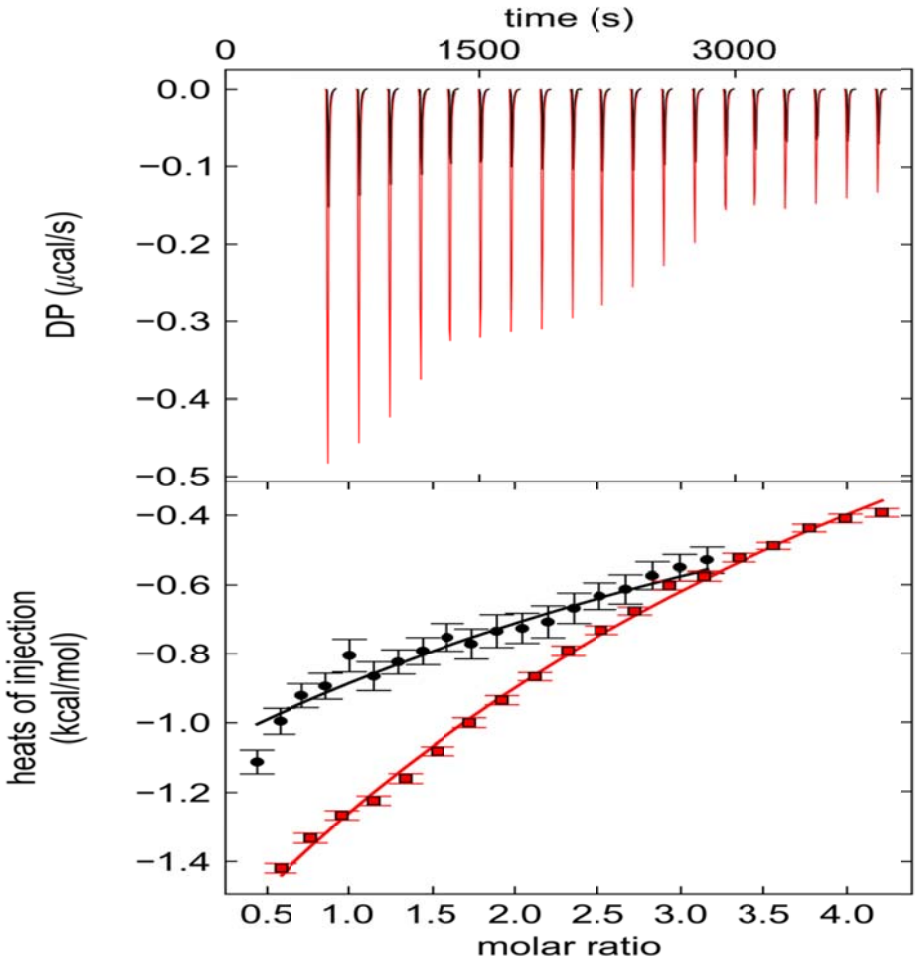

Figure 3.10: ITC analysis of the UCH37-RPN13N268 complex showed a weak interaction with ubiquitin, K_D: 1.6 ± 0.7 mM.

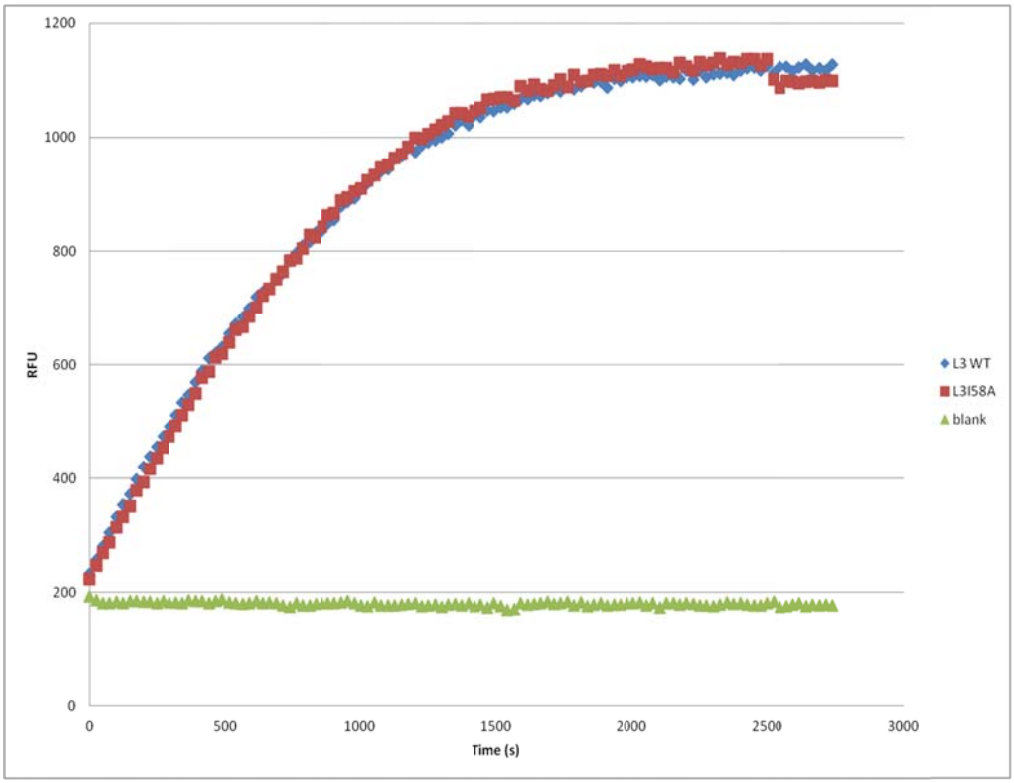

Figure 3.11: Isoleucine to alanine mutation (I58A) in hUCHL3 shows no change in catalysis, suggesting that this residue is not involved in Ub-AMC catalysis.

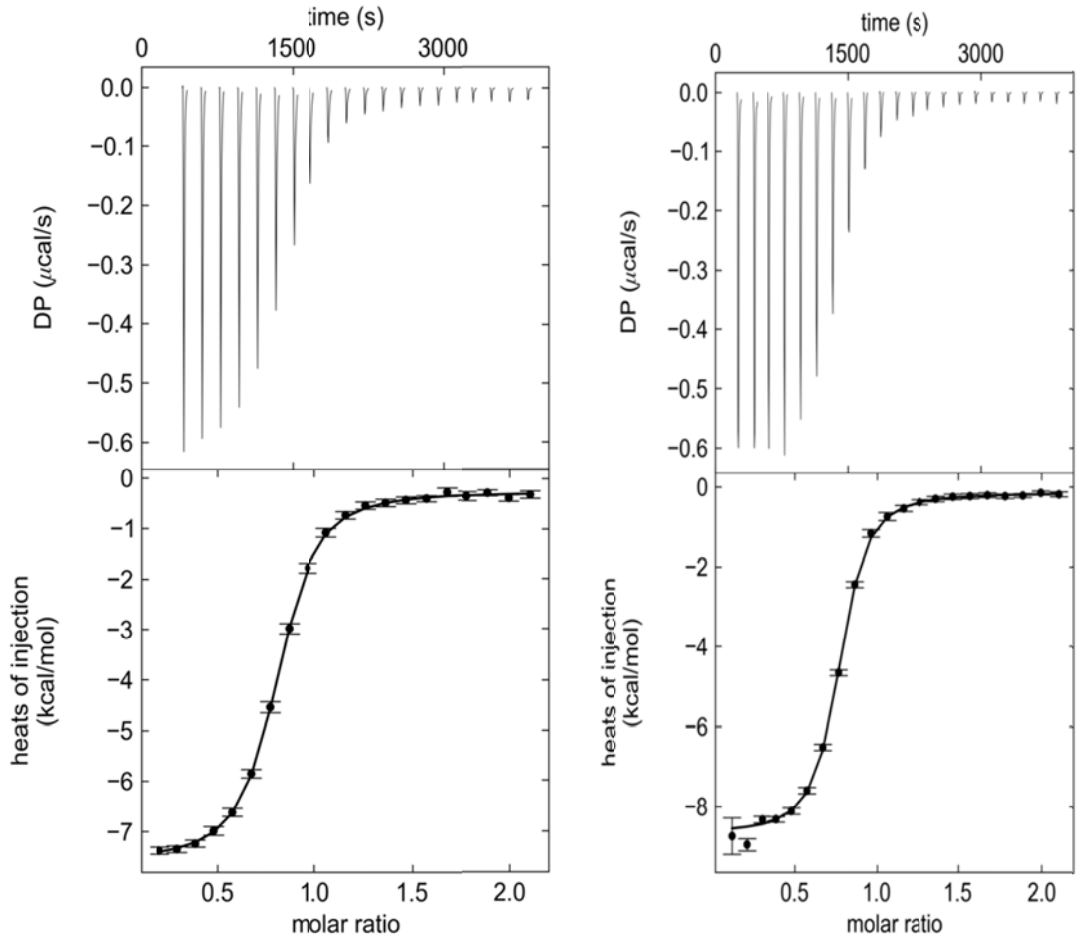

Figure 3.12: ITC analysis of (A) hUCHL3 and (B) the I58A mutant showed no change in Ub affinity K_D's= 669 ± 60 nM and 456 ± 62 nM, respectively.

CHAPTER 4: C—H•••O HYDROGEN BONDS IN CYSTEINE PROTEASES

4.1 Abstract

Cysteine proteases have been extensively studied for their importance in a wide variety of biological processes such as apoptosis (Caspases), regulated proteolysis (ubiquitin hydrolases), and calcium signaling (Calpains). The mechanism of these proteolytic enzymes is relatively well known: it involves a catalytic diad of a cysteine-histidine pair, or a triad with additional help of either an aspartic acid or asparagine. An analysis of structurally characterized cysteine proteases found in Merops Database reveals the presence of a close contact between the catalytic (His)C_{ε} and, most often, the O=C_{δ} of the putative oxyanion hole residue glutamine or a backbone carbonyl oxygen. This contact follows the requirements of a C-H---O hydrogen bond as previously reported for serine proteases (1). We speculate that this C-H---O interaction may play a role in the catalysis by either altering the pKa of the general- base His and/or by keeping the oxyanion-stabilizing side chain in a productive orientation. Upon further analysis, we found that the oxyanion-stabilizing side chain, glutamine of ubiquitin carboxyl terminal hydrolases are engaged in a C—H•••O hydrogen-bonding interaction with the catalytic histidine, a feature that is common in most cysteine proteases, including papain, belonging to families with the QCH(N/D) type of active-site configuration. It is possible that removal of the glutamine side chain might have abolished this interaction, which

typically accounts for 2 kcal/mol of stabilization, leading to an effect on catalysis observed here. We investigated this further by making an additional mutation of the glutamine to glutamic acid and lysine in UCHL3.

4.2 Introduction

C—H•••O hydrogen bonds have generally been identified by Taylor and Kenard[2] where a carbon is directly adjacent to a neutral or positively charged nitrogen, having an electron withdrawing effect. The result is that the carbon is more acidic and willing to donate its proton to a ready proton acceptor as long as the stereochemistry of the protein allows for it. It has been estimated that energy of this bond is 2.5 to 3.5 kcal/mol in vaccuo [3]. In recent years several studies have identified C—H•••O hydrogen bonds as having an important role in the stabilization of transmembrane helices[4], β sheets[5] and Schellman motifs[6]. However the role of this weak hydrogen bond in the activation of proteins is still not fully understood.

C—H•••O hydrogen bonds have also been identified in the active sites of serine protease.[7] Derewenda et al. surmise that the significance of the C—H•••O hydrogen bond is to provide an even charge distribution in the imidazole ring of histidine leading to the deprotonation of the $N_{\varepsilon 2}$ during the cleavage step of acylation and deacylation of the enzyme[7]. Also that the bonds role is not necessary for stabilization of the imidazole ring because of the observed preferred trans conformation[7]. However, it has not been determined if these bond are present in the active sites of cysteine protease. Using generally accepted distance and angle measurements for C—H•••O hydrogen bonds in

macromolecules we have determined the presence of C—H•••O hydrogen bond in the active sites of cysteine proteases.

4.3 Materials and Methods

Using the Merops[1] a dataset of 94 non-homologous structurally characterized cysteine protease were selected. Each of their coordinate files were downloaded from the Protein Data bank[8]. A cutoff was for resolution at 3.0 Å and sequence homology of < 80 %. Hydrogen's were added to the protein database coordinate files using the reduce program of Molprobity[9]. The stereo chemistry of the C—H•••O bond was analyzed using the 4 different parameters and seen in Figure 1: C-O bond distance (D); O-H bond distance (D_H); C—H•••O angle (ζ); and H—O=C angle (ξ). Geometric parameters used in previous C—H•••O studies can be found in Table 1. The parameters as applied to this study limited the C-O bond distance (D) < 4.0Å, O-H bond distance (D_H) <2.8Å, C—H•••O angle (ζ) > 120 (°)and the H—O=C angle (ξ) was measured but no specific cutoff was set. The calculation of the bond distances and angles were calculated using Pymol[10] and recorded into a table 4.4

4.4 Results

4.4.1 C—H•••O Hydrogen Bond In Most Cysteine Protease Active Sites

An analysis of the data reveals the presence of the C—H•••O hydrogen bond in the active sites of cysteine proteases. We identified 94 structurally characterized cysteine protease using the Merops[1]. Out of the 94 just 45 (48%) examples were identified as

having a distance C—H•••O (D) of < 4.0 Å and an H—O (D_H) distance of $\leq$ 2.8 Å with an average of 3.52Å and 2.50Å respectively. Figure 3A and 3B show the relative distribution of measured distances in the structures. It reveals that a majority of the C—H•••O distances are between 3.5Å and 4.0Å. Also the H—O distances vary greatly but between 2.0Å to 2.8Å.

The C_ε-H--O (ζ) angles were also well within the defined criteria of >120^0 with an average of 156^0, while the average H—O=C (ξ) angle was 127^0. The distribution of angle measurements seen in Figure 3B and 3C are very spread out for the C_ε-H--O (ζ) angle and relatively tight for the H—O=C (ξ) angle. These values are consistent with previously identified C—H•••O hydrogen bonds as reported in previous C—H•••O analysis in literature.

The C_ε-H--O hydrogen bond may have its importance in contributing to the effect on the charge distribution of the catalytic imidazole as suggested by Derewenda et al[7]. However we also noticed that glutamine was observed to be the most frequent proton acceptor in the analysis, involved in 32 (34%) of the total 94 proteins studied and is most noted to be the member of the putative oxyanion hole of cysteine protease. Previous studies have shown the importance of the oxyanion hole for the stabilization of the tetrahedral intermediate in the cysteine reaction mechanism and how mutation at this residue contributes to the reduction in enzyme activity[11]. From its prevalence as the proton acceptor in the importance of the C-H--O interaction may be to position the glutamine for immediate stabilization of the tetrahedral intermediate. Figure 4 shows the presence of the C—H•••O hydrogen bond in UCHL3 (PDB entry **1UCH**), a notably very efficient cysteine protease. The glutamine is held in short contact with the catalytic

histidine. The CεH is approximately 2.0 Å away from the oxygen of the side-chain carbonyl group. Interestingly, this distance is less than the sum of their van der Walls radii. This distance, along with C—H•••O and H•••O=C angles of 171° and 122°, respectively, which meets the geometric criteria used for a C—H•••O hydrogen bond and therefore qualifies as a significant interaction [3, 4, 12-14]. Inspection of the active sites of UCHL1 (PDB ID: **3IFW**) (bound with ubiquitin vinylmethylester) and UCHL5N240 (PDB ID: **3RIS**) also reveals the presence of the same interaction (Table 2), suggesting that the C—H•••O hydrogen bond involving the active site histidine and glutamine is a common feature of the UCH enzymes discussed herein [6, 12, 15].

4.4.2 UCHL3 Lysine and Glutamine Mutants Activity not as Expected

In order to better understand the role of the glutamine side chain in the catalytic reaction, additional mutations converting the glutamine to either a glutamate or a lysine were carried out (Figure 6). Since results for the glutamine to alanine mutation were consistent across the three UCH enzymes tested, we limited the experiments to just UCHL3, which displayed the best geometry for the C—H•••O hydrogen bond among the UCH enzymes. Mutation of the glutamine to glutamate would allow for a stronger C—H•••O bond but would eliminate its contribution to oxyanion stabilization. Furthermore, it would introduce a negative charge that is expected to destabilize the oxyanion species. Mutation to lysine, on the other hand, would take away the possibility of the C—H•••O bond while allowing for stronger oxyanion stabilization, assuming that the side-chain NH_3^+ group of the lysine would occupy a position similar to the NH_2 group of the glutamine's side chain. As seen in the previous alanine mutants, replacing the glutamine

residue with either a glutamate or lysine lowered k_{cat}, while K_M remains relatively unchanged (Table 3). Surprisingly, the Q89E mutation resulted in only a 5-fold reduction in k_{cat} compared to the wild-type enzyme, an effect that is significantly lower than what would be expected from the combined effect of both eliminating hydrogen-bonding and introducing charge-charge repulsion between the glutamate side chain and the oxyanion. In the case of Q89K, despite our expectation that the mutation would lead to better oxyanion stabilization, we see a 15-fold loss in k_{cat}, which is roughly the value we see in the UCHL3 Q89A mutant (compare Table 3.1 with Table 2.1).

In the analysis of 94 structurally characterized cysteine proteases we have seen evidence of the C—H•••O hydrogen bond in about half of the cysteine protease that we have analyzed. 45 of the 94 exhibited C—H•••O hydrogen bond from the active site Histidine (48%)[16]. 32 cases were between the Histidine active site residue and the Glutamine oxyanion residue (34%). We speculate that this interaction gives a greater importance for the role of the oxyanion hole residue in cysteine proteases by either altering the pKa of the general- base His and/or by keeping the oxyanion-stabilizing side chain in a productive orientation. An alternative explanation of the difference in magnitude of Ub-AMC hydrolysis seen between the glutamine to alanine mutants compared to the wild-type enzymes can be made by invoking the loss of the C—H•••O contact in the mutant. Inspection of active sites of the UCH enzymes reveal that the glutamine is in short contact with the catalytic histidine, which satisfies the geometric constraints for a C—H•••O hydrogen bond. Intrigued by this, we looked at a larger dataset of QCH(N/D) type of cysteine proteases in the Merops database, which revealed most cysteine proteases, including papain, possess a conserved glutamine that is within

C—H•••O bonding distance of the catalytic histidine. It should be noted that in papain, the glutamine (Gln19) is also known to be involved in an N—H•••O hydrogen bond with the NH group of the side chain of Trp177 [17], a catalytically important side chain. This is an example of a carbonyl group simultaneously engaged in hydrogen bonding with a CH and an NH donor, a situation commonly observed among protein β-sheets, in which the backbone carbonyl groups of one strand are engaged in C—H•••O and N—H•••O hydrogen bonds with an adjacent strand's CαH and backbone NH groups, respectively [18]. However this 'bifurcated' situation does not exist in UCH enzymes, as there is no other hydrogen bond donor with accepted distance other than the imidazole group of the catalytic histidine. The observation of the C—H•••O contact presented here extends the parallels between serine and cysteine proteases. Dewerenda et al. first observed a C—H•••O contact involving the catalytic histidine and a backbone carbonyl as the hydrogen bond donor in the active site of serine proteases [12]. The possibility that such an interaction plays a role in the catalytic mechanism of cysteine proteases, as has been suggested for their serine counterparts, cannot be ruled out. Interestingly, the change in free energy of transition-state stabilization (close to 2 kcal/mol) upon mutation in our system, as well as in the case of papain, happens to be very much within the range of the strength of a C—H•••O hydrogen bond [3], [19].

The C—H•••O hydrogen bond can be thought of as an additional force that stabilizes the imidazole side chain in a productive orientation such that it acts both as a general base and a proton donor during catalysis. Additionally, the C—H•••O hydrogen bonding would serve to enhance the histidine's ability to specifically act as a general base by transferring some electron density from the glutamine carbonyl to the imidazole ring

of histidine. A stronger general base would mean a better ability to extract proton from water to activate it for nucleophilic attack, facilitating the formation of the tetrahedral transition state during deacylation (Scheme 2.1). Although different cysteine proteases would employ different mechanisms for hydrolysis, a better general-base histidine will in general contribute to efficient catalysis. However, the exact mechanism of how the active-site C—H•••O interaction may play a role in transition-state stabilization needs to be further investigated by computational work.

We conducted additional studies on UCHL3 to dissect the role of the glutamine side chain in the deubiquitination reaction. If the sole purpose of glutamine were to stabilize the oxyanion, removal of the hydrogen-bonding (N-H•••O) donor plus the placement of a negative charge would substantially destabilize the transition state, leading to an effect on k_{cat} that would be greater than the alanine mutant. Interestingly, the glutamine to glutamate mutant (with only a 5-fold decrease in k_{cat}) proved to be a better catalyst than the alanine mutant, which is inconsistent with the idea that the glutamine is acting as an oxyanion stabilizer. Instead, the data appears to support that the C—H•••O hydrogen bond contributes to catalysis. It is likely that the carboxylate side chain of glutamate in the Q89E mutant makes a stronger C—H•••O interaction with the CεH group of the catalytic histidine than the carboxamide group of glutamine resulting in a better catalyst than the wild-type protein, but this effect is compensated to some degree by the unfavorable electrostatics between the negatively charged side chain and the oxyanion. It should be noted that a previous study showed that Q19E mutation in papain resulted in an approximately 20-fold decrease in k_{cat}, to a similar level as seen in the Q19A mutant, leading the authors of that study to propose that he negative charge was

tolerated in the active site [20]. It is tempting to propose that in papain, the accommodation of the unfavorable charge in the mutant might have also been due to the compensatory effect of the C—H•••O hydrogen bond.

We then mutated the glutamine to lysine, which produced an enzyme with activity comparable to the alanine mutant. This is also surprising because lysine side chain has two components, NH groups for hydrogen bonding with the oxygen of the oxyanion, and the charge for favorable electrostatic interaction, and we expected that the combination of the two, assuming that right geometry is maintained for the N-H•••O bond, would cause better stabilization of the oxyanion than in the wild-type protein. However, this mutant showed similar level of catalytic activity as the alanine mutant, indicating that placement of positive charge near the active site does not appreciably enhance the stability of the oxyanion species, presumably because the glutamine in the wild-type enzyme was not playing a role in oxyanion stabilization. Alternatively, the longer side chain of lysine may be oriented away from the oxyanion with little interaction between the two, and therefore, the lysine mutant may not be reporting if the glutamine were stabilizing the oxyanion. On the other hand, since the Q89K mutant lacks the ability to form the C—H•••O hydrogen bond as the Q89A mutant, the reduction in $k_{cat,}$ to nearly the same extent as seen in Q89A, might reflect this deficiency.

4.5 Discussion

Earlier we have shown that the active-site glutamine in UCH enzymes contributes to rate enhancement, but the relatively modest value of transition-state stabilization is more indicative of a weaker interaction, such as the C—H•••O bond between the

glutamine and catalytic histidine, than the conventional N-H•••O type of hydrogen bond that was proposed to stabilize the oxyanion [21]. We now conclude as a result for the UCHL3 Q89K and Q89E that this active site glutamine gives all the characteristics of a C—H•••O hydrogen bond. The observation that the glutamate mutant of UCHL3 is more active than the alanine mutant suggests that the conserved glutamine is unlikely to contribute to oxyanion stabilization, rather may play a role in catalysis via the C—H•••O hydrogen bond with the catalytic histidine.

4.5 References

1. Rawlings ND, Morton FR, Barrett AJ. MEROPS: the peptidase database. Nucleic Acids Res. 2006;34(Database issue):D270-2. Epub 2005/12/31. doi: 34/suppl_1/D270 [pii]

10.1093/nar/gkj089. PubMed PMID: 16381862; PubMed Central PMCID: PMC1347452.

2. Taylor R, Kennard O. Crystallographic Evidence for the Existence of C-H...O, C-H...N, and C-H...C1 Hydrogen-Bonds. Journal of the American Chemical Society. 1982;104(19):5063-70. PubMed PMID: ISI:A1982PH54900012.

3. Scheiner S, Kar T, Gu YL. Strength of the (CH)-H-alpha center dot center dot O hydrogen bond of amino acid residues. Journal of Biological Chemistry. 2001;276(13):9832-7. PubMed PMID: ISI:000167996400035.

4. Senes A, Ubarretxena-Belandia I, Engelman DM. The C alpha-H center dot center dot center dot O hydrogen bond: A determinant of stability and specificity in transmembrane helix interactions. Proceedings of the National Academy of Sciences of the United States of America. 2001;98(16):9056-61. PubMed PMID: ISI:000170216900027.

5. Fabiola GF, Krishnaswamy S, Nagarajan V, Pattabhi V. C-H center dot center dot center dot O hydrogen bonds in beta-sheets. Acta Crystallographica Section D-Biological Crystallography. 1997;53:316-20. PubMed PMID: ISI:A1997XB25600011.

6. Madan Babu M, Kumar Singh S, Balaram P. A C-H triplebond O hydrogen bond stabilized polypeptide chain reversal motif at the C terminus of helices in proteins. J Mol Biol. 2002;322(4):871-80. Epub 2002/09/25. doi: S0022283602007155 [pii]. PubMed PMID: 12270720.

7. Derewenda ZS, Derewenda U, Kobos PM. (His)C-Epsilon-H...O=C Hydrogen-Bond in the Active-Sites of Serine Hydrolases. Journal of Molecular Biology. 1994;241(1):83-93. PubMed PMID: ISI:A1994PA94700009.

8. Bernstein FC, Koetzle TF, Williams GJB, Meyer EF, Brice MD, Rodgers JR, et al. Protein Data Bank - Computer-Based Archival File for Macromolecular Structures. Journal of Molecular Biology. 1977;112(3):535-42. PubMed PMID: ISI:A1977DK67100014.

9. Chen VB, Arendall WB, Headd JJ, Keedy DA, Immormino RM, Kapral GJ, et al. MolProbity: all-atom structure validation for macromolecular crystallography. Acta Crystallographica Section D-Biological Crystallography. 2010;66:12-21. doi: Doi 10.1107/S0907444909042073. PubMed PMID: ISI:000273758800003.

10. The PyMOL Molecular Graphics System V, Schrödinger, LLC.

11. Menard R, Carriere J, Laflamme P, Plouffe C, Khouri HE, Vernet T, et al. Contribution of the glutamine 19 side chain to transition-state stabilization in the oxyanion hole of papain. Biochemistry. 1991;30(37):8924-8. Epub 1991/09/17. PubMed PMID: 1892809.

12. Derewenda ZS, Lee L, Derewenda U. The Occurrence of C-H-Center-Dot-Center-Dot-Center-Dot-O Hydrogen-Bonds in Proteins. Journal of Molecular Biology. 1995;252(2):248-62. PubMed PMID: ISI:A1995RU75200009.

13. Steiner T. C—H•••O hydrogen bonding in crystals. Crystallography Reviews. 2003;9:177-228.

14. Desiraju GR. The C-H center dot center dot center dot O hydrogen bond: Structural implications and supramolecular design. Accounts of Chemical Research. 1996;29(9):441-9. PubMed PMID: ISI:A1996VG79600006.

15. Chakrabarti P, Chakrabarti S. C-H center dot center dot center dot O hydrogen bond involving proline residues in alpha-helices. Journal of Molecular Biology. 1998;284(4):867-73. PubMed PMID: ISI:000077467300003.

16. Rajan S, Baek K, Yoon HS. C-H...O hydrogen bonds in FK506-binding protein-ligand interactions. J Mol Recognit. 2013;26(11):550-5. doi: 10.1002/jmr.2299. PubMed PMID: 24089362.

17. Gul S, Hussain S, Thomas MP, Resmini M, Verma CS, Thomas EW, et al. Generation of nucleophilic character in the Cys25/His159 ion pair of papain involves Trp177 but not Asp158. Biochemistry. 2008;47(7):2025-35. Epub 2008/01/30. doi: 10.1021/bi702126p. PubMed PMID: 18225918.

18. Fabiola GF, Krishnaswamy S, Nagarajan V, Pattabhi V. C-H...O hydrogen bonds in beta-sheets. Acta Crystallogr D Biol Crystallogr. 1997;53(Pt 3):316-20. Epub 1997/05/01. doi: 10.1107/S0907444997000383

S0907444997000383 [pii]. PubMed PMID: 15299935.

19. Starikov EB, Steiner T. Computational support for the suggested contribution of C-H center dot center dot center dot O=C interactions to the stability of nucleic acid base pairs. Acta Crystallographica Section D-Biological Crystallography. 1997;53:345-7. PubMed PMID: ISI:A1997XB25600020.

20. Menard R, Plouffe C, Laflamme P, Vernet T, Tessier DC, Thomas DY, et al. Modification of the electrostatic environment is tolerated in the oxyanion hole of the cysteine protease papain. Biochemistry. 1995;34(2):464-71. Epub 1995/01/17. PubMed PMID: 7819238.

21. Boudreaux D, Chaney J, Maiti TK, Das C. Contribution of active site glutamine to rate enhancement in ubiquitin C-terminal hydrolases. FEBS J. 2012. Epub 2012/01/31. doi: 10.1111/j.1742-4658.2012.08507.x. PubMed PMID: 22284438.

22. Steiner T. Effect of Acceptor Strength on C-H...O Hydrogen-Bond Lengths as Revealed by and Quantified from Crystallographic Data. Journal of the Chemical Society-Chemical Communications. 1994;(20):2341-2. PubMed PMID: ISI:A1994PN86900013.

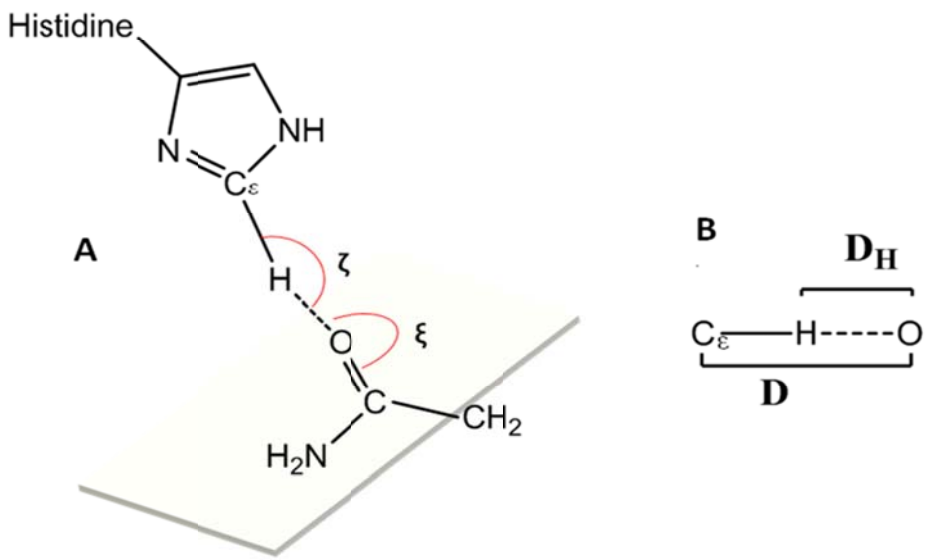

Figure 4.1: Definition of geometrical parameters A. Angular parameters. B. Distance parameters. Nomenclature according to Derewenda et al.[1]

Table 4.1: Geometric Parameters used in previous studies[6]

D (Å)	**D_H (Å)**	**C_ε-H--O (ζ) (°)**	**H—O=C (ξ) (°)**	**Reference**
≤3.5	<2.7	>120	--	[4]
--	<2.7	>90	~120	[12]
--	<2.8	>90	--	[22]
4.0-30	<2.8	>110	120-140	[14]

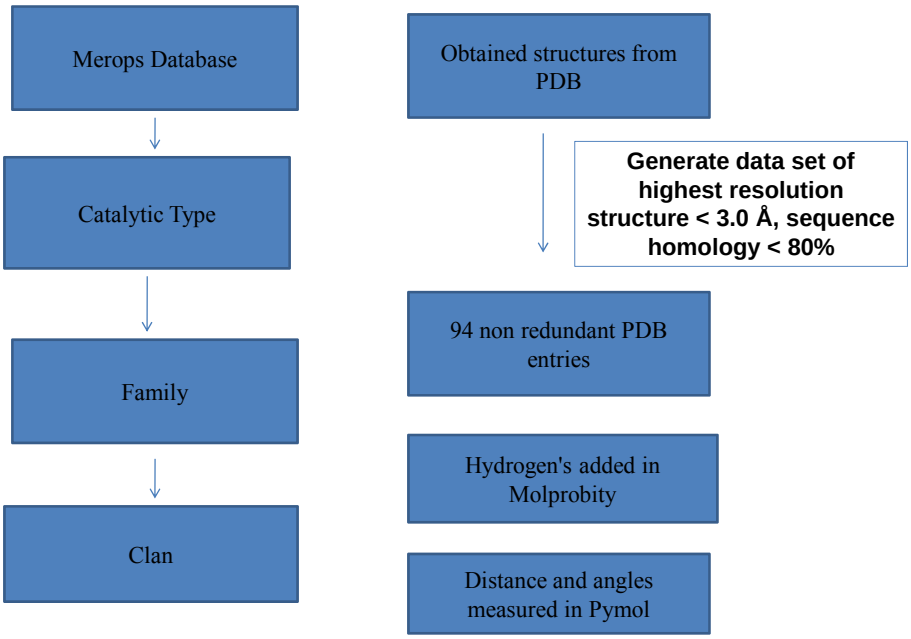

Figure 4.2: Flowchart used to create database. Structurally characterized proteins identified in the Merops Database[1] which segregates proteins by catalytic type, family's by sequence similarity, clan's by evolutionary relationship. The pdbs were downloaded from the Protein Data Bank[8]. The C—H•••O distances and angles were then measured in Pymol[10]

Table 4.2: C—H•••O hydrogen bond parameters observed in 45 of 94 structurally characterized cysteine proteases. Hydrogen bond donor and acceptor in bold. ([a])Acceptor is backbone carbonyl oxygen of W280. ([b]) Acceptor is backbone carbonyl oxygen of G24 280

Pdb ID	**Resolution (Å)**	**Active site residues**	**D (Å)**	**D_H**	**C_ε-H--O (ζ)>120 (^{0})**	**H--O-C (ξ) (^{0})**
9PAP	1.65	C25, **H159**, N175**,Q19**	3.84	2.79	158.6	115.9
1YAL	1.70	C25, **H159,** N179 ,**Q19**	3.72	2.60	172.4	125.2
1PPO	1.80	C25, **H159**, N179, **Q19**	3.69	2.68	153.0	130.4
1MDW	1.95	C105, **H262**, N286, **Q99**	2.97	1.90	164.0	128.4
1KXR	2.07	S115, **Q109**, **H272**, N296	3.23	2.30	141.7	119.0
1ZIV	2.31	C97, **H254**, N278, **Q91**	3.26[a]	2.50	128.2	139.6
3IFW	2.4	C90, **H161**, D176, **Q84**	3.71	2.79	141.6	159.1
1UCH	1.80	**C95**, H169, D184, **Q89**	3.11	2.00	171.6	122.1
2GFO	2.00	C786, **H1067**, D1085, **N781**	3.31	2.20	172.2	121.0
1VJV	1.74	C118, **H447**, N113, **N465**	3.10	2.10	147.3	102.4

Table 4.2: continued

Pdb ID	**Resolution (Å)**	**Active site residues**	**D (Å)**	**D_H**	**C_ε-H--O (ζ)>120 (^{0})**	**H--O-C (ξ) (^{0})**
1QMY	1.90	C51, **H148**, N46, A163	3.27	2.20	156.8	126.2
3K8U	1.90	C17, **H96**, A112, **Q11**	3.59	2.70	136.2	153.6
1CV8	1.75	C24, **H120**, N141, **Q18**	3.50	2.40	160.4	138.3
2CY7	1.90	C74, D278, **H280, Y54**	3.09	2.10	141.9	128.3
3DKB	2.50	C103, **H256, N98**	3.96	2.88	167.2	74.7
1Y08	1.93	C94, **H262**, D284, **D286**	3.30	2.28	153.7	88.9
2Z84	1.70	C53, **H177**, D175, **Y41**	3.62	2.75	135.5	161.2
2BU3	1.40	C70, **H183**, D201, **Q64**	3.51	2.41	179.0	150.6

Table 4.2: continued

Pdb ID	**Resolution (Å)**	**Active site residues**	**D (Å)**	**D_H**	**C_ε-H--O (ζ)>120 (^{0})**	**H--O-C (ξ) (^{0})**
3C0R	2.31	C120,**H222, D117**	3.25	2.44	128.8	127.2
3BIJ	2.50	C135, **H84**	3.14[b]	2.34	128.6	88.9
1EUV	1.60	C580,**H514**, D531,**Q574**	3.90	2.84	160.0	118.0
2CKG	2.45	C602,**H533**, D550,**Q596**	3.82	2.78	157.5	113.5
3EAY	2.40	C926,**H794**, D873,**Q920**	3.59	2.59	151.5	137.4
1XT9	2.20	C163,**H102**, D119,**Q157**	3.29	2.20	176.7	136.4
1A2Z	1.73	C143, E80, **H167**	3.72	2.82	139.7	100.8
2HWK	2.45	C477, **H546**	3.70	2.90	129.5	128.8
1GEC	2.10	C25, **H159**, Q19	3.61	2.06	179.1	150.0

Table 4.2: continued

Pdb ID	**Resolution (Å)**	**Active site residues**	**D (Å)**	**D_H**	**C_ε-H--O (ζ)>120 (^{0})**	**H--O-C (ξ) (^{0})**
1S4V	2.00	C26, **H163**, **Q20**	3.79	2.69	174.6	138.3
1EF7	2.67	C31, **H180**, N200, **Q22**	3.88	2.81	163.9	144.6
1CQD	2.10	C27, **H161**, N181, **Q21**	3.98	2.97	152.4	120.8
2FO5	2.20	C28, **H167**, N188, **Q22**	3.66	2.60	162.2	118.0
1CS8	1.80	C25, **H163**, **Q19**	3.68	2.59	168.8	131.4
1GLO	2.20	C25, **H164**, **Q19**	3.33	2.27	161.4	119.7
7PCK	3.20	C25, **H162**, **Q19**	3.48	2.38	173.9	154.1
1YVB	2.70	C25, **H159**, **Q19**	3.83	2.78	159.5	112.1
1HUC	2.10	C29,**H199**, **Q23**, N219	3.55	2.54	153.3	122.5

Table 4.2: continued

Pdb ID	**Resolution (Å)**	**Active site residues**	**D (Å)**	**D_H**	**C_ε-H--O (ζ)>120 (^{0})**	**H--O-C (ξ) (^{0})**
3BWK	2.42	C51, **H183**, N182, **Q45**	3.99	2.98	152.8	140.7
1IWD	1.63	C25, **H159**, N178, **Q19**	3.63	2.54	169.1	137.0
2BDZ	2.10	C25, **H159**, N175, **Q19**	3.57	2.49	168.8	130.2
2PNS	1.90	C25, **H157**, N173, **Q19**	2.88	2.01	132.6	101.0
3F75	1.99	C31, **H167**, N189, **Q25**	3.48	2.38	174.0	139.5
2B1M	2.00	G26, **H168**, N175	3.40	2.38	154.7	137.7
1CB5	2.59	C73, **H372**, N396, **Q67**	3.71	2.65	162.1	114.6
1GCB	2.20	C73, **H369**, N392, **Q67**	3.75	2.68	165.9	126.7
		Average	**3.52**	**2.50**	**156.1**	**127.0**

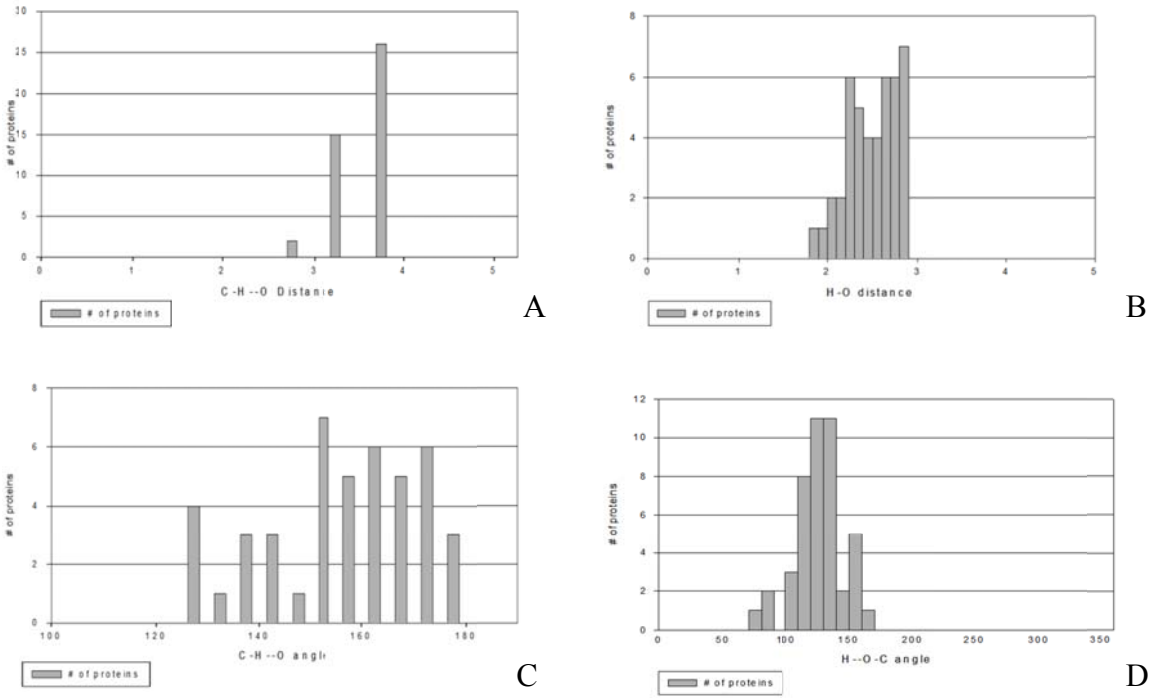

Figure 4.3: A. Distribution of distances (*D*) between the active site Histidine Cε-H—O contact of the side chain or backbone carbonyl. B. Distribution of distances (D_H) between the H—O. C. Distribution of angle between Cε-H—O (ζ). Distribution of angle between H—O=C (ξ) contact of the side chain or backbone carbonyl.

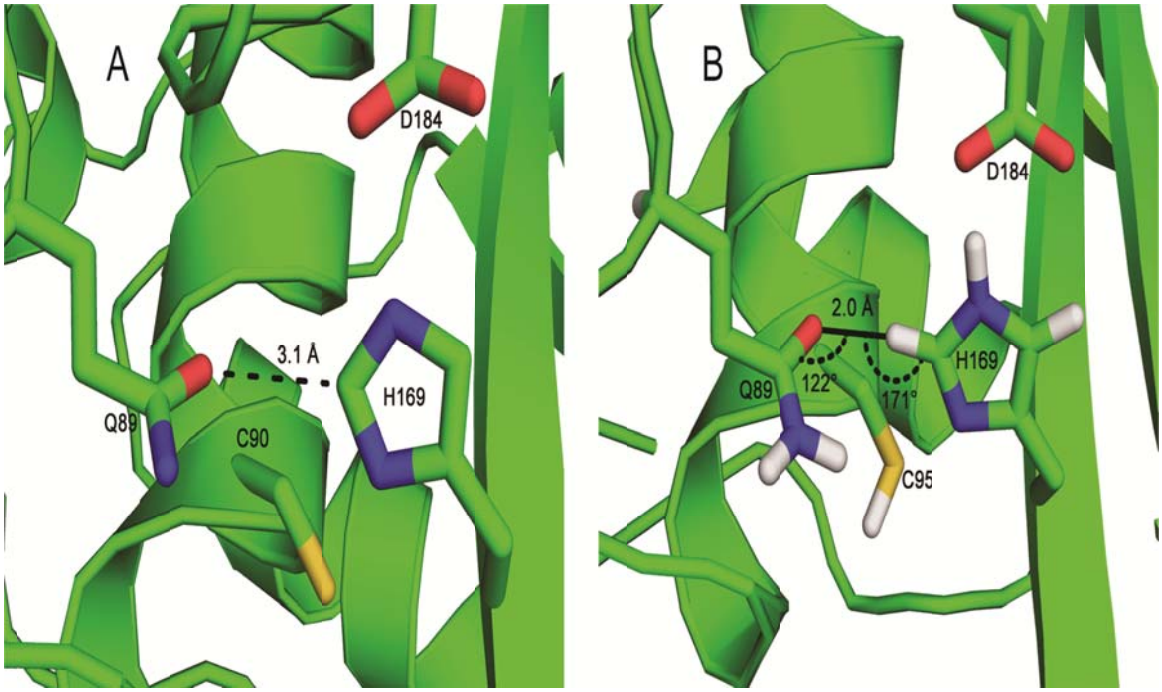

Figure 4.4: C—H•••O bonding seen in UCHL3 with the catalytic residues and the glutamine shown as sticks. (A) The D distance. (B) The D_H distance along with the ξ and ζ angles.

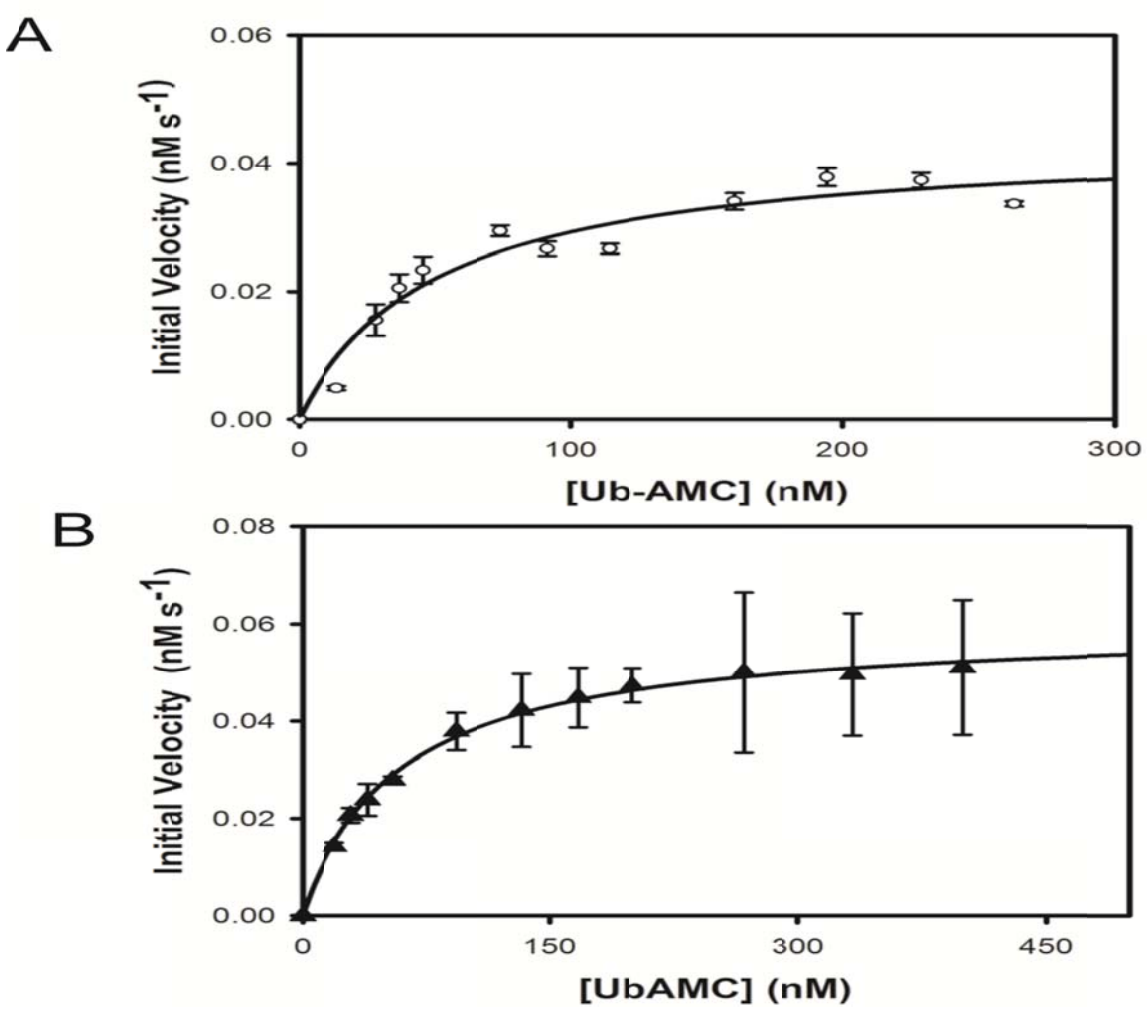

Figure 4.5: (A) Glutamine to glutamate and (B) lysine mutants in UCHL3. The glutamate mutant showed far less decrease in k_{cat}, only 5 fold . The lysine mutants were similar to the alanine mutant

Table 4.3: Kinetic Parameters for UCHL3 Glu and Lys mutants showing decrease in k_{cat}/K_M from wild type

	K_M (nM)	**k_{cat} (s^{-1})**	**$k_{cat}/K_M \times 10^4$ (M^{-1} s^{-1})**	**$\Delta\Delta G^{\neq}$ (kcal/mol)**
UCHL3 Q89E	**49.8 ± 11.0**	**3.65 ± 0.00**	**7329**	**0.72**
UCHL3 Q89K	**58.5 ± 2.9**	**1.20 ± 0.00**	**1931**	**1.51**

VITA

VITA

Joseph Rashon Chaney, Jr was born to Joseph and Janetta Chaney on December 5, 1979 in Baton Rouge, LA. He survived the mean streets of Baton Rouge by spending most of his time in school or at church. He attended Scotlandville Magnet High School in where he would graduate in 1997. Each summer of high school, Joseph attended the Timbuktu Academy at Southern University, run by his mentors Dr. Diola Bagayoko and Dr. Ella Kelly. The program gave Joseph early introduction to scientific research and his eventual college major, Chemistry. Upon graduation Joseph attended Southern University on a Timbuktu Academy scholarship. While at Southern, Joseph met the love of his life and greatest supporter, Millicent. Upon graduation, Joseph obtained a job in the Louisiana petrochemical industry as a Project Manger and Lab Technician at Dow Chemical. While at Dow, Joseph received several awards for his leadership and technical skill. In the mean time he married Millicent and had one child, Joshua. At this time he was encouraged to pursue his Ph.D. and subsequently enrolled at Purdue University. While at Purdue, Joseph and Millicent welcomed their second child, Caleb. Joseph met many wonderful people from many different cultures and backgrounds. He was also afforded the opportunity to travel to several major conferences and workshops. He would later get the opportunity to write about some of his early experiences in graduate school in a book published by the graduate school to go along with co-authoring three

publications in peer-reviewed journals. Joseph was offered a post doctoral position in Dr. Sunyoung Kim's lab at Louisiana State University Health Science Center in his wife's home city of New Orleans. He will be the first of his and his wife's family to earn a Ph.D. and hopes that his journey will encourage others to follow their dreams.

PUBLICATION

the FEBS Journal

Contribution of active site glutamine to rate enhancement in ubiquitin C-terminal hydrolases

David A. Boudreaux*, Joseph Chaney*, Tushar K. Maiti† and Chittaranjan Das

Department of Chemistry, Purdue University, West Lafayette, IN, USA

Keywords
CHO hydrogen bond; cysteine proteases; deubiquitinases; oxyanion hole; UCH enzymes

Correspondence
C. Das, Department of Chemistry, Purdue University, 560 Oval Drive, West Lafayette, IN 47906, USA
Fax: +1 765 494 0239
Tel: +1 756 494 5478
E-mail: cdas@purdue.edu

*These authors contributed equally to this work

†**Present address**
180, Udyog Vihar Phase I, Gurgaon 122016 Haryana, India

(Received 23 September 2011, revised 22 December 2011, accepted 18 January 2012)

doi:10.1111/j.1742-4658.2012.08507.x

Ubiquitin C-terminal hydrolases (UCHs) are cysteine proteases featuring a classical Cys–His–Asp catalytic triad, and also a highly conserved Gln that is thought to be a part of the oxyanion hole. However, the contribution of this side chain to catalysis by UCHs is not known. Herein, we demonstrate that the Gln side chain contributes to rate enhancement in UCHL1, UCHL3, and UCHL5. Mutation of the Gln to Ala in these enzymes impairs the catalytic efficiency, mainly because of a 16-fold to 30-fold reduction in k_{cat}, which is consistent with a loss of approximately 2 kcal·mol^{-1} in transition state stabilization. However, the contribution to transition state stabilization observed here is rather modest for the side chain's role in oxyanion stabilization. Interestingly, we discovered that the carbonyl oxygen of this side chain is engaged in a C–H···O hydrogen-bonding contact with the CεH group of the catalytic His. Upon further analysis, we found that this interaction is a common active site structural feature in most cysteine proteases, including papain, belonging to families with the QCH(N/D) type of active site configuration. It is possible that removal of the Gln side chain might have abolished the C–H···O interaction, which typically accounts for 2 kcal·mol^{-1} of stabilization, leading to the effect on catalysis observed here. Additional studies performed on UCHL3 by mutating the Gln to Glu (strong C–H···O acceptor but oxyanion destabilizer) and to Lys (strong oxyanion stabilizer but lacking C–H···O hydrogen-bonding capability) suggest that the C–H···O hydrogen bond could contribute to catalysis.

Introduction

Ubiquitin (Ub) C-terminal hydrolases (UCHs) belong to a larger group of enzymes collectively called deubiquitinases, which catalyze the hydrolysis of the peptide or isopeptide bond through which Ub is attached to other proteins or other Ub moieties in polyubiquitin chains [1–5]. The UCH family members are cysteine proteases featuring a classical Cys–His–Asp catalytic triad [6–10]. The active site of these enzymes also features a highly conserved Gln (Fig. 1), which is believed to be a part of the so-called oxyanion hole, an arrangement of spatially proximal peptide dipoles aligned in a way that creates a positively charged pocket facing the thiol group of the catalytic Cys. It is also possible that, by virtue of being located at the N-terminus of a helix, the electropositive character of this pocket is enhanced by the helix macrodipole effect [11]. In cysteine proteases, nucleophilic attack on the carbonyl group of the scissile peptide bond proceeds through a tetrahedral transition state bearing a negative charge on the oxygen atom of the carbonyl group. This negative charge is stabilized by electrostatic and hydrogen-bonding interactions with

Abbreviations
AMC, aminomethylcoumarin; PDB, Protein Data Bank; Ub, ubiquitin; Ubal, ubiquitin aldehyde; UCH, ubiquitin C-terminal hydrolase.

```
UCHL1     80 YFMKQTIGNSCGTIGLIHAVANN 102
UCHL3     85 YFMKQTISNACGTIGLIHAIANN 107
UCHL5     78 FFAKQVINNACATQAIVSVLLNC 100
BAP1      81 FFAHQLIPNSCATHALLSVLLNC 103
Yuh1      80 IWFKQSVKNACGLYAILHSLSNN 102

UCHL1    159 NFHFILFNNVDGHLYELDGRMPF 181
UCHL3    167 DLHFIALVHVDGHLYELDGRKPF 189
UCHL5    162 AFHFVSYVPVNGRLYELDGLREG 184
BAP1     167 AFHFVSYVPITGRLFELDGLKVY 189
Yuh1     164 NLHYITYVEENGGIFELDGRNLS 186
```

Fig. 1. Sequence alignment of the human UCHs and the yeast homolog Yuh1. Residues corresponding to the catalytic triad are in red, and the putative oxyanion residue is in blue.

the oxyanion hole, which are proposed to constitute one of the factors leading to the lowering of activation energy for the hydrolysis reaction [12].

The relative orientation of the carbonyl oxygen of the scissile peptide group with respect to the oxyanion-stabilizing groups, as in the tetrahedral transition state, may be approximately visualized in the crystal structure of the yeast Ub hydrolase Yuh1 bound covalently to the suicide substrate Ub aldehyde (Ubal) (Fig. 2) [13]. Attack of the catalytic thiol on Ubal results in the formation of the thiohemiacteal product, which mimics the oxyanion-bearing tetrahedral transition state (Fig. 2). As seen in Fig. 2, the hydroxyl oxygen of the thiohemiacetal moiety is within a relatively short distance from the backbone NH groups of the catalytic Cys90, Ala89 and Asn88 and the side chain NH_2 group of Gln84, the putative oxyanion-stabilizing side chain. It has been proposed that, in a general cysteine protease, the negatively charged oxygen in the tetrahedral transition state would occupy nearly the same position as the thiohemiacteal hydroxyl oxygen seen in the Yuh1–Ubal structure and would be coordinated through electrostatic and hydrogen-bonding interactions with the groups lining the oxyanion hole [13].

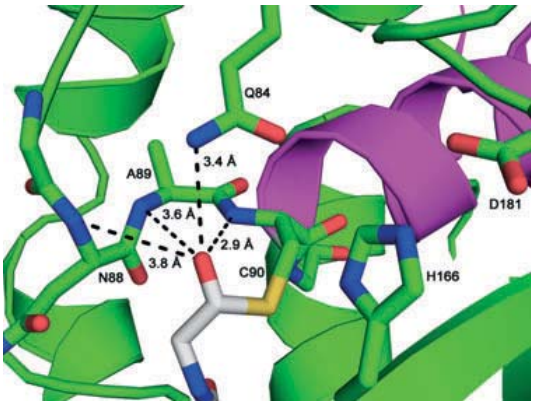

Fig. 2. Ubal (gray) covalently bound to Yuh1 (green). Hydrogen bonding distances are shown for Yuh1 residues stabilizing the thiohemiacetal hydroxyl oxygen on the aldehyde moiety. The helix of Yuh1 that may contribute to the macrodipole is in magenta.

Previous studies in papain revealed that Gln19, the oxyanion side chain in the protein, plays a role in the catalytic mechanism of the enzyme contributing to rate enhancement. Mutation of this side chain to Ala reduces the catalytic efficiency by approximately 60-fold, mostly affecting k_{cat} (20-fold lower), with a smaller change in K_m (three-fold higher) [12]. Ignoring the relatively small change in K_m, the 20-fold change in k_{cat} was attributed to a loss of the contribution of the Gln side chain to oxyanion stabilization. The catalytic Cys–His–Asp triad of structurally characterized UCHs, such as UCHL1, UCHL3, and UCHL5, adopts a similar geometric relationship as found in the Cys–His–Asn triad of papain and the triads of other papain-like cysteine proteases. Additionally, the active site Gln in UCH enzymes is located in an analogous position to Gln19 in the active site of papain. However, the role played by this side chain in catalysis by UCHs has not been studied thus far. Considering the importance of the UCH group of proteases in diseases such as Parkinson's disease and cancer, dissecting the role of active site residues in catalysis by these enzymes is an important endeavor, as it would advance our understanding of the mechanism of these enzymes [14–18]. In this study, we sought to determine the contribution to rate enhancement by the putative oxyanion-stabilizing side chain of the active site Gln by mutational analysis and comparison of the kinetic parameters with those of the wild-type proteins. This was investigated in all structurally characterized UCHs – UCHL1, UCHL3, and the catalytic domain of UCHL5 (residues 1–240, hereafter referred to as UCHL5N240) [6–10]. Breast cancer early-onset 1-associated protein 1, the remaining human UCH family member, was omitted from this study, as its crystal structure has yet to be determined.

Results

Active site Gln → Ala mutants of UCHs show significantly less activity than the wild-type enzymes

In order to determine whether the conserved Gln found in the active site of UCHs (Fig. 1) contributes to rate enhancement, hydrolysis assays with the fluorogenic substrate Ub-aminomethylcoumarin (AMC) were

conducted, with identical conditions for each enzyme and its Gln → Ala mutant. These results showed that the rate of hydrolysis leading to AMC release was significantly reduced for the mutants as compared with their wild-type counterparts (Fig. S1), suggesting a role for this side chain in contributing to rate enhancement in the catalytic mechanism of the enzymes. As Gln is located in the solvent-accessible active site of the enzymes, the mutation of this residue to Ala is not expected to cause any significant perturbation in the active site structure or gross changes in the three-dimensional fold of the protein. In fact, the CD spectra of the mutants produced patterns that were nearly identical in shape and intensity to those of their corresponding wild-type proteins (Fig. S2), confirming that the mutation has no observable structural effect in these proteins.

The reduction in catalytic activity observed upon mutation could be attributable to two possible factors: an increase in K_m, or a reduction in k_{cat}, the rate constant of the rate-determining step in the hydrolysis reaction. In order to determine which parameters are affected by the mutation, we set out to analyze the Michaelis–Menten kinetics of the mutants and the wild-type enzymes. Additional activity assays were conducted with varying substrate concentrations, and plots of the initial velocities versus substrate concentration are shown in Fig. 3. All enzymes, with the exception of UCHL5N240 Q82A, were fitted to the Michaelis–Menten equation (Fig. 3F). Nonlinear regression analysis of the plots yielded the kinetic parameters k_{cat} and K_m for each UCH variant, and their values are provided in Table 1. The values of the kinetic parameters obtained with wild-type enzymes were consistent with previously reported values [19–21]. For UCHL1 and UCHL3, the Gln → Ala mutants showed 30-fold and 18-fold decreases in k_{cat}, respectively, as compared with their corresponding wild-type enzymes. However, K_m values were relatively unchanged by the mutation, which is consistent with the hypothesis that the Gln is involved in the catalytic mechanism of the enzyme.

In the case of UCHL5N240 Q82A, k_{cat} and K_m could not be determined individually, because, even at concentrations of Ub-AMC as high as 12 μM, the Michaelis–Menten plot was still rising linearly with substrate concentration, not reaching the plateau that is diagnostic of saturation. Substrate concentrations > 12 μM result in dimethylsulfoxide concentrations higher than 5%, which can diminish the enzyme's activity. Instead, the k_{cat}/K_m ratio was determined by dividing the slope of this linear plot by the total enzyme concentration, as it can be assumed that, in this region of the Michaelis–Menten plot, [Ub-AMC] $\ll K_m$. Comparison of this value for the wild-type and Q82A variant of UCHL5N240 showed a 16-fold reduction in catalytic efficiency, which was comparable to the reductions seen with UCHL1 and UCHL3, suggesting that Gln82 is probably performing the same function as in the other UCH enzymes.

In order to determine the effect of these mutations on the stabilization of the transition state, we sought to estimate the change in free energy of activation associated with the mutation. The calculation was carried out with Eqn (1) and the k_{cat}/K_m values mentioned above and reported in Table 1 [12]. The free energy change for the three enzymes was approximately 2 kcal·mol^{-1}, which is consistent with the value reported for the same mutation in papain [12].

$$\Delta\Delta G^{\neq} = -RT \ln \left[\frac{(k_{cat}/K_m)_{mutant}}{(k_{cat}/K_m)_{wild\text{-}type}} \right] \quad (1)$$

The active site Gln in UCHs is involved in a C–H···O hydrogen bond with CεH of the catalytic His

The loss in enzymatic activity seen in the Gln → Ala mutants prompted us to look closely at the interactions of the active site Gln with nearby residues. Figure 4 shows the active site neighbors of Gln in UCHL3 [Protein Data Bank (PDB) entry 1UCH]. Interestingly, the Gln is in close proximity to the catalytic His, with the CεH being 2.0 Å away from the oxygen of the side chain carbonyl group, a distance less than the sum of their van der Waals radii. This distance, along with C–H···O and H···O=C angles of 171° and 122°, respectively, meets the geometric criteria used for a C–H···O hydrogen bond, and this interaction therefore qualifies as a significant interaction [22–26]. Inspection of the active sites of UCHL1 (PDB ID: 3IFW) (bound with Ub vinylmethylester) and UCHL5N240 (PDB ID: 3RIS) also reveals the presence of the same interaction (Table 2), suggesting that the C–H···O hydrogen bond involving the active site His and Gln is a common feature of the UCHs discussed herein [22,27,28].

This observation led us to wonder whether such a hydrogen bond also exists in papain and other papain-like cysteine proteases. To this end, we created a dataset of structurally characterized cysteine proteases found in the MEROPS database that contain, in addition to the three members of the catalytic triad CH(N/D), the conserved Gln in their active site (see Experimental procedures) [29]. The list of all proteins in the dataset and relevant information about them is

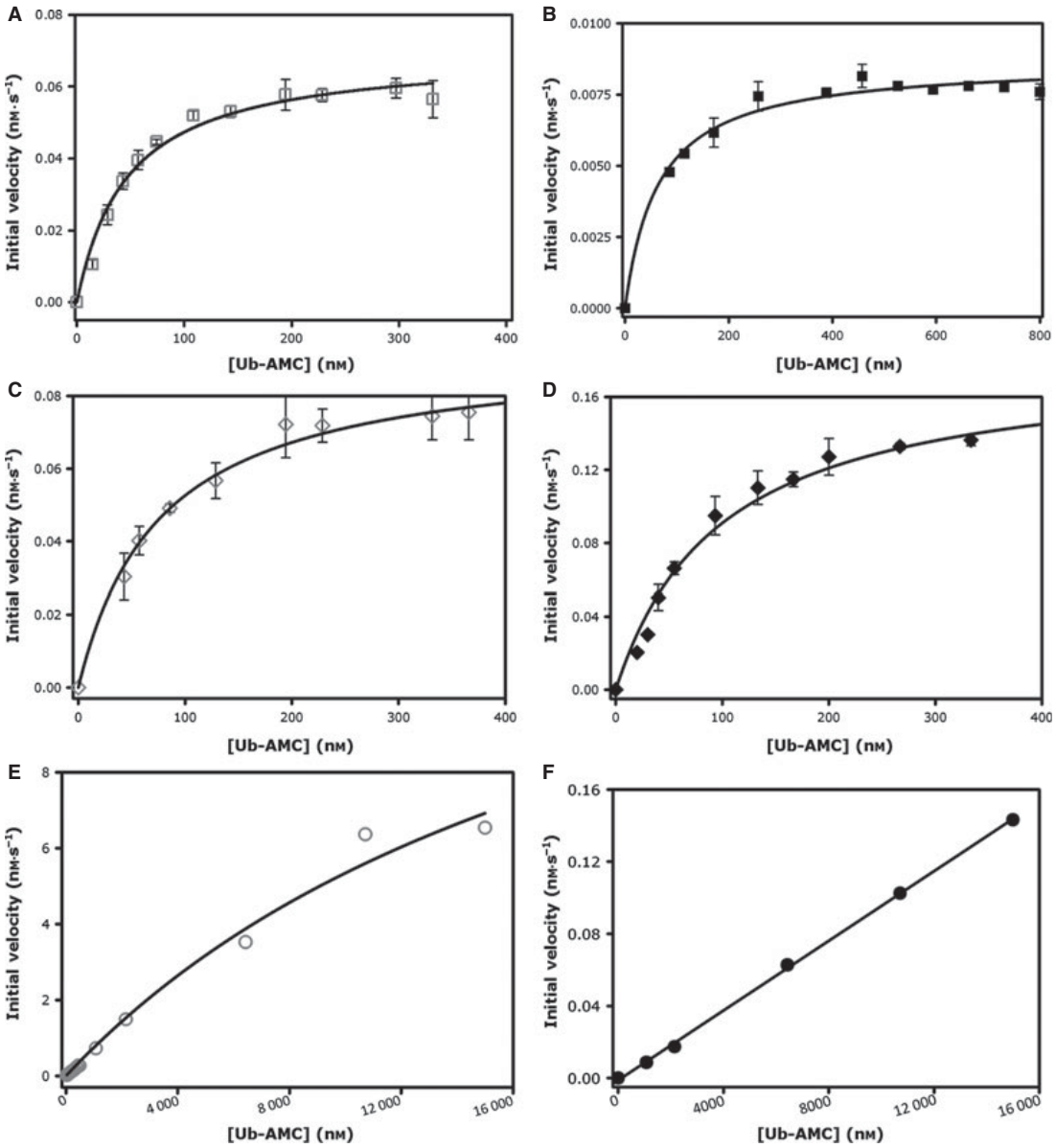

Fig. 3. Deubiquitination activity assay for determination of catalytic parameters. Data were fitted to the Michaelis–Menten equation to determine the k_{cat} and K_m parameters for each enzyme and the corresponding Gln → Ala mutants. Wild-type UCHL1 (A) and UCHL1 Q84A (B) are shown as squares, wild-type UCHL3 (C) and UCHL3 Q89A (D) are shown as diamonds, and wild-type UCHL5N240 (E) and UCHL5N240 Q82A (F) are shown as circles.

presented in Table 2. The His–Gln (Cε–Oδ) distance and angle distributions within the members of the dataset are shown as a histogram in Fig. 5. Of 46 structures, 80% (37) satisfied the criteria for a C–H···O interaction. The remaining nine proteins met the angular requirements for the C–H···O bond, but did not meet the distance requirements. However, it should be noted that, in general, a hydrogen bond has a significant electrostatic component, which will be functional even at relatively longer distances, albeit with a

Table 1. Kinetic parameters for UCHs.

Enzyme	K_m (nM)	k_{cat} (s^{-1})	$k_{cat}/K_m \times 10^4$ ($M^{-1}\cdot s^{-1}$)	$\Delta\Delta G^{\ddagger}$ ($kcal\cdot mol^{-1}$)
UCHL3	77.1 ± 8.2	18.60 ± 0.60	24 140	1.89
UCHL3 Q89A	99.1 ± 13.5	1.03 ± 0.05	1040	
UCHL1	47.0 ± 6.0	$(0.0348 \pm 1.25) \times 10^{-3}$	74.1	2.19
UCHL1 Q84A	56.1 ± 2.3	$(0.0011 \pm 1.50) \times 10^{-4}$	1.96	
UCHL5N240	21 493.2	33.67	15.7	1.68
UCHL5N240 Q82A	–	–	0.966	

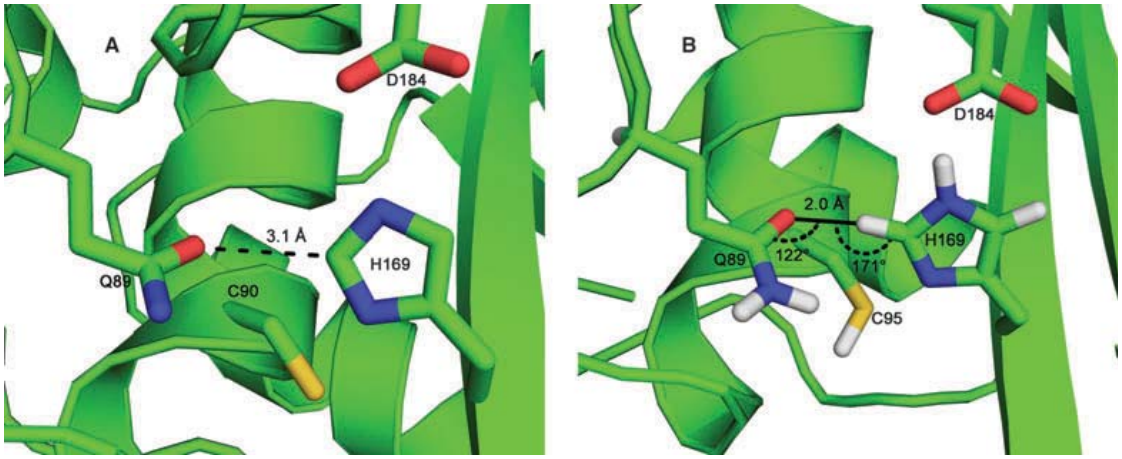

Fig. 4. Ribbon diagram of UCHL3 with the catalytic residues and the C–H···O bonding Gln shown as sticks. (A) The *D*-value. (B) The D_H-value along with the ξ and ζ angles.

weaker effect [24]. Among the 37 structures that met the criteria, there were five instances in the dataset where inactive forms of the protein did not meet C–H···O specifications; however the bond criteria were satisfied once the protein was in an active conformation upon complexation with either an inhibitor or a substrate mimic (Table 2). Table 2 shows that a majority of the C–H···O distances were between 3.1 and 4.5 Å, with a mean value of 3.7 Å. Additionally, the H···O distances varied between 2.1 and 3.3 Å with a mean value of 2.6 Å. The Cε–H···O (ζ) angles were also well within the defined criteria of > 120°, with a mean of 161°, whereas the mean H···O=C (ξ) angle was 134°.

In order to better understand the role of the Gln side chain in the catalytic reaction, additional mutations converting the Gln to either a Glu or a Lys were carried out (Fig. 6). As the results for the Gln → Ala mutation were consistent across the three UCHs tested, we limited the experiments to just UCHL3, which displayed the best geometry for the C–H···O hydrogen bond among the UCHs. Mutation of the Gln to Glu would allow for a stronger C–H···O bond, but would eliminate its contribution to oxyanion stabilization. Furthermore, it would introduce a negative charge that is expected to destabilize the oxyanion species. Mutation to Lys, on the other hand, would take away the possibility of the C–H···O bond while allowing for stronger oxyanion stabilization, on the assumption that the side chain NH_3^+ group of the Lys would occupy a position similar to the NH_2 group of the Gln side chain. As seen in the previous Ala mutants, replacing the Gln with either a Glu or a Lys lowered k_{cat}, whereas K_m remained relatively unchanged (Table 3). Surprisingly, the Q89E mutation resulted in only a five-fold reduction in k_{cat} as compared with the wild-type enzyme, an effect that is significantly lower than what would be expected from the combined effect of both eliminating hydrogen bonding and introducing charge–charge repulsion between the Glu side chain and the oxyanion. In the case of the Q89K mutant, despite our expectation that the mutation would lead

Table 2. C–H···O hydrogen bond parameters observed in 46 structurally characterized cysteine proteases with QCH(N/D)-type active site configurations from the MEROPS database.

Clan	Family	PDB	Protein	Resolution	Active site residues	D (Å)	D_H (Å)	ζ (°)	ξ (°)
CA	C1	1PE6	Papain	2.1	Q19, C25, H159, N175	3.7	2.6	167.4	135.6
		1YAL	Chymopapain	1.7	Q19, C25, H159, N179	3.7	2.6	172.4	125.2
		1PPO	Caricain	1.8	Q19, C25, H159, N179	3.7	2.7	153.0	130.4
		1GEC	Glycyl endopeptidase (*Carica papaya*)	2.1	Q19, C25, H159, N179	3.6	2.1	179.1	150.0
		2ACT	Actinidain	1.7	Q19, C25, H162, N182	3.5	2.5	162.0	124.0
		1FH0[a]	Cathepsin V	1.6	Q19, C25, H163, N187	4.2	3.2	162.7	137.9
		1S4V	Vignain	2.0	Q20, C26, H163, N183	3.8	2.7	174.6	138.3
		1EF7[b]	Cathepsin X	2.7	Q22, C31, H180, N200	3.9	2.8	163.9	144.6
		1CQD[a]	Zingipain	2.1	Q21, C27, H161, N181	4.0	3.0	152.4	120.8
		1M6D	Cathepsin F	1.7	Q19, C25, H159, N175	3.8	2.8	146.7	155.6
		2FO5	Endopeptidase B (barley-type)	2.2	Q22, C28, H167, N188	3.7	2.6	162.2	118.0
		1CS8	Cathepsin L	1.8	Q19, C25, H163, N187	3.7	2.6	168.8	131.4
		1GLO	Cathepsin S	2.2	Q19, C25, H164, N184	3.3	2.3	161.4	119.7
		7PCK	Cathepsin K	3.2	Q19, C25, H162, N182	3.5	2.4	173.9	154.1
		1NB5[b,c]	Cathepsin H	2.4	Q19, C25, H159, N158	3.4	2.4	152.3	162.4
		1YVB	Falcipain-2	2.7	Q19, C25, H159, N175	3.8	2.8	159.5	112.1
		1HUC[c]	Cathepsin B	2.1	Q23, C29, H199, N219	3.6	2.5	153.3	122.5
		3BPM	Falcipain-3	2.5	Q45, C51, H183, N182	3.9	2.8	165.0	98.9
		1K3B[c]	Dipeptidyl-peptidase I	2.2	Q228, C234, H381, N403	3.4	2.3	172.4	131.2
		2P86[a]	Rhodesain	1.2	Q19, C25, H162, N182	4.3	3.3	152.8	141.3
		1XKG	Peptidase 1 (mite)	1.6	Q108, C114, H250, N270	3.4	2.3	165.0	135.6
		1F2A[a]	Cruzipain	1.6	Q19, C25, H159, N175	4.1	3.0	164.0	137.7
		1IWD	Ervatamin B	1.6	Q19, C25, H159, N178	3.6	2.5	169.1	137.0
		1O0E[a]	Ervatamin C	1.9	Q19, C25, H157, N173	4.0	3.0	168.1	131.3
		2BDZ	Mexicain	2.1	Q19, C25, H159, N175	3.6	2.5	168.8	130.2
		3BCN[c]	Ervatamin A	2.8	Q19, C25, H157, N173	3.1	2.1	154.7	150.9
		3F75	TgCPL peptidase (*Toxoplasma gondii*)	2.0	Q25, C31, H167, N189	3.5	2.4	174.0	139.5
		2B1M	Papain-like protein SPE31 (*Pachyrhizus erosus*)	2.0	Q20, G25, H168, N188	3.4	2.4	154.7	137.7
		1CB5	Bleomycin hydrolase (animal)	2.6	Q67, C73, H372, N396	3.7	2.7	162.1	114.6
	C2	1KXR	Calpain-1	2.1	Q109, C115, H272, N296	3.2	2.3	141.7	119.0
		1MDW	Calpain-2	2.0	Q99, C105, H262, N286	3.0	1.9	164.0	128.4
	C12	3IFW[b]	Ubiquitinyl hydrolase L1	2.4	Q84, C90, H161, D176	3.7	2.8	141.6	159.2
		1UCH	Ubiquitinyl hydrolase L3	1.8	Q89, C95, H169, D184	3.1	2.0	171.6	122.1
		1CMX[c]	Ubiquitinyl hydrolase YUH1	2.3	Q84, C90, H166, D181	4.1	3.1	159.4	140.8
		3IHR	Ubiquitin C-terminal hydrolase L5	3.0	Q82, C88, H164, D179	3.6	2.8	133.6	160.1
	C39	3K8U	Bacteriocin-processing peptidase	1.9	Q11, C17, H96, D112	3.6	2.7	136.2	153.6
	C47	1CV8	Staphopain A	1.8	Q18, C24, H120, N141	3.5	2.4	160.4	138.3
		1X9Y[a]	Staphopain B	2.5	Q237, C243, H340, N360	4.0	2.9	164.6	123.4
CE	C83	2BU3[c]	γ-Glutamylcysteine dipeptidyltranspeptidase	1.4	Q64, C70, H183, D201	3.5	2.4	179.0	150.6
	C5	1AVP[a]	Adenain	2.6	Q115, C122, H54, E71	4.5	3.5	156.5	100.5
	C48	3EAY	SENP7 peptidase	2.4	Q920, C926, H794, D873	3.6	2.6	151.5	137.4
		1XT9	SENP8 peptidase	2.2	Q157, C163, H102, D119	3.3	2.2	176.7	136.4
		1EUV[b]	Ulp1 peptidase	1.6	Q574, C580, H514, D531	3.9	2.8	160.0	145.6
		2CKG	SENP1 peptidase	2.5	Q596, C602, H533, D550	3.8	2.8	157.5	118.0
		1TH0[a]	SENP2 peptidase	2.2	Q542, C549, H478, D495	3.9	2.9	154.4	122.3
					AVG	3.7	2.6	161.1	133.7

[a] Does not meet our criteria for CHO hydrogen bond. [b] Satisfies our criteria upon complex formation. [c] MOLPROBITY strongly suggested flipping of Gln or His.

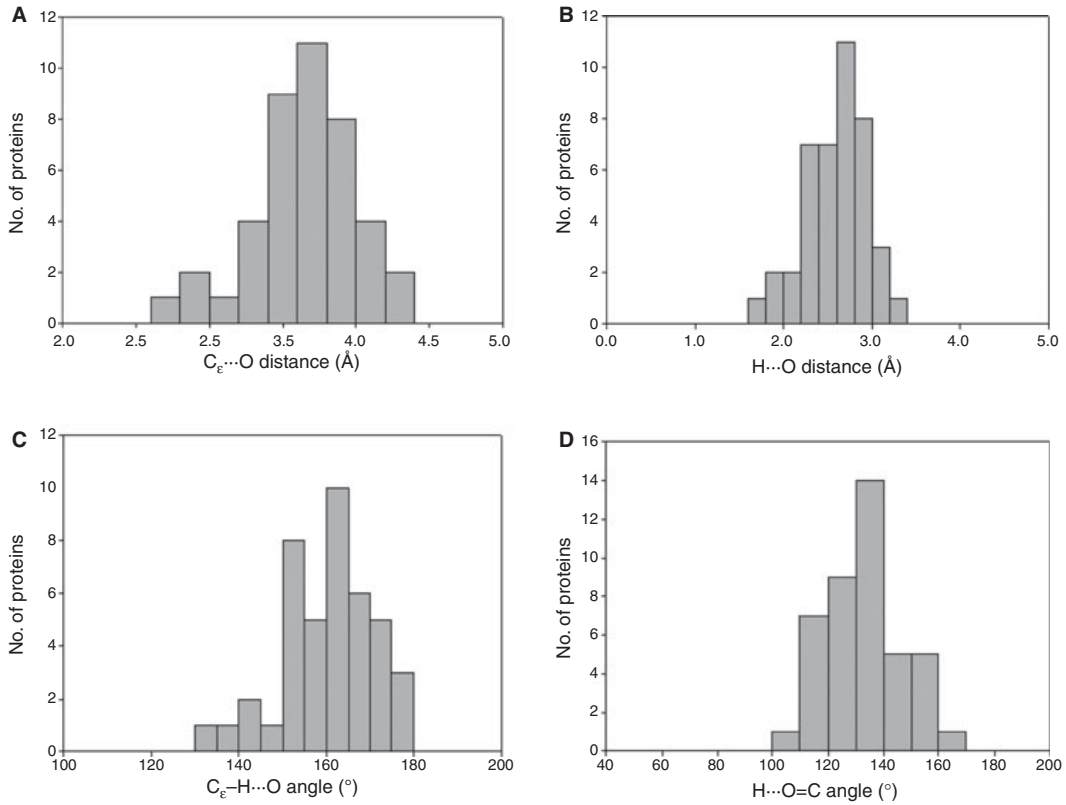

Fig. 5. (A) Distribution of distances (*D*) between the active site His Cε–H···O contact of the side chain or backbone carbonyl. (B) Distribution of distances (D_H) H···O–C. (C) Distribution of angles between Cε–H···O (ζ). (D) Distribution of angles between the H···O–C (ξ) contact of the side chain or backbone carbonyl.

to better oxyanion stabilization, we saw a 15-fold reduction in k_{cat}, which is approximately the value that we saw in the UCHL3 Q89A mutant (compare Table 1 with Table 3).

Discussion

The UCH subfamily of deubiquitinases are cysteine proteases with a catalytic triad similar to that seen in the papain family. In each member of this family, as in papain, there is a conserved Gln located in the active site of the enzymes that is believed to stabilize the incipient negative charge on the carbonyl of the scissile bond during the transition state of the hydrolysis reaction (Scheme 1). Indeed, mutation of the Gln19 in papain to Ala resulted in a 60-fold decrease in catalytic efficiency, owing mainly to a diminished catalytic rate (20-fold) and a small loss in substrate binding (three-fold). These results support the claim that the conserved Gln side chain contributes to the stabilization of the oxyanion transition state. Given the similarity in certain active site residues between papain and members of the UCH family, we wondered whether the Gln would perform a similar role in the UCH family. The study presented herein sought to address the role of the conserved Gln in rate enhancement in three UCHs.

Through site-directed mutagenesis, the active site Gln in three structurally characterized members of the UCH family was replaced with Ala, in order to assess the contribution of this side chain to rate enhancement. Deubiquitination assays show there is a significant loss of activity in mutant enzymes as compared with their wild-type counterparts. Comparison of the kinetic parameters shows a 16-fold to 30-fold reduction (~ 2 kcal·mol^{-1}) in the catalytic efficiency for the Gln mutants, which is attributable mainly to a decrease in the k_{cat} parameter, as seen in UCHL1 and UCHL3

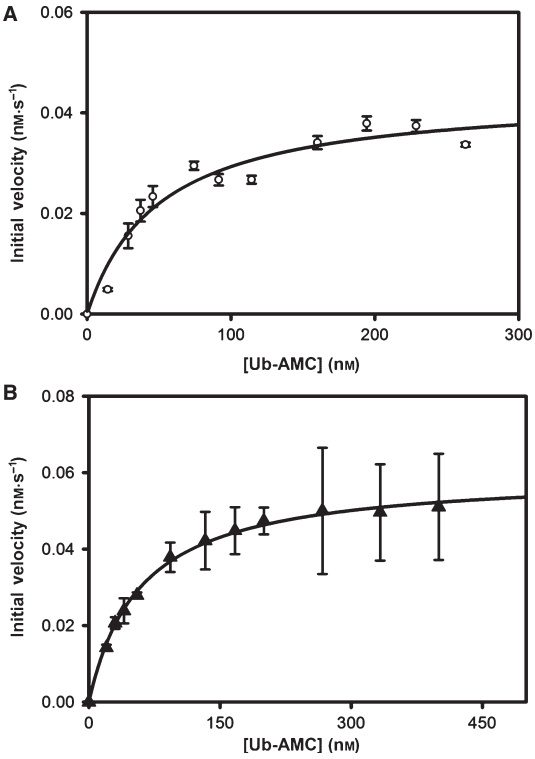

Fig. 6. Activity assay for UCHL3 mutants fitted to the Michelis–Menten equation for determination of K_m and k_{cat}. (A) UCHL3 Q89E is shown as open circles. (B) UCHL3 Q89K is shown as filled triangles.

(for the mutant UCHL5, k_{cat} and K_m could not be separately determined). These results are in agreement with the aforementioned results for papain, although the UCHs did not exhibit the same change in K_m value. The kinetic scheme for UCHL1 has been worked out by Case and Stein, using the same Ub-AMC substrate [20]. Their study showed that the rate of acylation is rate-limiting for k_{cat}, which means that K_m is reduced to the dissociation constant (K_d) of the Michaelis complex. The fact that we do not see any significant change in K_m suggests that Gln84 in UCHL1 does not contribute to the enzyme–ground state–substrate complex. Therefore, in UCHL1, according to our studies, the active site Gln does not make any appreciable contact with the substrate in the Michaelis complex; rather, it helps to stabilize the transition state.

Table 3. Kinetic parameters for UCHL3 mutants.

	K_m (nM)	k_{cat} (s^{-1})	$k_{cat}/K_m \times 10^4$ ($M^{-1}\cdot s^{-1}$)	$\Delta\Delta G^{\neq}$ (kcal·mol^{-1})
UCHL3 Q89E	49.8 ± 11.0	3.65 ± 0.00	7329	0.72
UCHL3 Q89K	58.5 ± 2.9	1.20 ± 0.00	1931	1.51

The kinetic scheme for UCHL3 remains to be worked out. However, k_{cat} values of UCHL3-catalyzed hydrolysis of Ub ethylester and Ub-lysine are very similar to that obtained with Ub-AMC as the substrate, suggesting that deacylation might be the rate-limiting step [19]. In such a case, K_m is not the simple dissociation constant of the Michaelis complex. Nevertheless, the fact that K_m changes only slightly upon Gln → Ala mutation in UCHL3 is consistent with the inference that the Gln does not appreciably contribute to the Michaelis complex.

As discussed before, we could not separately measure k_{cat} and K_m for UCHL5N240 Q82A; rather, the ratio was measured, which is about 16-fold less than that for the wild-type protein. It is possible that the ratio reflects a change mostly in k_{cat}, as for UCHL1 and UCHL3, because of the structural similarity between the proteins. However, it cannot be ruled out that UCHL5N240 employs a different mechanism from UCHL1 and UCHL3. It is possible that there was a much larger change in k_{cat} that was compensated for by an opposite change in K_m. Alternatively, there was little or no change in k_{cat} and the observed effect was attributable mostly to a change in K_m. The latter possibility seems rather unreasonable, as the Gln is located in an almost identical position as in the other enzymes, and its effect on stabilizing the Michaelis–Menten complex is therefore expected to be the same.

Our results indicate that the mutation of Gln to Ala results in a significant reduction in the catalytic rate, supporting the hypothesis that Gln functions to stabilize the transition state intermediate(s). However, one would expect the change to be much > 30-fold, as seen in our system, if the mechanism acted through the stabilization of the oxyanion, which has been proposed to involve hydrogen bonding between the NH_2 group of the side chain of Gln and the negatively charged oxygen ion, given that such hydrogen bonds are particularly strong. For example, mutation of the oxyanion-stabilizing residue Tyr16 to Phe in ketosteroid isomerase results in a 20 000-fold (6.3 kcal·mol^{-1}) reduction in k_{cat} [30]. One explanation for the discrepancy between the result of the mutation of the oxyanion-stabilizing side chain in ketosteroid isomerase and our system is that, in the latter, the side chain of Gln is not solely responsible for stabilizing the oxyanion

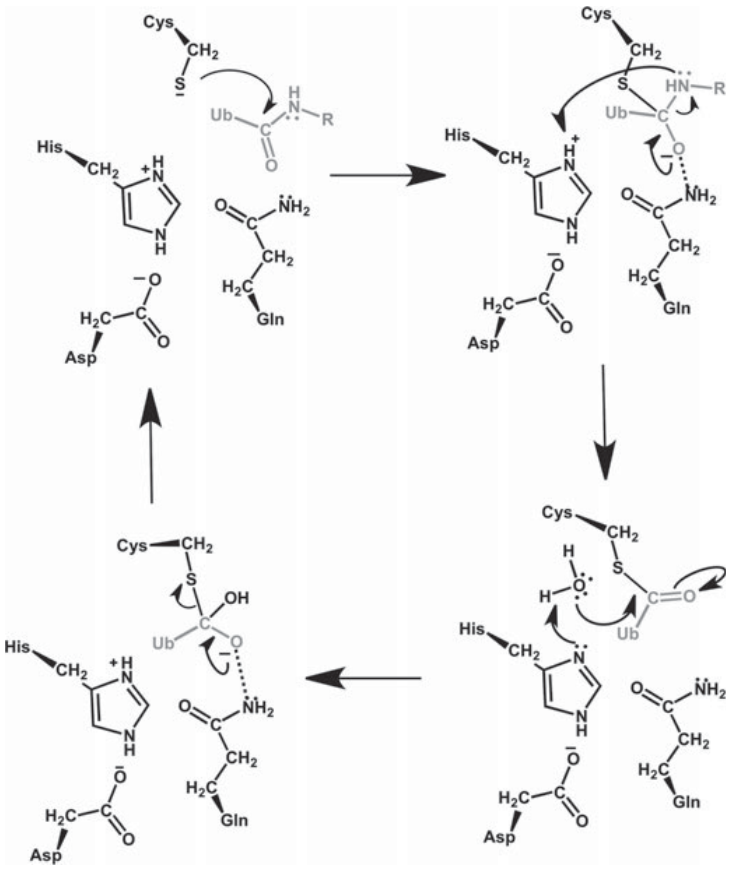

Scheme 1. Mechanism for the hydrolysis of ubiquitinated constructs by UCHs. Active site residues of the enzyme are in black, and the ubiquitinated substrate is in gray. The oxyanion interaction is indicated with dashed lines.

through hydrogen bonding; rather, it plays a role in contributing to the overall electropositive character of the oxyanion hole. As shown in Fig. 2, a number of αNH dipoles from surrounding backbone residues can still support a significant degree of oxyanion stabilization even in the absence of the Gln side chain. As main chain atoms cannot be removed by traditional mutagenesis methods, the individual contribution of each atom cannot be determined, and nor can we determine whether the Gln plays a more significant role than the individual backbone atoms. The alternative possibility, that the transition state stabilization by the Gln side chain reflects a somewhat weaker hydrogen bond, owing to a longer distance between the donor and the acceptor (Fig. 2), cannot be ruled out.

An alternative explanation for the difference in magnitude of Ub-AMC hydrolysis seen between the Gln → Ala mutants and the wild-type enzymes involves the loss of the C–H···O contact in the mutant. Inspection of active sites of the UCHs reveals that the Gln is in close proximity to the catalytic His, which satisfies the geometric constraints for a C–H···O hydrogen bond. Intrigued by this, we looked at a larger dataset of QCH(N/D)-type cysteine proteases in the MEROPS database, and this revealed that most cysteine proteases, including papain, possess a conserved Gln that is within C–H···O bonding distance of the catalytic His. It should be noted that, in papain, Gln19 is also known to be involved in an N–H···O hydrogen bond with the NH group of the side chain of Trp177 [31], a catalytically important side chain. This is an example of a carbonyl group being simultaneously engaged in hydrogen bonding with a CH and an NH donor, a situation that is commonly observed among

protein β-sheets, in which the backbone carbonyl groups of one strand are engaged in C–H···O and N–H···O hydrogen bonds with an adjacent strand's CαH and backbone NH groups, respectively [32]. However this 'bifurcated' situation does not exist in UCHs, as there is no other hydrogen bond donor with an acceptable distance other than the imidazole group of the catalytic His. The observation of the C–H···O contact presented here extends the parallels between serine and cysteine proteases. Dewerenda *et al.* first observed a C–H···O contact involving the catalytic His and a backbone carbonyl as the hydrogen bond donor in the active site of serine proteases [22]. The possibility that such an interaction plays a role in the catalytic mechanism of cysteine proteases, as has been suggested for their serine counterparts, cannot be ruled out. Interestingly, the change in free energy of transition state stabilization (close to 2 $kcal \cdot mol^{-1}$) upon mutation in our system, as well as in the case of papain, happens to be very much within the range of the strength of a C–H···O hydrogen bond [26].

The C–H···O hydrogen bond can be thought of as an additional force that stabilizes the imidazole side chain in a productive orientation such that it acts both as a general base and as a proton donor during catalysis. Additionally, the C–H···O hydrogen bonding would serve to enhance the His residue's ability to specifically act as a general base by transferring some electron density from the Gln carbonyl to the imidazole ring of His. A stronger general base would mean a better ability to extract a proton from water to activate it for nucleophilic attack, facilitating the formation of the tetrahedral transition state during deacylation (Scheme 1). Although different cysteine proteases would employ different mechanisms for hydrolysis, a better general base His will, in general, contribute to efficient catalysis. However, the exact mechanism by which the active site C–H···O interaction may play a role in transition state stabilization needs to be further investigated by computational work.

We conducted additional studies on UCHL3 to dissect the role of the Gln side chain in the deubiquitination reaction. If the sole purpose of Gln were to stabilize the oxyanion, removal of the hydrogen-bonding (N–H···O) donor plus the placement of a negative charge would substantially destabilize the transition state, leading to an effect on k_{cat} that would be greater than that in the Ala mutant. Interestingly, the Gln → Glu mutant (with only a five-fold decrease in k_{cat}) proved to be a better catalyst than the Ala mutant, which is inconsistent with the idea that the Gln is acting as an oxyanion stabilizer. Instead, the data appear to support the idea that the C–H···O hydrogen bond contributes to catalysis. It is likely that the carboxylate side chain of Glu in the Q89E mutant undergoes a stronger C–H···O interaction with the CεH group of the catalytic His than the carboxamide group of Gln, resulting in a better catalyst than the wild-type protein, but this effect is compensated for to some degree by the unfavorable electrostatics between the negatively charged side chain and the oxyanion. It should be noted that a previous study showed that Q19E mutation in papain resulted in an approximately 20-fold decrease in k_{cat}, to a similar level as seen in the Q19A mutant, leading the authors of that study to propose that the negative charge was tolerated in the active site [33]. It is tempting to propose that, in papain, the accommodation of the unfavorable charge in the mutant might have also been attributable to the compensatory effect of the C–H···O hydrogen bond.

We then mutated the Gln to Lys, which produced an enzyme with activity comparable to that of the Ala mutant. This is also surprising, because the Lys side chain has two components, NH groups for hydrogen bonding with the oxygen of the oxyanion, and the charge for favorable electrostatic interaction, and we expected that the combination of the two, assuming that right geometry is maintained for the N–H···O bond, would cause better stabilization of the oxyanion than in the wild-type protein. However, this mutant showed a similar level of catalytic activity as the Ala mutant, indicating that placement of a positive charge near the active site does not appreciably enhance the stability of the oxyanion species, presumably because the Gln in the wild-type enzyme was not playing a role in oxyanion stabilization. Alternatively, the longer side chain of Lys may be oriented away from the oxyanion with little interaction between the two. On the other hand, as the Q89K mutant lacks the ability to form the C–H···O hydrogen bond, the reduction in k_{cat} to nearly the same extent as seen in the Q89A mutant might reflect this deficiency.

In conclusion, we have shown that the active site Gln in UCHs contributes to rate enhancement, but the relatively modest value of transition state stabilization is more indicative of a weaker interaction, such as the C–H···O bond between the Gln and catalytic His, than the conventional N–H···O type of hydrogen bond that was proposed to stabilize the oxyanion. The observation that the Glu mutant of UCHL3 is more active than the Ala mutant suggests that the conserved Gln is unlikely to contribute to oxyanion stabilization, and rather may play a role in catalysis via the C–H···O hydrogen bond with the catalytic His.

Experimental procedures

General

The Ub-AMC used for hydrolysis assays was purchased from Boston Biochem (Boston, MA, USA). The glutathione affinity column (GSTPrep FF 16/10), gel filtration column (HiLoad 16/60 Superdex 75) and PreScission protease were purchased from GE Biosciences (Piscataway, NJ, USA). All fluorescence assays were performed on a TECAN Genios microplate spectrofluorometer. Buffer and salt components were purchased from either Sigma-Aldrich (St Louis, MO, USA) or RPI Corp. (Mount Prospect, IL, USA).

Mutagenesis, expression and purification of proteins

The genes for UCHL1, UHCL3 and UCHL5N240 were cloned into the pGEX-6P-1 vector with standard protocols, and subsequently used to mutate the active site Gln to Ala through PCR reactions with the Quickchange II (Agilent, Santa Clara, CA, USA) site-directed mutagenesis kit. All plasmids were transformed into Rosetta2 *Escherichia coli* cells and grown to a $A_{600\ nm}$ of 0.6 in LB medium supplemented with 100 μg·mL^{-1} ampicillin, and then induced with 0.5 mM isopropyl thio-β-D-thiogalactoside and grown overnight at 18 °C. Cells were harvested at 6000 ***g*** and resuspended in 1× NaCl/P_i + 400 mM KCl (buffer A). Cells were passed through a French press twice at 1200 p.s.i., and the lysate was cleared by centrifugation at 30 000 ***g*** for 1 h. The supernatant was loaded onto a glutathione affinity column, washed with three column volumes of buffer A, and eluted with 250 mM Tris, 500 mM KCl, and 10 mM reduced L-glutathione (pH 8.0). The eluted sample was dialyzed against 1× NaCl/P_i, 400 mM KCl, and 1 mM dithiothreitol, to which Precission Protease was added to remove the glutathione *S*-transferase tag, which was captured on a glutathione–agarose affinity column. The resulting glutathione *S*-transferase-cleaved protein solution was passed through a Superdex S75 gel filtration column with 50 mM Tris/HCl (pH 7.6), 150 mM NaCl, and 1 mM dithiothreitol. Fractions containing purified protein were pooled, concentrated, and then flash-frozen in liquid nitrogen and stored at −80 °C until use.

Kinetic assay to measure K_m and k_{cat} values

Each of the UCHs was diluted in assay reaction buffer (50 mM Tris, pH 7.6, 0.5 mM EDTA, 0.1% BSA, 5 mM dithiothreitol), so that the final concentrations in the reaction were as follows: UCHL1, 2 nM; UCHL1 Q84A, 8 nM; UCHL3, 5 pM; UCHL3 Q89A, 175 pM; UCHL5N240, 500 pM; UCHL5N240 Q82A, 3 nM; UCHL3 Q89E, 12 pM; and UCHL3 Q89K, 50 pM. Enzyme was added to a 96-well plate, and incubated at 30 °C for 5 min prior to addition of Ub-AMC diluted in assay reaction buffer to initiate the reaction. Rates of Ub-AMC cleavage were monitored with an excitation wavelength of 380 nm and an emission wavelength of 465 nm at 30 °C. Initial reaction rates were calculated and plotted against Ub-AMC concentrations in SIGMAPLOT, and fitted to the Michaelis–Menten equation to determine K_m and k_{cat} values.

C–H···O analysis

From the MEROPS database, a dataset of 46 nonhomologous structurally characterized cysteine proteases were selected belonging to families with a QCH(N/D) type of active site configuration [29]. Structures with a resolution lower than 3 Å were excluded from the dataset. Each of the coordinate files was downloaded from the PDB, and hydrogens were added to the protein structures with the REDUCE program under MOLPROBITY [34,35]. The stereochemistry of the C–H···O bond was analyzed with the four different criteria for parameters shown in Fig. 7: C–O bond distance (D); H···O bond distance (D_H); C–H···O angle (ζ); and H···O = C angle (ξ). The geometric parameters used in the present and previous C–H···O studies can be found in Table 4. The bond distances and angles were calculated with PYMOL (DeLano Scientific) and are shown in Table 2.

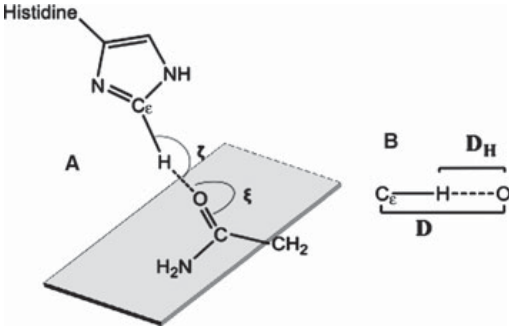

Fig. 7. Definition of geometric parameters. (A) Angular parameters. (B) Distance parameters.

Table 4. Geometric parameters for C–H···O hydrogen bonding

D (Å)	D_H (Å)	ζ (°)	ξ (°)	Reference
≤ 4.0	< 2.8	> 120	–	Present study
≤ 3.5	< 2.7	> 120	–	[23]
–	< 2.7	> 90	~ 120	[22]
–	< 2.8	> 90	–	[36]
4.0–3.0	< 2.8	> 110	120–140	[25]

Acknowledgements

We would like to acknowledge S. Schiener, Utah State University, for his helpful contribution to the manuscript. We are grateful to J.-C. Rochet for use of his fluorescence plate reader. Financial support from the National Institutes of Health (1R01RR026273) to C. Das is gratefully acknowledged. Financial support for D. A. Boudreaux was provided by the Purdue Research Foundation (204533), and financial support for to J. Chaney was provided by Alliances for Graduate Education and The Professoriate.

References

1 Komander D, Clague MJ & Urbe S (2009) Breaking the chains: structure and function of the deubiquitinases. *Nat Rev Mol Cell Biol* **10**, 550–563.
2 Komander D (2010) Mechanism, specificity and structure of the deubiquitinases. *Subcell Biochem* **54**, 69–87.
3 Love KR, Catic A, Schlieker C & Ploegh HL (2007) Mechanisms, biology and inhibitors of deubiquitinating enzymes. *Nat Chem Biol* **3**, 697–705.
4 Nijman SM, Luna-Vargas MP, Velds A, Brummelkamp TR, Dirac AM, Sixma TK & Bernards R (2005) A genomic and functional inventory of deubiquitinating enzymes. *Cell* **123**, 773–786.
5 Wilkinson KD (2009) DUBs at a glance. *J Cell Sci* **122**, 2325–2329.
6 Das C, Hoang QQ, Kreinbring CA, Luchansky SJ, Meray RK, Ray SS, Lansbury PT, Ringe D & Petsko GA (2006) Structural basis for conformational plasticity of the Parkinson's disease-associated ubiquitin hydrolase UCH-L1. *Proc Natl Acad Sci USA* **103**, 4675–4680.
7 Johnston SC, Larsen CN, Cook WJ, Wilkinson KD & Hill CP (1997) Crystal structure of a deubiquitinating enzyme (human UCH-L3) at 1.8 A resolution. *EMBO J* **16**, 3787–3796.
8 Misaghi S, Galardy PJ, Meester WJ, Ovaa H, Ploegh HL & Gaudet R (2005) Structure of the ubiquitin hydrolase UCH-L3 complexed with a suicide substrate. *J Biol Chem* **280**, 1512–1520.
9 Nishio K, Kim SW, Kawai K, Mizushima T, Yamane T, Hamazaki J, Murata S, Tanaka K & Morimoto Y (2009) Crystal structure of the de-ubiquitinating enzyme UCH37 (human UCH-L5) catalytic domain. *Biochem Biophys Res Commun* **390**, 855–860.
10 Boudreaux DA, Maiti TK, Davies CW & Das C (2010) Ubiquitin vinyl methyl ester binding orients the misaligned active site of the ubiquitin hydrolase UCHL1 into productive conformation. *Proc Natl Acad Sci USA* **107**, 9117–9122.
11 Warwicker J & Watson HC (1982) Calculation of the electric potential in the active site cleft due to alpha-helix dipoles. *J Mol Biol* **157**, 671–679.
12 Menard R, Carriere J, Laflamme P, Plouffe C, Khouri HE, Vernet T, Tessier DC, Thomas DY & Storer AC (1991) Contribution of the glutamine 19 side chain to transition-state stabilization in the oxyanion hole of papain. *Biochemistry* **30**, 8924–8928.
13 Johnston SC, Riddle SM, Cohen RE & Hill CP (1999) Structural basis for the specificity of ubiquitin C-terminal hydrolases. *EMBO J* **18**, 3877–3887.
14 Leroy E, Boyer R, Auburger G, Leube B, Ulm G, Mezey E, Harta G, Brownstein MJ, Jonnalagada S, Chernova T *et al.* (1998) The ubiquitin pathway in Parkinson's disease. *Nature* **395**, 451–452.
15 Saigoh K, Wang YL, Suh JG, Yamanishi T, Sakai Y, Kiyosawa H, Harada T, Ichihara N, Wakana S, Kikuchi T *et al.* (1999) Intragenic deletion in the gene encoding ubiquitin carboxy-terminal hydrolase in gad mice. *Nat Genet* **23**, 47–51.
16 Wicks SJ, Haros K, Maillard M, Song L, Cohen RE, Dijke PT & Chantry A (2005) The deubiquitinating enzyme UCH37 interacts with Smads and regulates TGF-beta signalling. *Oncogene* **24**, 8080–8084.
17 Eletr ZM & Wilkinson KD (2011) An emerging model for BAP1's role in regulating cell cycle progression. *Cell Biochem Biophys* **60**, 3–11.
18 Fang Y, Fu D & Shen XZ (2010) The potential role of ubiquitin c-terminal hydrolases in oncogenesis. *Biochim Biophys Acta* **1806**, 1–6.
19 Luchansky SJ, Lansbury PT Jr & Stein RL (2006) Substrate recognition and catalysis by UCH-L1. *Biochemistry*, **45**, 14717–14725.
20 Case A & Stein RL (2006) Mechanistic studies of ubiquitin C-terminal hydrolase L1. *Biochemistry*, **45**, 2443–2452.
21 Dang LC, Melandri FD & Stein RL (1998) Kinetic and mechanistic studies on the hydrolysis of ubiquitin C-terminal 7-amido-4-methylcoumarin by deubiquitinating enzymes. *Biochemistry* **37**, 1868–1879.
22 Derewenda ZS, Lee L & Derewenda U (1995) The occurrence of C-H···O hydrogen-bonds in proteins. *J Mol Biol* **252**, 248–262.
23 Senes A, Ubarretxena-Belandia I & Engelman DM (2001) The C alpha-H···O hydrogen bond: a determinant of stability and specificity in transmembrane helix interactions. *Proc Natl Acad Sci USA* **98**, 9056–9061.
24 Steiner T (2003) C–H···O hydrogen bonding in crystals. *Crystallogr Rev* **9**, 177–228.
25 Desiraju GR (1996) The C-H···O hydrogen bond: structural implications and supramolecular design. *Acc Chem Res* **29**, 441–449.
26 Scheiner S, Kar T & Gu YL (2001) Strength of the (CH)-H-alpha···O hydrogen bond of amino acid residues. *J Biol Chem* **276**, 9832–9837.

27 Chakrabarti P & Chakrabarti S (1998) C-H···O hydrogen bond involving proline residues in alpha-helices. *J Mol Biol* **284**, 867–873.
28 Madan Babu M, Kumar Singh S & Balaram P (2002) A C-H triplebond O hydrogen bond stabilized polypeptide chain reversal motif at the C terminus of helices in proteins. *J Mol Biol* **322**, 871–880.
29 Rawlings ND, Morton FR & Barrett AJ (2006) MEROPS: the peptidase database. *Nucleic Acids Res* **34**, D270–D272.
30 Kraut DA, Sigala PA, Fenn TD & Herschlag D (2010) Dissecting the paradoxical effects of hydrogen bond mutations in the ketosteroid isomerase oxyanion hole. *Proc Natl Acad Sci USA* **107**, 1960–1965.
31 Gul S, Hussain S, Thomas MP, Resmini M, Verma CS, Thomas EW & Brocklehurst K (2008) Generation of nucleophilic character in the Cys25/His159 ion pair of papain involves Trp177 but not Asp158. *Biochemistry* **47**, 2025–2035.
32 Fabiola GF, Krishnaswamy S, Nagarajan V & Pattabhi V (1997) C-H...O hydrogen bonds in beta-sheets. *Acta Crystallogr D Biol Crystallogr* **53**, 316–320.
33 Menard R, Plouffe C, Laflamme P, Vernet T, Tessier DC, Thomas DY & Storer AC (1995) Modification of the electrostatic environment is tolerated in the oxyanion hole of the cysteine protease papain. *Biochemistry* **34**, 464–471.
34 Bernstein FC, Koetzle TF, Williams GJB, Meyer EF, Brice MD, Rodgers JR, Kennard O, Shimanouchi T & Tasumi M (1977) Protein Data Bank – computer-based archival file for macromolecular structures. *J Mol Biol* **112**, 535–542.
35 Chen VB, Arendall WB, Headd JJ, Keedy DA, Immormino RM, Kapral GJ, Murray LW, Richardson JS & Richardson DC (2010) MolProbity: all-atom structure validation for macromolecular crystallography. *Acta Crystallogr D Biol Crystallogr* **66**, 12–21.
36 Steiner T (1994) Effect of acceptor strength on C–H...O hydrogen-bond lengths as revealed by and quantified from crystallographic data. *J Chem Soc Chem Commun*, **20**, 2341–2342.

Supporting information

The following supplementary information is available:
Fig. S1. Comparative activity assays of wild-type and mutant UCHs.
Fig. S2. Far-UV CD spectroscopy shows that the oxyanion-stabilizing mutations of Gln to Ala do not perturb the gross structure of the UCHs.
Data S1. Methods.

This supplementary material can be found in the online version of this article.

Please note: As a service to our authors and readers, this journal provides supporting information supplied by the authors. Such materials are peer-reviewed and may be reorganized for online delivery, but are not copy-edited or typeset. Technical support issues arising from supporting information (other than missing files) should be addressed to the authors.

JOHN WILEY AND SONS LICENSE
TERMS AND CONDITIONS

Apr 08, 2015

This Agreement between Joseph R Chaney ("You") and John Wiley and Sons ("John Wiley and Sons") consists of your license details and the terms and conditions provided by John Wiley and Sons and Copyright Clearance Center.

License Number	3601470996814
License date	Apr 03, 2015
Licensed Content Publisher	John Wiley and Sons
Licensed Content Publication	FEBS Journal
Licensed Content Title	Contribution of active site glutamine to rate enhancement in ubiquitin C-terminal hydrolases
Licensed Content Author	David A. Boudreaux,Joseph Chaney,Tushar K. Maiti,Chittaranjan Das
Licensed Content Date	Feb 27, 2012
Pages	13
Type of use	Dissertation/Thesis
Requestor type	Author of this Wiley article
Format	Print and electronic
Portion	Full article
Will you be translating?	No
Title of your thesis / dissertation	BIOCHEMICAL INVESTIGATION OF UBIQUITIN CARBOXY-TERMINAL HYDROLYSES
Expected completion date	May 2015
Expected size (number of pages)	120
Requestor Location	Joseph R Chaney 120 Washington St LAFAYETTE, IN 47905 United States Attn: Joseph R Chaney
Billing Type	Invoice
Billing Address	Joseph R Chaney 120 Washington St LAFAYETTE, IN 47905 United States Attn: Joseph R Chaney
Total	0.00 USD

http://olabout.wiley.com/WileyCDA/Section/id-410895.html

Other Terms and Conditions:

v1.9

Questions? customercare@copyright.com or +1-855-239-3415 (toll free in the US) or +1-978-646-2777.

Gratis licenses (referencing $0 in the Total field) are free. Please retain this printable license for your reference. No payment is required.
